HAL
open science

Modèle de second gradient adapté aux milieux faiblement continus et mécanique d'Eshelby appliquée à l'indentation du verre

Nirmal Antonio Tamarasselvame

▶ **To cite this version:**

Nirmal Antonio Tamarasselvame. Modèle de second gradient adapté aux milieux faiblement continus et mécanique d'Eshelby appliquée à l'indentation du verre. Mathématiques [math]. Université Rennes 1, 2010. Français. NNT : . tel-00557871

HAL Id: tel-00557871

https://theses.hal.science/tel-00557871v1

Submitted on 20 Jan 2011

HAL is a multi-disciplinary open access archive for the deposit and dissemination of scientific research documents, whether they are published or not. The documents may come from teaching and research institutions in France or abroad, or from public or private research centers.

L'archive ouverte pluridisciplinaire **HAL**, est destinée au dépôt et à la diffusion de documents scientifiques de niveau recherche, publiés ou non, émanant des établissements d'enseignement et de recherche français ou étrangers, des laboratoires publics ou privés.

N^o d'ordre : 4230 ANNÉE 2010

THÈSE / UNIVERSITÉ DE RENNES 1
sous le sceau de l'Université Européenne de Bretagne

pour le grade de

DOCTEUR DE L'UNIVERSITÉ DE RENNES 1

Mention : Mathématiques et Applications

Ecole doctorale MATISSE

présentée par

Nirmal ANTONIO TAMARASSELVAME

préparée à l'UMR 6625 CNRS - IRMAR
Institut de Recherche Mathématiques de Rennes
U.F.R de Mathématiques

Intitulé de la thèse :

Modèle de second gradient adapté aux milieux faiblement continus et mécanique d'Eshelby appliquée à l'indentation du verre

Thèse soutenue à Rennes le 23 novembre 2010

devant le jury composé de :

Pr. Jean-François GANGHOFFER
Institut Nat. Polytechnique Lorraine / président

Pr. Gérard A. MAUGIN
Université Pierre et Marie Curie / rapporteur

Pr. Qi-Chang HE
Université Marne-La-Vallée / rapporteur

Pr. Jean-Christophe SANGLEBOEUF
Université Rennes 1 / examinateur

Pr. Lalaonirina R. RAKOTOMANANA
Université Rennes 1 / directeur de thèse

Mcf. Manuel BUISSON
Université Rennes 1 / co-directeur de thèse

Cette thèse est dédiée à la mémoire de Salomon Ange et Bruno Veron.

Remerciements

Mes premiers remerciements s'adressent, comme le veut la tradition, à ceux qui ont contribué à ce que ces travaux de thèse puissent un jour aboutir : Lalaonirina R. Rakotomanana, le Directeur de thèse, et Manuel Buisson, le co-Directeur de thèse. La hiérarchie est ainsi établie et ce n'est pas chose facile de s'y tenir, mais le plus important restera le fait que tous les deux ont toujours oeuvré ensemble pour l'intérêt du doctorant. Je vous remercie messieurs pour la confiance que vous m'avez accordée en me confiant ce projet, d'avoir assuré mon intégration au sein du laboratoire dans les meilleures conditions et pour les nombreuses réunions (LN, MN, LMN) que nous avons partagées dans l'objectif d'améliorer sans cesse mon travail et ma formation, pas seulement dans le cadre de la thèse.

Pour la suite, mes remerciements s'adressent aux membres du jury de thèse : Gérard A. Maugin et Qi-Chang He, les rapporteurs, Jean-Christophe Sangleboeuf et Jean-François Ganghoffer, les examinateurs. Soyez assurés chers professeurs de ma plus grande reconnaissance à votre égard pour avoir pris en considération mon travail.

Je remercie Loic Le Marrec et Fulgence Razafimahéry, membres de notre équipe, pour leur accueil et les échanges enrichissants centrés sur des thèmes de recherche et d'enseignement, et bien d'autres très souvent ponctués d'une touche d'humour. Je ne peux oublier les doctorants (anciens et nouveaux) dont j'ai eu la joie de croiser et que je continue à cotoyer : Anne-Claire Bennis, Anjara Zafindravaka (honneur aux dames), Polynice Eyi, Nicolas Bideau (et Solena), Hani Ali, Adil El Baroudi et Benjamin Mahiou. D'une manière générale je tiens à citer dans ces remerciements tous les membres de l'équipe mécanique ainsi que l'ensemble des enseignants chercheurs de la tour des maths. J'exprime toute ma reconnaissance aux enseignants chercheurs de l'INSA de Rennes dans le département de mathématiques pour la confiance qu'ils m'ont accordée pour les enseignements en mathématiques : Laurent Monier, Loïc Hervé, Marc Briane, Erwan Le Gruyer, Paul Sablonnière, Jean-Bernard Gravereaux...et aussi l'indispensable Evelyne Martinez. Je termine ce paragraphe par exprimer ma reconnaissance aux membres du LARMAUR, un autre laboratoire du campus de Beaulieu, pour une collaboration qui aura renforcé mes travaux de thèse et qui continuera je l'espère avec beaucoup de motivation.

Un laboratoire de recherche ne peut fonctionner dans de bonnes conditions sans un service administratif, informatique et de documentation de qualité tant sur le plan professionnel que sur le plan des relations humaines. Merci mesdemoiselles, mesdames et messieurs : Claude Boschet, Marie-Aude Verger, Karine Falc'Hon, Chantal Halet, Hélène

Rousseaux, Marie-Annick Paulmier, Dominique Hervé, André Rebour, Patrick Perez...

Bien entendu, une thèse conduit à la rencontre de nombreux doctorants issus d'horizons divers et variés. Laissez moi vous présenter l'équipe 434, dans laquelle j'ai conservé une place de titulaire : Alina Crudu, Maher Kachour et Adrien Saumard composent l'équipe A, Anna Morra, Julien Frézard et Kodjo Kpognon composent l'équipe B. Viennent ensuite les remplaçants (jokers de luxe) : Matthieu Saumard (et Marianne), Nicolas Popoff, Pierre Carcaud, Damien Passemier (et Noémie), Adrien Richou (et Anne-Sophie et Jean), Lin Yiqing (et Xi Song), Julien Dhondt, Arnaud Jobin...et je n'oublie pas les anciennes gloires : Thomas Sierocinski et Audrey Houiller, Jiaqi Chen, Victor Peron, Jonathan Marco, Ludovic Goudenège, Jimmy Lamboley, Colas Bardavid, Rodolphe Richard. Puis je continue avec une liste non exhaustive d'éléments qui ont effectué un essai : Jacques Lim, Jean-Louis Marchand, Gaël Cousin, Mathieu Calvez, Baptiste Olivier, et ceux et celles que nous avons tenté de recruter pour affiner notre tactique : Mathilde Herblot, Marie Baudouin, Aurélien Klak, Sébastien Breteaux, Lionel Chaussade, Clément Dunand, Gweltaz Chatel... Je tiens également à citer Pierre et Jacqueline Gougeon, que j'ai eu le plaisir de rencontrer dès mon arrivé sur Rennes et avec lesquels les discussions mensuelles autour d'une tasse de thé sont un réel plaisir. Durant les trois dernières années rennaises, mes collègues et amis rencontrés représentent une des plus belles expériences humaines qu'il m'ait été donnée de vivre, et que j'entretiendrai pour longtemps.

Je n'oublie pas d'où je viens et ce qui m'a permis d'arriver à ce niveau. Je tiens ainsi à remercier les enseignants chercheurs de l'université de Versailles-Saint-Quentin-en-Yvelines, en particulier ceux du département de mathématiques, et ceux de Paris Dauphine (CEREMADE) dans le cadre du Master de Recherche. Puis une grande pensée pour les membres de l'École des Ponts et Chaussées de Champs-sur-Marne, avec les deux encadrants du stage de Master de Recherche : Silvano Erlicher (laboratoire LAMI) et Rui Pedro Carreira (campus de Recherche et Développement Décathlon de Villeneuve-d'Ascq). Cela a constitué un véritable tremplin pour une poursuite en thèse.

Enfin je parachève ces remerciements en m'adressant à mes proches. Je commence par mes amis parisiens et versaillais, en particulier Christian Gaudumet, Marc Kaissarlian et Olivier Rayar pour leur amitié qui dure, et tous les autres que je ne peux citer sans en oublier. Puis la famille, chose essentielle, dont les membres ont toujours une pensée pour moi à proximité et du côté de Pondichéry en Inde, où j'ai fait mes premiers pas. Mes parents, Gandy "attai", tonton "mama" et le trio germain (Bernard, Agnès, Thierry) forment en tout et pour tout ma famille d'abord, sans qui je n'y serais pas parvenu. Merci à vous tous...

Résumé

Dans une première partie, notre étude porte sur les milieux faiblement continus avec une approche basée sur la géométrie non riemannienne. Nous considérons un corps solide déformable modélisé par une variété riemannienne munie d'une connexion affine. Un tel modèle est une extension d'un autre qui considère une connexion euclidienne, laquelle dérive du tenseur métrique imposé par l'espace ambiant. La masse par unité de volume peut être supposée non constante et le corps peut contenir des défauts décrits par des champs de discontinuité de champs scalaires ou de champs vectoriels définis sur la variété. Dans ce cas, en plus du tenseur métrique, nous utilisons nécessairement la torsion introduite par Cartan ou la courbure, deux tenseurs associés à la connexion affine. Nous disposons ainsi d'un modèle de milieu continu du second gradient. Les investigations prennent en compte les effets de ces champs tensoriels dans l'analyse de la déformation du corps. Comme application, nous décrivons l'atténuation spatiale d'une onde propagée dans un milieu non homogène. Dans une seconde partie, notre étude porte sur une modélisation de l'indentation Vickers du verre. Nous considérons un modèle qui utilise le schéma d'inclusion d'Eshelby dans une matrice semi-infinie, pour analyser les champs de contrainte et de déplacement durant le processus de charge. L'objectif est de déterminer la densification du verre sous l'indenteur. Les résultats semi-analytiques obtenus sont confrontés de manière positive avec des données expérimentales fournies par le LARMAUR.

Abstract

In a first part, we deal with the weakly continuous media according to non Riemannian geometry. We consider a solid body modelled by a Riemannian manifold endowed with an affine connection. This model is an extension of the one which considers an Euclidean connection, which derives from the metric tensor induced by the ambiant space. The mass per volume unit may be assumed non constant and some defects, described by discontinuity fields of scalar fields or vectorial fields defined on the manifold, may appear in the body. In a such case, in addition of the metric, we necessary use the torsion introduced by Cartan or the curvature, both tensors associated with the affine connection. This corresponds to a second gradient continuum model. The investigations take into account the effects of these tensor fields on the analysis of the deformation of the body. As application, we describe the attenuation of wave propagation within a non homogeneous body. In a second part, we deal with the modelling of the Vickers indentation of glass. We consider a model which uses the schema of inclusion of Eshelby into a semi-infinite matrix, to analyse the stress and displacement fields during the loading process. The objective is to determine the densification of the glass beneath the indenter. The semi-analytical results are positively compared with experimental data which are issue from LARMAUR.

Préface

Le concept de milieu continu occupe une place essentielle dans la mécanique des solides déformables. En effet, sa simplicité (continuité des fonctions définies sur le milieu) est un point de départ pour modéliser la déformation des solides mais ce type de modélisation est souvent artificiel. Par exemple on observe dans les matériaux, à l'échelle microscopique, des micro-fissures qui accentuent la déformation, souvent irréversible, de ces matériaux. Les micro-fissures génèrent une discontinuité dans l'organisation des structures géométriques, observée en particulier dans les cristaux. On parle de dislocations lorsque ces discontinuités sont repérables dans le circuit de Burgers. À ce sujet, la description par les milieux simples de Noll, en 1958, est ainsi limitée par des phénomènes de discontinuité dans le matériau. La problèmatique suivante est de pouvoir modéliser les discontinuités en généralisant les milieux simples de Noll.

A travers les siècles, le développement des concepts mathématiques, notamment en géométrie différentielle, a fortement été stimulé pour les besoins de la mécanique. Il est courant de modéliser un corps solide par une variété différentielle et les imperfections du milieu peuvent être décrites au moyen des outils tels que le tenseur métrique (mesures des angles et distances) et ses dérivées, et la connexion affine (outil approprié pour le transport des champs tensoriels). La connexion n'est pas un tenseur mais elle définit deux tenseurs fondamentaux : la torsion et la courbure. Notre attention portera sur les travaux en géométrie différentielle de B. Riemann (1826-1866) et E. Cartan (1869-1951). Généralement dans la géométrie de Riemann, la connexion affine utilisée est celle de Levi-Civita, introduite dans le théorème fondamental de Riemann. Celle-ci dérive du tenseur métrique et la torsion associée est nulle. Un espace de Riemann est analogue à un corps (solide) décrit par un milieu continu : les outils (métrique et connexion) suffisent à décrire un point du corps et ses distances relatives par rapport à un autre point. L'analogue du tenseur de déformation en élasticité est le tenseur métrique, et le tenseur (symétrique) de contrainte est alors la réponse à une variation de la métrique. Les travaux de Cartan ont permis d'enrichir la géométrie de Riemann avec l'introduction d'une torsion non nulle. Un espace de Cartan peut être rebaptisé espace de Riemann-Cartan. Il faut cependant distinguer deux types d'approches pour étudier et modéliser les matériaux dits hétérogènes, par exemple avec des micro-fissures : l'approche riemannienne et l'approche non-riemannienne. La différence se situe dans le choix d'une torsion non nulle ou pas. Historiquement, on peut attribuer à Riemann la notion de courbure et à Cartan la notion de torsion, définies à partir de la connexion affine.

Une approche puissante de modélisation des milieux hétérogènes est le modèle des milieux de Cosserat, publié en 1909 par les frères Eugène (1866-1931) et François (1852-1914) Cosserat. Le principe de cette approche est celui de considérer un corps déformable comme un ensemble de granules (milieu continu) en mouvement les uns par rapport aux autres. Au cours du vingtième siècle, cela constitua une vision originale, une source d'inspiration pour plusieurs avancées scientifiques en mécanique des milieux continus et en science physique-mathématique des matériaux. Notamment cela fut le cas pour Cartan dans le développement de la géométrie. Un espace de Riemann-Cartan peut être réalisé par un milieu généralisé de Cosserat. Une combinaison des points de vue de Cartan et des frères Cosserat a mené à de nombreuses investigations sur les milieux hétérogènes, dont une théorie dite du gradient. Dans cette théorie, la notion de gradient est associée au tenseur de déformation (tenseur d'ordre 2). Il est courant de trouver dans la littérature la théorie du second gradient pour laquelle le gradient est associé au déplacement (tenseur d'ordre 1). Cette approche est utilisée pour décrire les imperfections du matériaux. Par exemple, en partant du circuit de Cartan, une classe de milieux faiblement continus a été introduite par Rakotomanana (1997). Le corps solide est modélisé par une variété riemannienne munie d'une métrique et d'une connexion affine compatible avec la métrique. Les discontinuités des champs scalaires et vectoriels sont définies en termes de tenseurs de torsion et de courbure associés à la connexion affine. Une telle approche, non riemannienne, nous conduit à un modèle de type second gradient. Une interaction avec les milieux de Cosserat est également établie.

Dans ce travail de thèse nous démontrons, au moyen des outils en géométrie différentielle et en analyse tensorielle, des propriétés qui concernent un modèle de type second gradient dans le cadre d'une approche non-riemannienne. Nous utilisons ensuite une version adaptée de ce type de modèle pour étudier la propagation d'ondes élastiques dans un milieu hétérogène. Pour terminer, nous nous focalisons sur l'expérience d'indentation du verre en présentant un modèle analytique qui utilise en particulier le schéma d'inclusion d'Eshelby. Ces trois contributions seront détaillées à la fin du chapitre suivant.

Notations

Chapitres 1

- $\mathcal{B}$: continuum = differential manifold / variété différentielle
- $T_M\mathcal{B}$: tangent space of $\mathcal{B}$ at M / espace tangent à $\mathcal{B}$ en M
- $\mathbf{g}$: metric / tenseur métrique
- $[\ ,\ ]$: Lie-Jacobi bracket / crochet de Lie-Jacobie
- ∇ : affine connection / connexion affine
- $\overline{\nabla}$: connection of Levi-Civita / connexion de Levi-Civita
- $\aleph$: torsion / tenseur de torsion
- $\mathfrak{R}$: curvature / tenseur de courbure
- $\mathcal{W}$: strain energy function / fonction d'énergie potentielle
- $\mathbf{E}$: strain tensor / tenseur de déformation
- $\aleph_0$: 1-form of Cartan / vecteur covariant de Cartan
- $\aleph^{\gamma}_{0\alpha\beta}$: constants of structure of Cartan / constantes de structure de Cartan

Chapitres 2

- $\mathcal{W}$: strain energy density / densité d'énergie potentielle
- $\mathcal{L}$: Lagrangean density / densité lagrangienne
- $E_{\alpha\beta}$: Green-Lagrange strain components / composantes du tenseur de déformation (Green-Lagrange)
- $g_{\alpha\beta}$: Cauchy-Green components / composantes du tenseur métrique (Cauchy-Green)
- $\Gamma^{\gamma}_{\alpha\beta}$: components of affine connection / composantes de la connexion affine
- $\overline{\Gamma}^{\gamma}_{\alpha\beta}$: components of connection of Levi-Civita / composantes de la connexion de Levi-Civita
- $\nabla^2 = \nabla \circ \nabla$: biconnection / biconnexion
- $\Gamma^{\gamma}_{\alpha\beta,\lambda} + \Gamma^{\mu}_{\alpha\beta}\Gamma^{\gamma}_{\lambda\mu}$: components of biconnection / composantes de la biconnexion
- $\aleph^{\gamma}_{\alpha\beta}$: components of torsion / composantes du tenseur de torsion
- $\mathfrak{R}^{\gamma}_{\alpha\beta\lambda}$: components of curvature / composantes du tenseur de courbure

Chapitre 3

- ρ : mass density / masse volumique
- ψ : strain energy / énergie potentielle
- λ_0, μ_0 : Lamé constants / constantes de Lamé
- c_L^2 : longitudinal velocity / vitesse longitudinale
- c_T^2 : transversal velocity / vitesse transversale
- c^2 : velocity ratio / rapport de vitesses
- σ : stress tensor / tenseur de contrainte
- ε : strain tensor in small deformations / tenseur de déformation en petites déformations
- $\mathbf{u}$: displacement vector / vecteur déplacement
- θ : angular rotation (example of Timoshenko beam) / vecteur rotation (exemple de la poutre de Timoshenko)
- $\aleph_0$ / $\tilde{\aleph}_0$: 1-form of Cartan / vecteur de Cartan
- $\aleph_1$ / $\aleph_2$: 1-form of Cartan (example of Timoshenko beam) / vecteur de Cartan (exemple de la poutre de Timoshenko)
- ω : stop-pass frequency / fréquence de coupure
- ω_n : n^{th} eigenfrequency / n-ième fréquence propre
- $\mathcal{M}$: Kummer function of first kind / fonction de Kummer de première espèce
- $\mathcal{U}$: Kummer function of second kind / fonction de Kummer de seconde espèce
- $\mathcal{J}_n$: n-order Bessel function of first kind / fonction de Bessel d'ordre n de première espèce
- $\mathcal{Y}_n$: n-order Bessel function of second kind / fonction de Bessel d'ordre n de seconde espèce

Chapitre 4

- B : characteristic of the plasticity-densification / paramètre caractéristique de la plasto-densification
- R : radius on the interface inclusion-matrix / rayon à l'interface inclusion-matrice
- p : vertical uniform pressure / pression vertical uniforme
- q : lateral uniform pressure / pression latérale uniforme
- P : load of the indenter / charge de l'indenteur
- σ^{Bo} : stress field of Boussinesq / champs de contrainte de Boussinesq
- $\mathbf{u}^{Bo}$: displacement field of Boussinesq / champs de déplacement de Boussinesq
- σ^{bl} : blister stress field / champs d'ampoule (contrainte)
- $\mathbf{u}^{bl}$: blister displacement field / champs d'ampoule (déplacement)
- h : displacement of the indenter in loading configuration / déplacement de l'indenteur en configuration de chargement
- ΔV : variation of the volume (densification) / volume densifié

Table des matières

1 Introduction générale **1**

1.1 Géométrie et mécanique . . . 2

1.1.1 Rappels en géométrie différentielle . . . 2

1.1.2 Milieu continu et limitations . . . 4

1.1.3 Introduction des milieux faiblement continus . . . 7

1.2 Champs d'application . . . 9

1.2.1 Milieux de Cosserat : présentation . . . 10

1.2.2 Théorie du gradient : exemples de lois constitutives . . . 11

1.2.3 Géométrie de Cartan et modèle de Cosserat . . . 12

1.3 Contribution du travail de thèse . . . 15

1.3.1 Invariance des champs . . . 15

1.3.2 Propagation d'onde . . . 16

1.3.3 Indentation du verre . . . 17

2 Invariance des champs dans un espace de Riemann **19**

2.1 Introduction . . . 20

2.1.1 Lagrangian function . . . 20

2.1.2 Invariance principles . . . 21

2.1.3 Objectives . . . 22

2.2 Mathematical preliminaries and framework . . . 23

2.2.1 Coordinate systems . . . 23

2.2.2 Components of tensor . . . 24

2.2.3 Affine connection . . . 25

2.2.4 Holonomic and nonholonomic transformations . . . 27

2.3 Quotient law . . . 29

2.4 Dependence with respect to the metric . . . 31

2.4.1 Metric tensor . . . 32

2.4.2 Introduction of tensors . . . 33

2.4.3 Theorem . . . 35

2.4.4 Discussion . . . 36

2.5 Invariance with respect to the connection . . . 36

2.5.1 Preliminary . . . 37

2.5.2 Application . . . 39

2.5.3 Synthesis . . . 40
2.6 Strain gradient continuum . . . 41
2.6.1 Interpretation . . . 41
2.6.2 Comparison . . . 43
2.7 Concluding remarks . . . 44

3 Propagation d'onde dans un corps hétérogène 47
3.1 Introduction . . . 48
3.2 Wave propagation equation . . . 48
3.3 Classification of waves in this non homogeneous continuum . . . 51
3.3.1 Wave orthogonal to non homogeneity . . . 51
3.3.2 Wave parallel to non homogeneity . . . 53
3.4 Thick-walled cylinder . . . 55
3.4.1 Kinematics and equation of motion . . . 55
3.4.2 Resolution for $\Delta \neq 0$ . . . 57
3.4.3 Resolution for $\Delta = 0$ . . . 60
3.4.4 Discussion on the direction of wave . . . 60
3.5 Bending of beams . . . 62
3.5.1 Kinematics and equation of motion . . . 62
3.5.2 Resolution for $\Delta_\Theta < 0$ . . . 65
3.5.3 Figures . . . 67
3.6 Discussion . . . 67
3.7 Concluding remarks . . . 73

4 Une étude analytique de l'indentation du verre 75
4.1 Présentation . . . 76
4.1.1 Indentation du verre . . . 76
4.1.2 Inclusion de type Eshelby . . . 76
4.2 Densification of glass beneath an indenter . . . 77
4.3 Models of Yoffe and mechanics of Eshelby . . . 78
4.3.1 Preliminaries . . . 78
4.3.2 Definition of defect . . . 78
4.3.3 Elasticity . . . 79
4.3.4 Plasticity and densification . . . 79
4.3.5 Bilan of defect . . . 79
4.3.6 Definition of the matrix . . . 79
4.4 Analytical results . . . 80
4.4.1 Stress field . . . 81
4.4.2 Inclusion-matrix interface . . . 82
4.4.3 Fourier's series method . . . 82
4.5 Comparison with the experimental . . . 83
4.5.1 Densification capacity . . . 84
4.5.2 Densification volume according to the load . . . 84
4.5.3 Development of the blister shape . . . 86

4.6 Conclusion 87

Conclusion générale **89**

Perspectives **91**

Appendices **93**

A Calcul indiciel **95**
A.1 Connection and tensors 95
A.2 Indentification of coefficients 96
A.3 Components of biconnection 97

B Équation des ondes **101**
B.1 Wave propagation equation 101
B.1.1 Units 101
B.1.2 Equation 101
B.2 Confluent hypergeometric equation 102
B.3 Cylinder 103
B.4 Beam 105

C Modèle d'indentation **109**
C.1 Identification of parameters 110
C.1.1 Fourier series : recalls 110
C.1.2 Approximation in Fourier series 111
C.2 Polar equations 114
C.3 Auto-similarity 116
C.4 Equations in cylindrical system 116

Liste des figures **119**

Bibliographie **121**

Chapitre 1

Introduction générale

Dans ce chapitre nous présentons une synthèse sur l'étude des milieux continus généralisés par une approche géométrique. Nous rappelons quelques définitions basées sur la théorie des variétés à connexion affine de E. Cartan (1923). Nous introduisons les limitations des milieux simples de Noll (1958) avant de présenter la notion de milieux faiblement continus introduite initialement par Rakotomanana (1997). Nous faisons le lien entre le modèle des milieux de Cosserat (1909) et des exemples de lois constitutives basées sur la théorie du second gradient. Nous terminons par indiquer dans quels contextes se situe notre travail de thèse et quels en sont les objectifs.

In this chapter we remind a synthesis of the generalized continuous media by a geometric approach. We recall some definitons of the theory on manifold endowed with an affine connection according to E. Cartan (1923). We introduce the limits of simple media according to Noll (1958) before presenting the so-called weakly continuous media introduced by Rakotomanana (1997). We deal with the link between the model of Cosserat (1909) and the elastic constitutive laws based on the strain gradient theory. Finally the context and the objectives of the thesis are mentioned.

1.1 Géométrie et mécanique

Dans cette partie nous rappelons quelques outils en géométrie différentielle, le concept de mécanique des milieux continus puis les milieux dits faiblement continus.

1.1.1 Rappels en géométrie différentielle

Considérons un espace vectoriel E de dimension quelconque et une variété différentielle $\mathcal{B}$ plongée dans E. On désigne par $T_M\mathcal{B}$ l'espace tangent en $M \in \mathcal{B}$ et un champ est une fonction (par exemple tensorielle) qui est définie localement en un point $M \in \mathcal{B}$. Puis nous introduisons deux outils essentiels : un tenseur métrique $\mathbf{g}$ et une connexion affine ∇. Nous rappelons qu'une métrique est un tenseur deux fois covariant symétrique et inversible, c'est un outil qui permet de mesurer les distances et les angles. Nous rappelons que E muni de $\mathbf{g}$, $(E, \mathbf{g})$, est un espace euclidien et que $\mathcal{B}$ muni de $\mathbf{g}$, $(\mathcal{B}, \mathbf{g})$, est une variété riemanienne. Nous définissons maintenant la connexion affine :

Définition 1.1.1 *(Connexion affine) Une connexion affine notée ∇ est définie pour deux champs de vecteurs quelconques :*

$$\nabla : (\boldsymbol{u}, \boldsymbol{v}) \in T_M\mathcal{B} \times T_M\mathcal{B} \longrightarrow \nabla_{\boldsymbol{u}}\boldsymbol{v} \in T_M\mathcal{B}, \tag{1.1.1}$$

qui admet les propriétés suivantes (λ et μ sont des scalaires, ϕ est un champ scalaire et $\boldsymbol{u}(\phi)$ est la dérivée directionnelle de ϕ dans la direction du vecteur $\boldsymbol{u}$)

$$\left\{\begin{array}{rcl} \nabla_{\lambda\boldsymbol{u}_1+\mu\boldsymbol{u}_2}\boldsymbol{v} & = & \lambda\nabla_{\boldsymbol{u}_1}\boldsymbol{v} + \mu\nabla_{\boldsymbol{u}_2}\boldsymbol{v} \\ \nabla_{\boldsymbol{u}}(\lambda\boldsymbol{v}_1 + \mu\boldsymbol{v}_2) & = & \lambda\nabla_{\boldsymbol{u}}\boldsymbol{v}_1 + \mu\nabla_{\boldsymbol{u}}\boldsymbol{v}_2 \\ \nabla_{\phi\boldsymbol{u}}\boldsymbol{v} & = & \phi\nabla_{\boldsymbol{u}}\boldsymbol{v} \\ \nabla_{\boldsymbol{u}}(\phi\boldsymbol{v}) & = & \phi\nabla_{\boldsymbol{u}}\boldsymbol{v} + \boldsymbol{u}(\phi)\boldsymbol{v} \end{array}\right. \tag{1.1.2}$$

Le champ de vecteur $\nabla_{\mathbf{u}}\mathbf{v}$ permet de calculer la valeur de $\mathbf{v}$ en un point $M \in \mathcal{B}$ transporté en un autre point $M' \in \mathcal{B}$ par le champ vectoriel $\mathbf{u}$, [18] :

$$\mathbf{v}(M') = \mathbf{v}(M) + \nabla_{\mathbf{u}}\mathbf{v}(M), \tag{1.1.3}$$

Une connexion affine induit une dérivée covariante qui généralise la notion de dérivée directionnelle dans une variété : $\nabla_{\mathbf{u}}\mathbf{v}$ est la dérivée covariante de $\mathbf{v}$ selon $\mathbf{u}$ par rapport à ∇. Plus généralement une connexion affine peut être utilisée pour décrire la variation d'un champ de tenseur sur une variété. Nous définissons maintenant le crochet de Lie-Jacobi :

Définition 1.1.2 *(Crochet de Lie-Jacobi) Le crochet de Lie-Jacobi de deux champs de vecteurs $(\boldsymbol{u}, \boldsymbol{v}) \in T_M\mathcal{B} \times T_M\mathcal{B}$ est un champ de vecteurs noté $[\boldsymbol{u}, \boldsymbol{v}]$ et défini par (ϕ est un champ scalaire) :*

$$[\boldsymbol{u}, \boldsymbol{v}](\phi) = \boldsymbol{u}\boldsymbol{v}(\phi) - \boldsymbol{v}\boldsymbol{u}(\phi), \tag{1.1.4}$$

$\boldsymbol{u}\boldsymbol{v}$ est la dérivée de Lie de $\boldsymbol{u}$ par rapport à $\boldsymbol{v}$, et $\boldsymbol{v}\boldsymbol{u}$ est la dérivée de Lie de $\boldsymbol{v}$ par rapport à $\boldsymbol{u}$.

Le crochet de Lie-Jacobi est un vecteur (tenseur d'ordre 1) mais la connexion affine n'est pas un tenseur. On désigne par $(T_M\mathcal{B})^*$ le dual de $T_M\mathcal{B}$ et on définit deux tenseurs associés à la connexion affine : la torsion et la courbure.

Définition 1.1.3 *(Torsion) La torsion notée $\aleph$ est un tenseur d'ordre 3 défini pour $(\boldsymbol{u}, \boldsymbol{v}, \omega) \in T_M\mathcal{B} \times T_M\mathcal{B} \times (T_M\mathcal{B})^*$:*

$$\aleph(\boldsymbol{u}, \boldsymbol{v}, \omega) = \omega\left(\nabla_{\boldsymbol{u}}\boldsymbol{v} - \nabla_{\boldsymbol{v}}\boldsymbol{u} - [\boldsymbol{u}, \boldsymbol{v}]\right) \tag{1.1.5}$$

Définition 1.1.4 *(Courbure) La courbure notée $\mathfrak{R}$ est un tenseur d'ordre 4 défini pour $(\boldsymbol{u}, \boldsymbol{v}, \boldsymbol{w}, \omega) \in T_M\mathcal{B} \times T_M\mathcal{B} \times T_M\mathcal{B} \times (T_M\mathcal{B})^*$:*

$$\mathfrak{R}(\boldsymbol{u}, \boldsymbol{v}, \boldsymbol{w}, \omega) = \omega\left(\nabla_{\boldsymbol{u}}\nabla_{\boldsymbol{v}}\boldsymbol{w} - \nabla_{\boldsymbol{v}}\nabla_{\boldsymbol{u}}\boldsymbol{w} - \nabla_{[\boldsymbol{u},\boldsymbol{v}]}\boldsymbol{w}\right) \tag{1.1.6}$$

La Figure (1.1.1) qui suit, adaptée de [40], donne un interprétation géométrique de la dérivée covariante (au sens de la connexion affine), du crochet de Lie-Jacobi et de la torsion. Une interprétation en mécanique des milieux continus de la torsion et de la

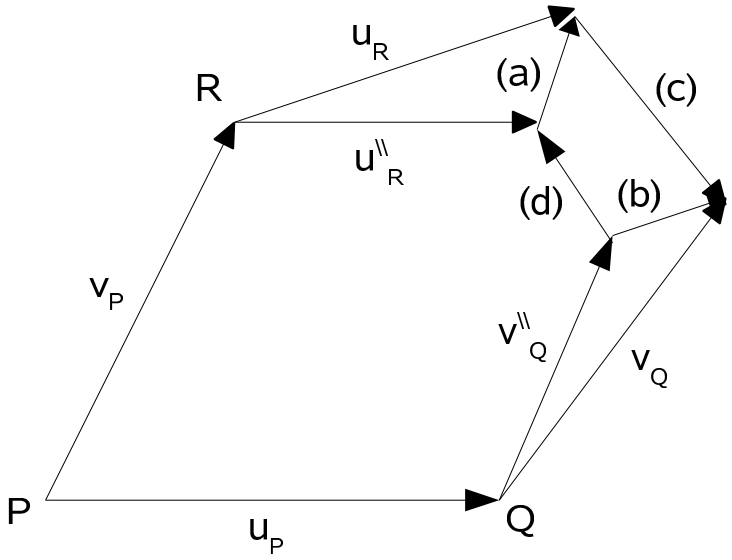

FIG. 1.1.1 – Interprétation géométrique de la torsion : Deux champs de vecteurs $\mathbf{u}$ et $\mathbf{v}$. De tout point P, le transport parallèle de $\mathbf{u}$ et $\mathbf{v}$ le long de $\mathbf{v}$ ou $\mathbf{u}$ donne respectivement $\mathbf{u}_R^{||}$ et $\mathbf{v}_Q^{||}$. (a) $= \nabla_{\mathbf{v}}\mathbf{u}$, (b) $= \nabla_{\mathbf{u}}\mathbf{v}$, (c) $= [\mathbf{u}, \mathbf{v}]$ et (d) $= \aleph(\mathbf{u}, \mathbf{v})$. Cf [40].

courbure sera donnée plus loin.

La métrique $\mathbf{g}$ est imposée par l'espace ambiant E mais il y a une infinité de choix pour la connexion affine ∇.

Définition 1.1.5 *(Connexion compatible) Une connexion affine est compatible avec la métrique si $\nabla_{\boldsymbol{w}}[g(\boldsymbol{u}, \boldsymbol{v})] = 0$ pour tout champ de vecteurs $\boldsymbol{u}$, $\boldsymbol{v}$, $\boldsymbol{w}$. On note $\nabla \boldsymbol{g} = 0$.*

Nous rappelons le théorème suivant :

Théorème 1.1.1 *(Théorème fondamental en géométrie riemanienne) Dans tout variété riemanienne $(\mathcal{B}, g)$, il existe une unique connexion affine compatible avec la métrique et à torsion nulle. Cette connexion est appelée la connexion de Levi-Civita et notée $\overline{\nabla}$: $\overline{\nabla}\boldsymbol{g} = 0$, $\aleph_{\overline{\nabla}} = 0$. [18]*

Définition 1.1.6 *Soit une variété riemanienne $\mathcal{B}$ muni d'une connexion affine compatible, [74] :*

- $\boldsymbol{g} = cst$ *($\nabla\boldsymbol{g} = 0$), $\aleph = 0$, $\mathfrak{R} = 0$: $\mathcal{B}$ est un espace euclidien (equivalence affine avec E).*
- $\nabla\boldsymbol{g} = 0$, $\aleph = 0$, $\mathfrak{R} = 0$ *ou* $\mathfrak{R} \neq 0$ *: $\mathcal{B}$ est un espace de Riemann (connexion de Levi-Civita).*
- $\nabla\boldsymbol{g} = 0$, $\aleph \neq 0$, $\mathfrak{R} = 0$ *ou* $\mathfrak{R} \neq 0$ *: $\mathcal{B}$ est un espace de Cartan.*

Par abus de langage, une variété riemanienne, c'est à dire muni d'une métrique, et muni d'une connexion affine mais qui n'est pas compatible avec la métrique est appelée un espace non-riemanien. Dans la suite, nous aurons à distinguer le "cas riemanien" du "cas non-riemanien" dans les différentes approches de modélisation des milieux continus. Ce qui distingue ces deux cas est le fait de considérer ou pas une torsion nulle.

1.1.2 Milieu continu et limitations

En mécanique des solides, un corps $\mathcal{B}$ est un ensemble de particules ou points matériels. On identifie chaque point matériel $M \in \mathcal{B}$ avec la position $\mathbf{X}$ du point de l'espace qu'il occupe à un instant $t_0 \in \mathbb{R}$. Ceci revient à identifier le corps solide avec la région de l'espace qu'il occupe. Cette région est appelée configuration : la configuration initiale est notée $\mathcal{B}_0$. Cependant par abus de langage, on parlera de point matériel appartenant au corps : $\mathbf{X} \in \mathcal{B}$.

La position actuelle $\mathbf{x}$, à l'instant t, de chaque point matériel est définie par la fonction vectorielle

$$\varphi : (\mathbf{X}, t) \in \mathbb{R}^3 \times \mathbb{R} \longrightarrow \mathbf{x} = \varphi\,(\mathbf{X}, t) \in \mathbb{R}^3. \tag{1.1.7}$$

Cette fonction, en général non linéaire, est appelée le mouvement du corps $\mathcal{B}$. Le mouvement correspond à la transformation par φ d'un point du corps. Un milieu continu est un modèle de domaine matériel (solides, fluides,...) dans lequel les propriétés physiques sont supposées varier d'une manière continue d'un point à un autre. En particulier, la distribution de la masse est supposée varier d'une manière continue. Les deux hypothèses de continuité du mouvement (unité du corps) $\varphi \in \mathcal{C}^0$ et $\varphi^{-1} \in \mathcal{C}^0$ sont à l'origine du concept du milieu continu. L'étude d'une transformation quelconque φ, non linéaire dans la plupart des cas, d'un milieu continu, est fondée sur l'analyse locale du mouvement relatif de deux points voisins $\mathbf{X}$ et $\mathbf{X} + d\mathbf{X}$. La continuité du mouvement impose que ces deux points matériels voisins ($\mathbf{X} + d\mathbf{X}$ appartient à une boule de centre $\mathbf{X}$ et d'un certain rayon τ) restent voisins tout au long du mouvement de $\mathcal{B}$. À l'inverse, deux particules voisines dans la configuration actuelle étaient nécessairement voisines dans la configuration

initiale. Dans ce cas, on peut écrire la dérivée directionnelle

$$\varphi\ (\mathbf{X} + d\mathbf{X}, t) = \varphi\ (\mathbf{X}, t) + \nabla\varphi\ (\mathbf{X}, t)[d\mathbf{X}] + \mathcal{O}(\|d\mathbf{X}\|), \tag{1.1.8}$$

dans laquelle en posant $d\mathbf{x} := \varphi\ (\mathbf{X} + d\mathbf{X}, t) - \varphi\ (\mathbf{X}, t)$, on peut définir le gradient de la transformation $\mathbf{F} := \nabla\varphi(\mathbf{X}, t)$ (transformation linéaire tangente) :

$$\mathbf{F} : (d\mathbf{X}, t) \in \mathbb{R}^3 \times \mathbb{R} \longrightarrow d\mathbf{x} = \mathbf{F}(d\mathbf{X}, t) \in \mathbb{R}^3. \tag{1.1.9}$$

On dit qu'une fibre matérielle $d\mathbf{X}$ dans la configuration initiale est transformée, par $\mathbf{F}$, en la fibre $d\mathbf{x}$ dans la configuration actuelle. Un milieu fortement continu répond à la définition $\mathbf{F} \in \mathcal{C}^0$ et $\mathbf{F}^{-1} \in \mathcal{C}^0$, c'est à dire $\varphi \in \mathcal{C}^1$ et $\varphi^{-1} \in \mathcal{C}^1$ (unité et régularité du corps). Tout cela est schématisé par la Figure (1.1.2).

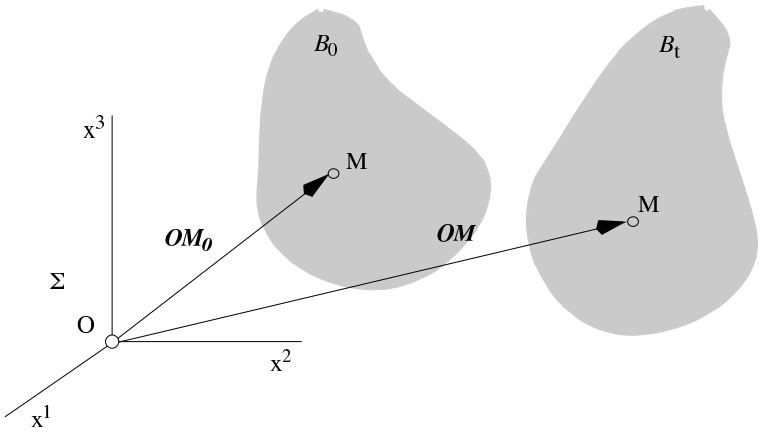

FIG. 1.1.2 – Transformation d'un point $\mathbf{M}$ par φ et d'une fibre $\mathbf{OM}$ par $\nabla\varphi$. Cf [75]

Cette description est relative aux milieux simples de Noll (1958). Un milieu (corps matériel dans une configuration de référence) est dit uniforme au sens de Noll-Truesdell si pour toute paire de points matériels il existe un isomorphisme matériel entre ces points (voisinages). Le milieu est dit homogène au sens de Noll-Truesdell s'il existe une configuration pour laquelle tous les isomorphismes matériels sont égaux à l'identité. L'intérêt de ces définitions, que l'on peut trouver dans [23], est de pouvoir considérer les lois constitutives localement autour d'un seul point matériel. Par conséquent, on peut par exemple dire que pour un milieu uniforme la densité de masse est continue dans la configuration de référence, et que pour un milieu homogène il existe une configuration dans laquelle la densité de masse est la même en tout point. La notion d'uniformité se base sur une configuration donnée du milieu, tandis que celle d'homogénéité décrit la capacité du corps à se retrouver dans un état particulier. Pour la suite (chapitre 3) nous utiliserons les termes d'uniformité et d'homogénéité sans faire référence à ceux introduits par Noll-Truesdell.

Cependant, on est confronté rapidement à l'insuffisance du milieu simple : les microfissurations. La motivation est à la fois physique et mathématique. En effet du point

de vue mathématique, si la transformation $\varphi \in \mathcal{C}^1$ et $\varphi^{-1} \in \mathcal{C}^1$ presque partout, nous sommes en présence de milieux dits faiblement continus, dont nous allons étendre la définition. À titre d'exemple un solide purement élastique sans fissures est considéré comme un milieu fortement continu, tandis qu'un solide plastique emdommagé représente un milieu faiblement continu. Des informations sur φ nous parviennent après confrontation des configurations initiale et actuelle du milieu. À l'échelle macroscopique, une même transformation peut induire deux formes différentes $\varphi_1 \neq \varphi_2$, comme on peut le constater dans la Figure (1.1.3). Nous distinguons ainsi une transformation holonome à celle non holonome.

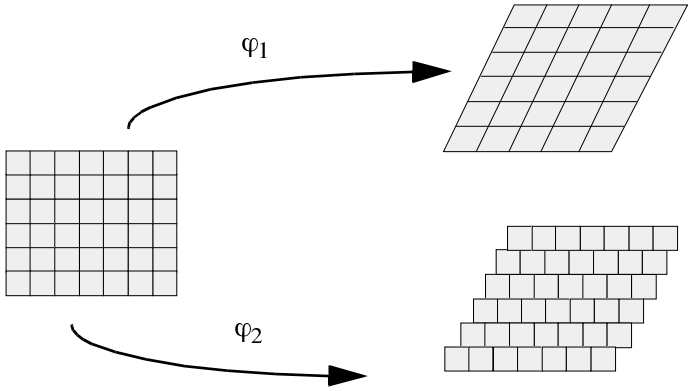

FIG. 1.1.3 – Déformations d'un solide : transformation holonome φ_1, transformation non-holonome φ_2. Cf [74]

Le milieu continu est modélisé de manière naturelle par une variété riemannienne $\mathcal{B}$ munie d'une métrique $\mathbf{g}$ et d'une connexion affine ∇ déduite du tenseur métrique (connexion euclidienne). Une généralisation possible de ces milieux continus consiste à considérer les connexions qui ne dérivent pas du tenseur métrique (induit par l'espace ambiant), dont le tenseur de torsion et le tenseur de courbure associés ne sont pas nécessairement nuls. Dans notre travail, nous aurons à considérer une connexion non euclidienne mais compatible avec la métrique (rappel : $\nabla \mathbf{g} = 0$). Le milieu continu généralisé est appelé un "continuum" e.g. [61].

Les deux tenseurs de torsion et de coubure modélisent les champs de dislocations et de disclinations de Volterra. Au début du vingtième siècle, les travaux du mathématicien Volterra sur la structure cristalline a fait naître la notion de dislocation. La construction dite "de Volterra" permet de créer formellement une dislocation, laquelle est un défaut linéaire correspondant à une discontinuité dans l'organisation de la structure cristalline. Une dislocation angulaire est plus communément appelée une disclination. Une dislocation peut être vue simplement comme un "quantum" de déformation élémentaire au sein d'un cristal possédant un champ de contrainte à longue distance. Elle est caractérisée par la direction de sa ligne et par un vecteur appelé "vecteur de Burgers" dont la norme représente l'amplitude de la déformation qu'elle engendre. Le vecteur de Burgers se dé-

finit comme étant le vecteur nécessaire pour boucler un circuit initialement fermé dans le cristal parfait et qui se trouve ouvert lorsqu'il enlace la ligne de dislocation (Figure (1.1.4)). Ce vecteur n'est pas quelconque dans un cristal mais représente une translation du réseau et physiquement, le vecteur de Burgers représente l'amplitude de la déformation transportée par une dislocation. Les dislocations de Volterra sont résumées sur la

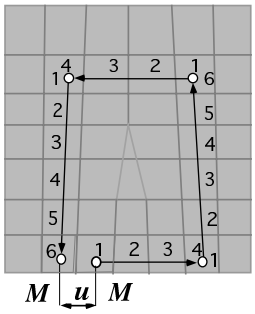

FIG. 1.1.4 – Circuit de Burgers dans un cristal. Cf [74]

Figure (1.1.5). À titre d'application, les dislocations peuvent aussi être engendrées à la suite d'un processus expérimental connu sous le nom d'indentation, pour lequel nous avons consacré un chapitre.

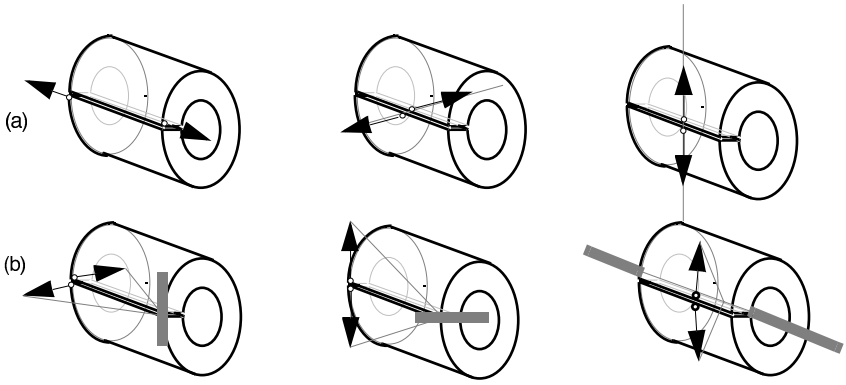

FIG. 1.1.5 – Dislocations de Volterra : (a) Translations relatives de deux surfaces (lèvres du cylindre). (b) Rotations relatives de deux surfaces (disclinations). Cf [74]

1.1.3 Introduction des milieux faiblement continus

Dans un milieu faiblement continu, la répartition de la matière est supposée continue mais des discontinuités des champs scalaires et vectoriels peuvent apparaître. Cette répartition de discontinuités dans la matière est continue et en nombre suffisament grand pour en admettre une répartition volumique. Parmi les champs scalaires on peut rescenser la

densité de masse et la température, parmi les champs vectoriels on recense entre autres la vitesse. On observe, à une certaine échelle, des discontinuités dans l'organisation des structures matérielles (micro-fissures, décohésions intragranulaires,...). Ces phénoménes de discontinuités ont été modélisés, via la géométrie différentielle, en généralisant les milieux simples de Noll. L'outil géométrique est basé dans ce cas sur les travaux de Riemann.

Il y a l'approche non-riemannienne. La modélisation des matériaux à discontinuités avec la géométrie non riemanienne se situe dans les travaux de Bilby [8] (1955), Kondo [48] (1955) et Kröner [49], [50] (1963, 1981). Sur le concept de connexion matérielle, la même année 1967, Noll introduit la notion de corps matériel uniforme simple et Wang les champs en mécanique des milieux continus. En se basant sur la structure cristalline et les matériaux simples, Noll [69] (1967) et Wang [85] (1967) ont défini les inhomogénéités d'un milieu (densité de discontinuités) au moyen des tenseurs de courbure et de torsion des connexions matérielles. Puis Edelen et Lagoudas [20] (1988) et Maugin [61] (1993) ont associé la géométrie des discontinuités et les équations de structure de Cartan [14], pour modéliser les dislocations dans les solides. Plus récemment dans l'étude de la structure cristalline, Le et Stumpf [55], [56] (1996) ont développé le concept de cristal de référence ("crystal reference") basés sur le tenseur métrique pour la modélisation des déformations élastiques et basés sur la connexion ("the crystal connection") pour la capture des dislocations. Ils ont montré que l'intégrabilité des lois consitutives requiert la nullité de la courbure associée à la connexion ("the crystal connection").

Dans la même voie que [20] et [61], Rakotomanana [73] (1997) a introduit une classe de milieux faiblement continus dont les champs de discontinuités scalaires et vectoriels sont définis à partir de torsion et de courbure non nulles. Lorsque la transformation est faiblement continue (rappel : $\varphi \in \mathcal{C}^1$ et $\varphi^{-1} \in \mathcal{C}^1$ presque partout), l'existence de surfaces de glissement ou dislocations est possible. Pour quantifier cette continuité faible, nous adoptons un schéma classique dû à Cartan [14] en suivant un champ scalaire θ (puis un champ vectoriel $\mathbf{w}$) suivant deux chemins sur le milieu continu issus d'un même point $M \in \mathcal{B}$ et se rejoignant à un autre point dont les directions sont données par deux séries de courbes intégrales de deux champs de vecteurs $\mathbf{u}_1$ et $\mathbf{u}_2$ (Figure (1.1.6)).

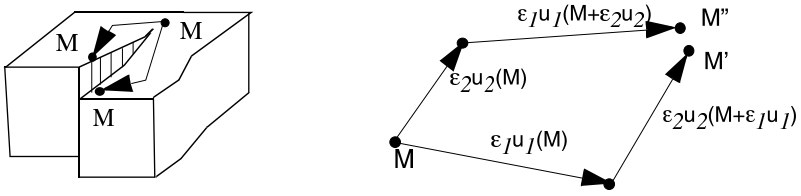

FIG. 1.1.6 – Circuit de Cartan. Cf [73]

Le principe de base est de calculer la variation de θ en posant

$$\theta' = \theta(M') - \theta(M), \qquad \theta'' = \theta(M'') - \theta(M) \tag{1.1.10}$$

Nous établissons :

$$\lim_{\varepsilon_1,\varepsilon_2\to 0} \frac{\theta'' - \theta'}{\varepsilon_1\varepsilon_2} = \theta[\aleph(\mathbf{u}_1, \mathbf{u}_2)] \tag{1.1.11}$$

Si la valeur prise par un champ scalaire θ défini sur $\mathcal{B}$ dépend du chemin choisi alors le champ du tenseur de torsion dans $\mathcal{B}$ est non nul et caractérise le saut subi par ce champ scalaire selon (1.1.11).

Puis, pour calculer la variation de $\mathbf{w}$, on pose

$$\mathbf{w}' = \mathbf{w}(M') - \mathbf{w}(M), \qquad \mathbf{w}'' = \mathbf{w}(M'') - \mathbf{w}(M) \tag{1.1.12}$$

Pour un champ scalaire arbitraire ω, nous établissons :

$$\lim_{\varepsilon_1,\varepsilon_2\to 0} \frac{\omega(\mathbf{w}'') - \omega(\mathbf{w}')}{\varepsilon_1\varepsilon_2} = \mathfrak{R}(\mathbf{u}_1, \mathbf{u}_2, \mathbf{w}, \omega) - \omega[\nabla_{\aleph(\mathbf{u}_1,\mathbf{u}_2)}\mathbf{w}] \tag{1.1.13}$$

Si la valeur prise par un champ vectoriel $\boldsymbol{w}$ défini sur $\mathcal{B}$ dépend du chemin choisi alors le champ du tenseur de torsion ou de courbure dans $\mathcal{B}$ sont non nuls et caractérisent le saut subi par ce champ vectoriel selon (1.1.13).

Les démonstrations sont dans [73]. Ces théorèmes établissent une interprétation de la torsion et de la courbure, en termes de discontinuités scalaires et vectorielles dans le continuum $\mathcal{B}$. La torsion $\aleph(\mathbf{x}, t)$ mesure seule le champ de discontinuités d'un scalaire, dont les dislocations. La courbure $\mathfrak{R}(\mathbf{x}, t)$ et la torsion mesurent le champ de discontinuités d'un vecteur, dont les disclinations. Le continuum $\mathcal{B}$ à connexion affine est affinement équivalent à l'espace ambiant euclidien E (corps de référence dépourvu de discontinuité) si et seulement si les champs de torsion et de courbure associés à la connexion sont identiquement nuls en tout point. Les discontinuités sont donc modélisées en introduisant la connexion affine comme variable indépendante en plus du tenseur métrique et sont entièrement capturées par la torsion et la courbure associées à cette connexion affine.

Il y a aussi l'approche riemannienne, qui consiste à utiliser les variétés riemaniennes relatives aux espace de Riemann (voir définition 1.1.6), comme supports géométriques des milieux et introduire des lois constitutives complexes, par exemple [56]. Cependant l'utilisation d'une telle variété riemannienne, à fortiori euclidienne (sans torsion et courbure), peut dès lors exclure la possibilité de modéliser les champs de discontinuités scalaires et vectoriels, compte tenu de l'approche non-riemannienne qui vient d'être présentée ci-dessus. Par exemple, la connexion de Levi-Civita (sans torsion) n'est ainsi pas adaptée pour modéliser les discontinuités des champs scalaires d'un milieu faiblement continu.

1.2 Champs d'application

Nous commencerons par présenter le modèle des milieux de Cosserat, introduit à l'origine au début du vingtième siècle par les frères Cosserat. Puis nous présenterons quelques exemples de lois contitutives basées sur la théorie dite du second gradient, leurs champs d'application et le lien avec le modèle Cosserat.

1.2.1 Milieux de Cosserat : présentation

Les milieux dits de Cosserat tirent leur nom des frères Cosserat (Eugène et François), suite à la parution à Paris en 1909 du livre intitulé "Théorie des corps déformables" [19]. Au cours du vingtième siècle, et surtout à partir de la deuxième moitié, la vision originale des deux frères Cosserat a inspiré plusieurs avancées scientifiques en mécanique des milieux continus et en science physique-mathématique des milieux matériels. Ils introduisirent un modèle de continuum avec un champ de rotation comme variable indépendante, en plus du champ de déplacement.

Considérons un référentiel galiléen Σ et un autre Σ' en mouvement à vitesse constante $\mathbf{v}_0$ par rapport à Σ. Le groupe fondamental de Galilée relatif à Σ et Σ' est un ensemble de transformations incluant les rotations $\mathbf{Q}$ et la vitesse $\mathbf{v}_0$. Les deux référentiels Σ et Σ' peuvent être associés à deux voisinages de points $\mathbf{x}$ et $\mathbf{x} + d\mathbf{x}$ de l'espace. On appelle microcosme l'ensemble d'un point et de son groupe de Galilée local : $\{\mathbf{x}, \mathbf{Q}, \mathbf{v}_0\}$. Le nom "microcosme" est du à Gonseth [34]. L'ensemble des microcosmes est un milieu de Cosserat. Physiquement un milieu de Cosserat est un ensemble de microstructures en mouvement les unes par rapport aux autres : rotation rigide (9 paramètres) et vitesse constante (3 paramètres). Chaque microcosme constitue un milieu continu avec sa propre métrique.

Nous rappelons qu'en mécanique des solides les variables fondamentales qui interviennent dans les lois consitutives sont le vecteur déplacement noté $\mathbf{u}$, le tenseur de contrainte (stress tensor) noté σ et le tenseur de déformation (strain tensor) noté $\mathbf{E}$ ou ε en petites déformations. Nous nous référons maintenant à [40]. Dans la théorie de l'élasticité classique, le vecteur déplacement $\mathbf{u}$ permet seul de définir la déformation. Dans un milieu de Cosserat, le mouvement de rotation des microstructures doit être pris en compte. On introduit alors deux tenseurs de déformation généralisée. Un tenseur d'ordre 2 noté β que l'on appelle "distortion" (distorsion)

$$\beta = \nabla \mathbf{u} - \omega \tag{1.2.1}$$

et un tenseur d'ordre 3 noté κ que l'on appelle "contortion" (contorsion)

$$\kappa = \nabla \omega \tag{1.2.2}$$

où ∇ est la connexion affine, $\mathbf{u}$ est le vecteur déplacement et ω est le bivecteur rotation associés au mouvement d'une microstructure. Si $\mathcal{H}$ représente l'énergie potentielle élastique, alors la contrainte de force noté Σ est définie par

$$\Sigma = \delta\mathcal{H}/\delta\beta \tag{1.2.3}$$

qui est un tenseur d'ordre 2. En petites déformations, nous identifions le tenseur de déformation élastique ε comme la partie symétrique[1] de β et le tenseur de contrainte σ comme la partie symétrique de Σ :

$$\varepsilon = \beta_{(\mathcal{S})}, \qquad \sigma = \Sigma_{(\mathcal{S})} \tag{1.2.4}$$

[1] La symétrie concerne ici la permutation des deux indices covariant (ou contravariant) du tenseur d'ordre 2.

Le mouvement de rotation dans un milieu de Cosserat, induit une nouvelle variable que l'on appelle (en anglais) "the spin moment stress" défini par

$$\tau = \delta\mathcal{H}/\delta\kappa \tag{1.2.5}$$

qui est un tenseur d'ordre 3. Finalement les variables (Σ, τ) caractérisent un milieu de Cosserat ("Cosserat continuum"). Les équations d'équilibre corespondantes sont les suivantes :

$$\nabla\Sigma + \mathbf{f} = 0, \qquad \nabla\tau - \Sigma_{(\mathcal{A})} + \mathbf{m} = 0 \tag{1.2.6}$$

où $\mathbf{f}$ et $\mathbf{m}$ représentent respectivement forces et moments de volume et $\Sigma_{(\mathcal{A})}$ est la partie antisymétrique de Σ. En élasticité classique $\tau = 0$ et $\mathbf{m} = 0$: d'une part $\mathcal{H}$ ne dépend pas de κ et d'autre part, via la deuxième équation, la contrainte est symétrique et notée tout simplement σ. Par conséquent, en petites déformations, la distorsion est aussi symétrique et notée ε. Il s'agit alors d'un modèle avec une loi constitutive qui dépend uniquement d'une déformation définie à partir du déplacement.

1.2.2 Théorie du gradient : exemples de lois constitutives

Pour établir les lois constitutives, le choix d'une fonction d'énergie potentielle, associée à un matériau élastique, élasto-plastique ou plastique, doit être fait. En élasticité, la loi de Hooke fait intervenir la fonction d'énergie potentielle $\mathcal{W} = \mathcal{W}(\mathbf{E})$ (ou densité d'énergie potentielle) qui dépend uniquement du tenseur de déformation $\mathbf{E}$. Au début des années 60, Toupin [81] et Mindlin [63] ont proposé une théorie adaptée pour les matériaux élastiques et connue sous le nom universel "strain gradient theory" (théorie du gradient de déformation), qui, de manière générale, introduit le gradient du tenseur de déformation comme variable supplémentaire dans la forme de l'énergie. Puis en 1965, Mindlin [65] introduit la notion de "second strain gradient theory" en élasticité linéaire, dans laquelle l'énergie est aussi fonction du second gradient de déformation. S'appuyant notamment sur les travaux de Toupin [81] et Mindlin [64], Germain [32] présente en 1973 une théorie du second gradient (premier gradient de déformation) à travers des investigations sur la méthode des puissances virtuelles en mécanique des milieux continus. Fin des années 90 et début des années 2000, la théorie du gradient se retrouve dans les travaux de Hutchinson et Fleck [28], [29], ceux de Nix, Gao et al. [30], [38], et ceux de Cermelli et Gurtin [15]. Ces investigations traitent essentiellement du comportement d'un matériau non purement élastique. La plupart des fonctions d'énergie introduites (voir [86]) dérivent du potentiel originel proposé par Mindlin [63]. Le gradient est généralement associé à la dérivation partielle par rapport aux coordonnées rectilignes, mais on trouve une description en coordonnées curvilignes dans [87], pour lequel on utilise la dérivée covariante au sens de Levi-Civita. L'introduction du gradient des variables dans les fonctions d'énergie prend en compte la présence de défauts dans le milieu continu ambiant, telles les dislocations et disclinations précédemment mentionnées. Les théories des milieux élastiques ou élasto-plastiques ont été développées en prenant en compte les dislocations et disclinations soit dans le cadre du "strain gradient theory" e.g. Gutkin et Aifantis [36], Le et Stumpf [56] ou

dans le cadre des connexions affines avec torsion e.g. Lazar [51], Noll [69], Rakotomanana [73], Wang [85].

Dans la suite, un milieu hétérogène sera défini comme un milieu faiblement continu (avec une répartition continu de défauts). Pendant plusieurs années, les milieux de Cosserat ont été utilisés pour modéliser des matériaux hétérogènes e.g. [27]. En utilisant des méthodes d'homogénéisation et d'analyse asymptotique, le modèle Cosserat a permis d'obtenir des propriétés effectives sur les matériaux hétérogènes. Une des extensions du modèle inclut la micro-inertie de chaque point matériel et a été rebaptisée milieu micropolaire ("micropolar continuum") par Eringen [22]. Dans un milieu micropolaire, la déformation est décrite au moyen du vecteur déplacement et d'un vecteur indépendant pour la rotation. Cette propriété rapproche les milieux micropolaires au modèle des milieux de Cosserat. Une extension des milieux micropolaires mène aux milieux micromorphes ("micromorphic continuum"), pour lesquels la déformation inclut une déformation macroscopique et un changement microscopique de la structure interne. Les modèles micropolaires élastiques à gradient ont ainsi été utilisés pour étudier les dislocations et disclinations et constituent de récents exemples de milieux micromorphes. Des exemples de milieux micropolaires sont donnés à la suite. Ils existent des approches en élasticité avec dislocations qui utilisent une densité d'énergie potentielle dépendant uniquement du tenseur de déformation et de son gradient e.g. [53]. Et ils existent des travaux qui exploitent la théorie des micro-couples en élasticité, e.g. [58] pour lequel l'énergie dépend également du gradient de déformation exprimé au moyen de gradient de rotation. Dans les travaux de Lazar, Maugin et Aifantis [54] on définit le tenseur de déformation comme la partie symétrique de la distorsion initialement introduite pour les milieux de Cosserat et la fonction d'énergie dépend en plus du gradient et du second gradient de la déformation. Dans les travaux de Lazar et Maugin [52], on définit un tenseur supplémentaire "wryness", définit comme la contorsion de Cosserat mais avec le vecteur rotation, ce qui en fait un tenseur d'ordre 2. Les deux variables (distorsion et "wryness") et leurs dérivées premières sont les arguments de la fonction d'énergie : nous avons une dépendance de gradient (au plus d'ordre 1) des arguments. Des études sur la dépendance par rapport aux gradients (d'ordre supérieur) des arguments de l'énergie seront faites dans le prochain chapitre.

1.2.3 Géométrie de Cartan et modèle de Cosserat

Le livre des frères Cosserat fut une source d'inspiration pour E. Cartan [13] pour la conception d'un modèle incluant le tenseur métrique qui mesure les changements de forme du continuum et la connexion affine pour pouvoir dériver les champs de tenseurs définis sur le continuum. Un concept qui utilise la connexion affine ∇, fut imaginé par Cartan pour pouvoir joindre deux microcosmes dans un milieu de Cosserat. Pour un champ de vecteurs

$$\mathbf{v}_0(\mathbf{x} + d\mathbf{x}) = \mathbf{v}_0(\mathbf{x}) + \nabla_{d\mathbf{x}}\mathbf{v}_0(\mathbf{x}), \tag{1.2.7}$$

et pour un champ de tenseurs

$$\mathbf{Q}(\mathbf{x} + d\mathbf{x}) = \mathbf{Q}(\mathbf{x}) + \nabla_{d\mathbf{x}}\mathbf{Q}(\mathbf{x}). \tag{1.2.8}$$

Une déformation dite non-holonome a lieu lorsque la variété, qui modélise le corps matériel, n'est plus affinement équivalente à l'espace ambiant euclidien. Les approches théoriques en géométrie s'ensuivent e.g. [61], [69], [85]. Le circuit de Cartan est utilisé par Kondo, Bilby et al. [9] et ceux de Kröner [72] dans l'objectif d'approfondir la modélisation d'une distribution continue de dislocations et disclinations. Une autre approche introduit des tenseurs relatifs aux dislocations ("geometrically necessary dislocations") e.g. [56]. Puis l'introduction d'une classe de milieux hétérogènes a été proposée par Rakotomanana [73] qui, on le rappelle, utilise torsion et courbure pour décrire les discontinuités des champs. L'introduction de la torsion comme variable cinématique supplémentaire pour le modèle peut être considérée comme une extension d'un modèle de Cosserat et plus généralement en physique et mécanique relativiste e.g. [40].

On rappelle qu'un continuum $\mathcal{B}$ est un ensemble de points matériels M modélisé par une variété. L'espace tangent (en M) est noté $T_M\mathcal{B}$. La déformation de $\mathcal{B}$ est une fonction φ qui transforme la configuration initiale $\mathcal{B}_0$ en la configuration actuelle (déformée) $\mathcal{B}$. Le point $M \in \mathcal{B}$ est localisé par $\mathbf{OM} = \varphi(\mathbf{OM}_0)$ et la différentielle $\mathbf{F} = d\varphi$ transforme un vecteur de l'espace tangent $\mathbf{f} = d\varphi(\mathbf{f}_0)$. Si nous considérons une base tangente locale $(\mathbf{f}_{01}, \mathbf{f}_{02}, \mathbf{f}_{03}) \in T_{M_0}\mathcal{B}_0$, alors la déformée est $(\mathbf{f}_1, \mathbf{f}_2, \mathbf{f}_3) \in T_M\mathcal{B}$

$$(\mathbf{f}_{01}, \mathbf{f}_{02}, \mathbf{f}_{03}) \longrightarrow (\mathbf{f}_1, \mathbf{f}_2, \mathbf{f}_3) \tag{1.2.9}$$

telle que $\mathbf{f}_a = d\varphi(\mathbf{f}_{0a})$. Pour une transformation holonome (Figure (1.1.3)), la déformation de $\mathcal{B}$ est définie à partir d'une connexion euclidienne notée $\overline{\nabla}$ qui dérive du tenseur métrique $\mathbf{g}$[2]. Et avec le vecteur déplacement $\mathbf{u}$ on définit le gradient de déformation $\mathbf{F} = \mathbb{I} + \overline{\nabla}\mathbf{u}$. Le tenseur métrique de l'espace ambiant est calculé par, e.g. [75],

$$\mathbf{g} = \mathbb{I} + \overline{\nabla}\mathbf{u} + \overline{\nabla}^T\mathbf{u} + \overline{\nabla}^T\mathbf{u}\overline{\nabla}\mathbf{u}. \tag{1.2.10}$$

Le tenseur de déformation noté $\mathbf{E}$ est défini par

$$\mathbf{E} = (1/2)(\overline{\nabla}\mathbf{u} + \overline{\nabla}^T\mathbf{u} + \overline{\nabla}^T\mathbf{u}\overline{\nabla}\mathbf{u}). \tag{1.2.11}$$

Le tenseur métrique $\mathbf{g} = \mathbb{I} + 2\mathbf{E}$ est couramment appelé le tenseur de déformation de Cauchy-Green. Nous pouvons ainsi assimiler la métrique avec le tenseur de déformation utilisé en mécanique. Pour des petites déformations, le tenseur de Cauchy noté ε est lié à la partie linéaire de la métrique (ou du tenseur de déformation) :

$$\varepsilon = (1/2)(\overline{\nabla}\mathbf{u} + \overline{\nabla}^T\mathbf{u}). \tag{1.2.12}$$

En présence d'une transformation non holonome (Figure (1.1.3)), il n'est plus possible de décrire la déformation du continuum uniquement avec la métrique (ou le tenseur de déformation). Le continuum n'est plus affinement équivalent à l'espace ambiant. Ainsi le tenseur de déformation ε est plus difficile à déterminer, puisque la connexion affine, qui est l'outil géométrique de dérivation, prend la forme suivante :

$$\nabla = \overline{\nabla} + \nabla^{inh}, \tag{1.2.13}$$

[2] La métrique est imposée par l'espace ambiant. La connexion euclidienne qui en dérive fut celle utilisée en mécanique pendant plus de deux siècles.

où ∇^{inh} ("inh" pour inhomogénéités) n'est pas symétrique par rapport aux indices covariant[3], [40], [68] (la torsion définie avec ∇ n'est donc pas nulle). La cinématique d'un milieu hétérogène (transformation non holonome) est décrite par les composantes du tenseur de déformation et les coefficients de structure de Cartan relatifs à la base $(\mathbf{f}_1, \mathbf{f}_2, \mathbf{f}_3)$. Les coefficients de structure de Cartan notés $\aleph^c_{0ab}$ [14], sont définis à partir du crochet de Lie-Jacobi[4] :

$$[\mathbf{f}_a, \mathbf{f}_b] = \aleph^c_{0ab}\mathbf{f}_c \tag{1.2.14}$$

D'après le théorème de Frobenius [68], $(\mathbf{f}_1, \mathbf{f}_2, \mathbf{f}_3)$ est une base locale holonome si elle est associée à un système de coordonnées curvilignes et $\aleph^c_{0ab} = 0$. Elle est non holonome dans le cas contraire et $\aleph^c_{0ab} \neq 0$. On pourra constater que les composantes de torsion et de courbure sont simplifiées si ces tenseurs sont projetés dans une base holonome (voir chapitre suivant). Le milieu hétérogène est ainsi décrit comme un ensemble de petits granules euclidiens, qui peuvent se déformer, se translater, subir des rotations les uns par rapport aux autres (microcosmes). Lors d'une transformation non holonome, étant donné que le crochet de Lie-Jacobi est antisymétrique [18], nous avons $\aleph^c_{0ab} = -\aleph^c_{0ba}$ et il y a donc 9 coefficients de structures indépendants. Un nouvel outil, du à Cartan [14], est alors introduit, un vecteur covariant (une 1-forme) :

$$\aleph_0 = \aleph^a_{0ab}\mathbf{f}^b. \tag{1.2.15}$$

Pour définir le vecteur covariant de Cartan $\aleph_0$, il est nécessaire de connaître 6 coefficients de structure, soit le même nombre de composantes d'un tenseur métrique (symétrique). Le lien avec les milieux de Cosserat est ainsi établi. Nous rappelons que, historiquement, un milieu de Cosserat est décrit par un champ de déplacement $\mathbf{u}$ et un champ de rotation, lequel peut être remplacé par un vecteur angulaire θ pour de petites rotations. Dans le modèle qui vient d'être exposé [73], [74], nous introduisons le vecteur de Cartan $\aleph_0$ comme variable additionnelle. Finalement, en général, le mouvement de $\mathcal{B}$, est entièrement décrit dans le temps par le déplacement $\mathbf{u}(M,t)$ et la torsion $\aleph(M,t)$ associée à la connexion affine. Pour les milieux hétérogènes, l'opérateur de divergence doit être reformulé. Par exemple dans [50], [74], la divergence est dédoublée comme somme d'une divergence classique et d'une contribution des champs d'inhomogénéités (discontinuité des champs), lesquels sont source de contraintes internes. On définit donc la divergence généralisée dans un milieu hétérogène par

$$\mathrm{div}(\sigma) = \overline{\mathrm{div}(\sigma)} + \sigma(\aleph_0). \tag{1.2.16}$$

La divergence classique est notée $\overline{\mathrm{div}(\sigma)}$ et le terme supplémentaire $\sigma(\aleph_0)$ capture la contribution d'effort des hétérogénéités et est attribué aux forces dites de configuration e.g. [37], [62], [72]. D'une manière générale, il peut être montré que la dépendance de l'énergie $\mathcal{W}(\varepsilon, \aleph_0)$ par rapport à la variable additionnelle $\aleph_0$ donne la loi de comportement e.g. [75]. Cette dépendance reflète la théorie du second gradient. Nous pouvons par la

[3]Les indices du bas sont covariants, ceux du haut sont contravariants. Plus de détails concernant les composantes des champs de tenseurs dans le chapitre suivant.

[4]Indices répétés : convention de sommation d'Einstein.

suite formuler les équations d'équilibre ou du mouvement dans un milieu hétérogène. Par exemple en petites déformations et pour faire simple avec une fonction d'énergie qui ne dépend pas de terme en gradient $\mathcal{W}(\varepsilon)$, la divergence généralisée prend la forme suivante (1.2.16), λ et μ étant les constantes de Lamé :

$$\mathrm{div}(\sigma) = (\lambda + \mu)\ \overline{\nabla}(\overline{\mathrm{div}}\mathbf{u}) + \mu\ \overline{\Delta}\mathbf{u} + \left[\lambda\ \overline{\mathrm{div}}\mathbf{u}\ \mathbb{I} + \mu\ (\overline{\nabla}\mathbf{u} + \overline{\nabla}^T\mathbf{u})\right] \aleph_0 \tag{1.2.17}$$

où la barre signifie qu'il s'agit des opérateurs différentiels classiques (gradient, divergence, laplacien) par rapport à un système de coordonnées donné. En annulant le nouveau terme $\aleph_0 = 0$, on retrouve l'opérateur divergence qui apparaît dans l'équation de Navier, bien connu.

1.3 Contribution du travail de thèse

Le travail de thèse comporte trois parties : la première porte sur l'invariance des champs dans un espace de Riemann munie d'une connection affine, la deuxième partie porte sur la propagation d'ondes élastiques dans un milieu hétérogène puis la troisième partie porte sur une modélisation de l'indentation du verre.

1.3.1 Invariance des champs

Dans cette première partie, nous poursuivons les investigations concernant l'utilisation de la géométrie de Cartan pour modéliser les milieux faiblement continus [73], [74]. La fonction d'énergie potentielle est traitée au moyen d'un champ scalaire défini dans un système de coordonnées curviligne associé à une base tangente locale. De plus, le travail se base sur le calcul tensoriel et les propriétés d'invariance des champs en physique. Le tenseur métrique est préféré au tenseur de déformation, pour le raisonnement et les calculs. Par exemple la métrique est inversible, ce qui n'est nécessairement pas le cas pour le tenseur de déformation fréquemment utilisé en mécanique. On peut faire le lien [75].

Dans un premier temps, l'objectif est d'étudier un résultat concernant la dépendance des champs scalaires, définis sur une variété riemannienne, par rapport aux dérivées du tenseur métrique. Ce résultat (théorème) a été publié par Lovelock et Rund [57] (1975) avec des hypothèses de symétrie concernant les variables introduites. Notre travail consiste à reprendre cette investigation dans un cadre plus général, sans hypothèse de symétrie, pour reformuler ce théorème puis de faire le lien avec les variables utilisées en mécanique. En identifiant le tenseur métrique au tenseur de déformation et les champs scalaires aux fonctions d'énergie, le modèle, construit selon [57], contredit les modèles issus de la théorie du gradient en élasticité ("first strain gradient elasticity" introduit à l'origine par Mindlin [64]) qui ne prennent pas en compte la dépendance par rapport au second gradient du tenseur de déformation.

Dans un second temps, nous introduisons en plus la connexion affine comme outil de calcul, suggérée par Cartan, mais qui n'est pas un tenseur. Nous nous intéressons toujours aux champs scalaires définis sur une variété riemannienne mais cette fois-ci avec une connexion affine compatible avec la métrique. Notre attention porte sur le principe

d'invariance des champs lors d'un changement de système de coordonnées curvilignes et sur les propriétés qui en découlent. Nous étudierons successivement un champ scalaire qui dépend de la métrique (toujours) et de la connexion compatible, de la biconnexion (dérivée seconde par rapport à la connexion) et des deux. Le travail démontre que la dépendence d'un champ scalaire par rapport aux tenseurs torsion et/ou courbure est une condition équivalente (nécessaire et suffisante) pour l'invariance du champ scalaire qui dépend, au départ, de la connexion affine associée. Ces propriétés sont citées dans [76] et elles seront démontrées dans cette thèse. Dans cette approche non-riemannienne des milieux faiblement continus, nous pouvons justifier l'utilisation systématique de la torsion et de la courbure comme arguments principaux de la fonction d'énergie, en plus de la métrique (ou du tenseur de déformation). La particularité d'un tel modèle se situe dans l'utilisation d'arguments tensoriels (torsion et/ou courbure) contrairement à d'autres modèles déjà existants, proposés initialement dans [65], dont les variables dérivées ne sont pas nécessairement des tenseurs.

Finalement, nous nous intéressons aux fonctions scalaires définies sur une variété riemannienne à connexion affine. Nous nous focalisons sur les arguments, et leurs dérivées, de ces fonctions en faisant le lien avec les variables introduites en mécanique et mécanique-géométrie. La première partie est ainsi intégrée dans l'étude des milieux faiblement continus avec une approche géométrique et dans la théorie du second gradient.

Ce travail constitue l'élaboration de [4] qui a récemment fait l'objet d'une contribution pour un congrès.

1.3.2 Propagation d'onde

La deuxième partie, plus appliquée, se situe dans le même cadre que la précédente, à savoir principalement les milieux faiblement continus. Il s'agit de développer un modèle de milieu hétérogène similaire aux milieux faiblement continus [73] et adapté pour l'étude de la propagation d'onde élastique dans un milieu hétérogène. Les motivations pour étudier la propagation des ondes dans un milieu hétérogène sont avant tout physiques, puisque une atténuation spatiale de l'onde est constatée expérimentalement e.g. [35], [41].

Le milieu hétérogène est décrit, de manière naturelle, à partir d'une densité de masse variable $\rho = \rho(\mathbf{x})$. Nous choisissons une densité de masse qui évolue de manière exponentielle, pour sa simplicité mathématique. Le terme qui définira le sens et l'amplitude de la variation est un vecteur noté $\aleph_0$. Ce dernier est un paramètre du modèle et apparaît dans la définition de la densité de masse du milieu. Pour faire simple, nous utilisons une densité d'énergie potentielle élastique $\mathcal{W}(\varepsilon)$, sans terme à gradient. L'équation du mouvement obtenue est celle obtenue pour les milieux hétérogènes à partir d'un opérateur divergence reformulé, e.g. [74] :

$$\overline{\mathrm{div}(\sigma)} + \sigma(\aleph_0) = \rho\ \mathbf{u}_{tt} \tag{1.3.1}$$

Sans pour l'instant faire le lien entre $\aleph_0$ et le vecteur covariant de Cartan [14], l'équation du mouvement est résolue pour deux exemples de milieu hétérogène : un cylindre infini à paroi épaisse et un modèle de poutre de Timoshenko. Les résultats analytiques obtenus permettent d'une part de mettre en évidence, par le calcul, l'atténuation de l'onde

propagée dans ce milieu hétérogène et d'autre part de relever la notion de fréquence de coupure pour l'onde. Ces caractéristiques sont bien évidemment liées au paramètre $\aleph_0$ introduit, et plus précisemment à un discriminant sous la forme $\Delta := \aleph_0^2 - \omega_n^2$, où ω_n désigne la n-ième fréquence propre.

Nous pouvons ensuite faire le lien avec les milieux hétérogènes introduits dans le cadre des modèles de Cosserat revisités par Cartan. Les équations obtenues dans les deux cas coïncident parfaitement. Le choix de la poutre de Timoshenko n'est pas aléatoire, car celle-ci peut être considérée comme un modèle de milieu de Cosserat e.g. [75].

Ce travail a fait l'objet d'une communication pour une conférence internationale[5] et d'un article en soumission [5].

1.3.3 Indentation du verre

La troisième et dernière partie se consacre à une étude pragmatique sur l'indentation du verre à faible charge. Plus particulièrement il s'agit de l'indentation de Vickers dont l'indenteur est un poinçon de forme pyramidale. Ce travail est une collaboration avec le laboratoire LARMAUR de l'Université de Rennes 1. En effet, les membres de ce laboratoire ont souhaité l'exploitation du travail de Yoffe [83] pour obtenir des résultats analytiques en particulier concernant l'influence du coefficient de Poisson. Nous avons alors vu le lien avec la mécanique d'Eshelby, dans la catégorie concernant les inclusions et les inhomogénéités [24], et l'exploitation du calcul formel [10]. L'empreinte à la surface du verre, suite à la charge puis décharge de l'indenteur, est ainsi modélisée avec un modèle analytique développé par Yoffe associé donc à une inclusion émergente de type Eshelby. Notre approche se veut empirique dans la mesure où nous disposons au départ des données expérimentales (fournies par le LARMAUR). Les expressions analytiques des champs de contrainte et de déplacement proviennent du modèle de Yoffe. Cependant la résolution des équations n'est pas purement analytique : notre objectif est de proposer des formes d'ampoules qui décrivent le comportement du verre, localement déformé, en réponse à la pression de l'indenteur. Ces formes ont également été observées expérimentalement. L'étude décrit un phénomène de densification du verre et se focalise sur l'influence du coefficient de Poisson sur les zones affectées. Les résultats semi-analytiques sont confrontés de manière positive avec les données expérimentales [43]. La poursuite de la collaboration avec le laboratoire LARMAUR, se traduit par la publication [12] présentée à un colloque[6] national puis une extension [3] présentée à une conférence[7] internationale.

Compte tenu de certaines approches e.g. [30], [39], la théorie du gradient de déformation ("strain gradient theory") est appliquée à l'indentation. Cela laisse envisager un lien potentiel entre la troisième partie et les deux précédentes parties. Cependant nous

[5] *Models of continua with scalar discontinuity distribution : theory and examples* présentée pour la Conférence internationale Euromech : Mechanics of Generalized Continua : a hundred years after the Cosserats, Paris, France, 13-16 mai.

[6] Colloque national sur l'indentation, Rennes, France, 7-8 nov.

[7] Conférence internationale sur la rupture (ICF12 : 12th International Conference on Fracture) 2009, Ottawa, Canada.

n'avons pas, dans ce mémoire, développé ce lien (voir perspectives).

Chapitre 2

Invariance des champs dans un espace de Riemann

Dans ce chapitre nos investigations portent sur les champs scalaires définis sur une variété riemannienne munie d'une connexion affine. Dans la première partie nous nous inspirons des travaux de Lovelock et Rund (1975) sur la dépendance du Lagrangien par rapport au tenseur métrique et ses dérivées. La seconde partie s'intéresse à la dépendance par rapport à la connexion affine, compatible avec la métrique. Nous prouvons la dépendance nécessaire par rapport aux tenseurs torsion et/ou courbure, associés à la connexion. La preuve est basée sur le principe d'invariance. Ce travail constitue la référence [4] : le lecteur est donc invité à substituer éventuellement l'expression "in this paper" par "in this chapter".

In this chapter we deal with the scalar fields defined on Riemannian manifold endowed with an affine connection. On the one hand we investigate the dependence with respect to the metric and its derivatives according to Lovelock and Rund (1975). And on the other hand we investigate the dependence with respect to the compatible connection. We prove the necessary dependence withe respect to the torsion and/or to the curvature assciated with the connection. The proof is based on the principle of invariance of fields. This work is associated with the reference [4] : the reader can thus replace the expression "in this paper" by "in this chapter".

2.1 Introduction

For analyzing the deformation of the elastic continuous media, the strain tensor and the stress are related by the constitutive laws. It is then convenient to introduce a potential energy function here denoted $\mathcal{W}$ and also called the strain energy function because of its dependence with respect to the strain. For extended model including couple-stress, the same kinematics as classical elasticity is used but the strain energy density is assumed to be a function of both the strain and the curl of strain e.g. [81]. Another extension of the model was the elastic continuum with micro-structure e.g. [63] where the strain energy density is function of the strain, the first gradient of the strain and the second gradient of the strain.

2.1.1 Lagrangian function

In continuum mechanics, the deformation is classically defined by means of the field of displacement vector $\mathbf{u}(\mathbf{x}, t) \in \mathbb{R}^3$ defined on a manifold, where $\mathbf{x} \in \mathbb{R}^3$ and $t \in \mathbb{R}_+$ defines a material point position within the space and the time respectively e.g. [60]. In theory of elasticity, one uses the strain energy function $\mathcal{W} = \mathcal{W}(\mathbf{E})$ which depends only on strain tensor $\mathbf{E}$ (Green-Lagrange strain tensor). The strain tensor $\mathbf{E} = (1/2)(\nabla\mathbf{u} + \nabla^T\mathbf{u} + \nabla^T\mathbf{u}\nabla\mathbf{u})$ is formulated by means of covariant derivatives of displacement field $\mathbf{u}$. The symbol ∇ represents more generally an affine connection introduced for the derivation of tensor fields defined on a Riemannian manifold e.g. [60]. The (material) metric tensor $\mathbf{g} = \mathbf{I} + 2\mathbf{E}$ is related to strain, and consequently to derivatives of displacement. In elasticity, the Lagrangian scalar density $\mathcal{L}(\mathbf{u}_t, \nabla\mathbf{u}) = (\rho/2)\|\mathbf{u}_t\|^2 - \mathcal{W}(\nabla\mathbf{u})$ is used in dynamic problems to obtain the equations of motion [60]. The first term is the kinetic energy and the second term one the strain energy density (per volume unit). For the sake of simplicity in this paper, we do not consider kinetic energy in the Lagrangian density. Consequently we limit ourself to the strain energy density $\mathcal{L} \equiv \mathcal{W}$, a third grade model accounting for the inertial terms may be found in e.g. [1] where they applied Noether's theorem for establishing conservation and balance laws. From another point of view, it may be observed that the introduction of the method of path-integration, or Cartan circuit method, allowed to point out the influence of the torsion tensor in the formulation of linear momentum conservation for discrete points e.g. [46] or continuous medium e.g. [50], [73].

In early 1960s, Toupin developed elastic continuum models with couple-stress [81] and observed that some components of the gradient of strain were not accounted for. Later he pointed out the correspondance of strain gradient elastic models and discrete lattice models of solids with nevertheless some flaws when considering centro-symmetric materials. To overcome this problem, Mindlin [63] have proposed a strain gradient theory, adapted for elastic material, in which the strain energy function is assumed to depend on both the strain, strain gradient, and second gradient of the strain. More recently, the correspondance of the second gradient strain continuum with fluid like material with heterogeneous density including capillarity effects was analyzed by Forest et al. [27]. It should be also noticed that the theory of second gradient of strain may find its roots in

the domain of solids with Volterra's dislocations where torsion and curvature tensors are involved e.g. [74]. More precisely, last 1999s and early 2000s, the strain gradient theory have been used notably in the works of Hutchinson and Fleck [28], [29], Nix, Gao and al. [30], [38], Cermelli and Gurtin [15]. The theories of elastic or elastic plastic continuous media were developed by accounting for the presence of dislocations and disclinations within the material (heterogeneous body), either with a strain gradient density e.g. [54], [56], or in the context of affinely connected manifold with torsion e.g. [51], [69], [74], [85]. Constitutive laws of heterogeneous solids are obtained by choosing free energy functions depending on higher order of displacement and rotation gradient e.g. [58], or on density dislocation tensor e.g. [72]. Most of them were derived from original potential proposed by Mindlin e.g. [63].

All of these previous results suggested us to consider, in the present work, higher gradient continuum elastic properties which are often resumed by a potential energy function $\mathcal{W}(E_{ij}, E_{ij,k}, E_{ij,kl})$ depending on higher derivatives of the components of the strain tensor $\mathbf{E}$. In this work, we slightly modify the dependence and thus consider a strain gradient elastic continuum defined by a Lagrangian function of the type $\mathcal{L}(g_{\alpha\beta}, g_{\alpha\beta|\lambda}, g_{\alpha\beta|\lambda|\mu})$ where the (material) metric tensor $g_{\alpha\beta} := \delta_{\alpha\beta} + \nabla_\alpha u_\beta + \nabla_\beta u_\alpha + \nabla_\alpha u^\gamma \nabla_\beta u_\gamma$ is formulated by means of derivatives of displacement field $\mathbf{u}$ ($g_{\alpha\beta}$ is usually called Cauchy-Green strain tensor). We notice that quantities $g_{\alpha\beta}$ are the components of the metric tensor onto a material base which deforms with the continuum. A generic function of the type $\mathcal{L}(\nabla_\alpha u_\beta, \nabla_\lambda \nabla_\alpha u_\beta, \nabla_\mu \nabla_\lambda \nabla_\alpha u_\beta)$ can be considered for elastic material of grade three e.g. [1]. Such a model is included in the class of materials we are studying in the present paper. The symbol $|$ denotes the covariant derivative with respect to an affine connection ∇. It is reminded that the affine connection is not a tensor. Such a Lagrangian function defines second / third grade continuum models e.g. [63]. As we previously mention, we do not consider kinetic energy in the Lagrangian function.

2.1.2 Invariance principles

Our investigations are focused on the invariance properties of the Lagrangian function, defined on a Riemannian manifold with an affine connection. It is necessary to define the notion of invariance of such function. We introduce three following notions of invariance : Euclidean-Frame-Indifference (EFI), Form-Invariance (FI) and Rigid-Motion-Indifference (RMI). These notions are more precisely defined in e.g. [79] :

- Euclidean-Frame-Indifference (EFI) : Invariance with respect to Euclidean observers.
- Form-Invariance (FI) : The Lagrangian function has the same mathematical shape in any coordinate system.
- Rigid-Motion-Indifference (RMI) : Invariance with respect to superimposed rigid body motions.

The term "invariance" is related to a mathematical function, it is then used for FI. Whereas the term "indifference" is related to the visions of Euclidean observers (see [79]), it is then used for EFI and RMI. In the present paper, a method is given to select the invariant variables under the action of the homeomorphism, upon which this model

must depend. Actually it will be the action of the diffeomorphism, since we work with a differential manifold and we will introduce some higher gradient variables. In physics, form-invariance is also known as diffeomorphism-invariance meaning that the expression of physical quantities (for instance the energy) have the same form under the arbitrary coordinate transformation. It is merely a kind of change of variable with a diffeomorphism. The term "Form-invariance" is used instead of "diffeomorphism-invariance", but both of them may be used hereafter. Since we are dealing with continuum evolving in an Euclidean ambient space, the condition EFI is required for any constitutive laws. And it is also proved in [79] that any two of previous notions automatically imply the third. Consequently, the additionnal condition of FI allows to ensure the indifference of the constitutive laws with respect to the surperimposed rigid body motion (RMI). In the following, central focus is the FI (under the action of the homeomorphisms, and more exactly of the diffeomorphisms in such a case) that appears like a mathematical condition for ensuring the principle of objectivity of constitutive laws of continuous medium. Principle based on homeomorphisms is unambiguously developed in lieu of the usual material frame-indifference.

2.1.3 Objectives

Many strain gradient models use an Euclidean connection which derives from the metric, e.g. [87] for which the connection is that of Levi-Civita. Any affine connection defines the tensor of torsion $\aleph$ and the tensor of curvature $\mathfrak{R}$ and according to the Fundamental theorem in Riemannian geometry, the torsion associated with the connection of Levi-Civita is null e.g. [18]. There exist some approaches based on Cartan geometry [14] with a connection which does not derive from the metric and for which the associated torsion and curvature do not necessarily vanish e.g [74]. The functions defined on Riemannian manifold should be tensors, which are used to represent physical fields. We aim to extend the form of the strain density $\mathcal{L}$, more precisely by analyzing the arguments of $\mathcal{L}$. For more generality we will consider a scalar field, also noted $\mathcal{L}$, rather than a density field. To obtain the corresponding density field, it is sufficient to multiply the scalar field by the volume-form, uniform and constant e.g. [76]. We will shed light on the invariance principle of the scalar field, or more precisely the Form-Invariance of the Lagrangian function. In a first part we consider a strain gradient elastic continuum defined by a Lagrangian function of the type $\mathcal{L}(\mathbf{g}, \nabla\mathbf{g}, \nabla^2\mathbf{g})$ which may be formulated as $\mathcal{L}(g_{\alpha\beta}, g_{\alpha\beta|\gamma}, g_{\alpha\beta|\gamma|\lambda})$, in an arbitrary coordinate system (x^α). The symbol $|$ denotes the covariant derivative with respect to an affine connection ∇ (we call bi-connection the operator second covariant derivative $\nabla^2 = \nabla \circ \nabla$). Lovelock and Rund have shown that if one assumes a dependence as $\mathcal{L}(g_{\alpha\beta}, g_{\alpha\beta,\gamma})$ (comma denotes a partial derivative), then by applying the form-invariance requirement, the scalar function takes necessarily the form of $\mathcal{L}(g_{\alpha\beta})$. The first part of the present work was inspired in part of results in Lovelock and Rund, [57] (1975). In their work, Lovelock and Rund have implicitly used the Levi-Civita affine connection. By applying the Lemma of Ricci, the covariant derivative of the metric tensor with respect to this connection is equal to zero e.g. [18].

Remark 2.1.1 *It should be stressed that our purpose in this paper is not to consider a particular form of constitutive laws satisfying the Euclidean Frame-Indifference and / or the Indifference with respect to Superimposed Rigid Body Motions. The term invariance is taken in the sense of Form-Invariance [79]. It is not limited to the so-called Euclidean objectivity. Indeed, by assuming that the potential energy density admits the metric tensor components as arguments, the Euclidean-Frame Indifference is a priori satisfied. We would like to go one step further for strain gradient continuum as in e.g. [80].*

In a second part we consider both independent arguments metric and affine connection which is compatible with the metric (meaning that $\nabla \mathbf{g} \equiv 0$). To obviate the problem of metric compatibility, we slightly extend the dependence of the Lagrangian function by proposing the form of $\mathcal{L}(\mathbf{g}, \nabla, \nabla^2)$. Applying the form-invariance principle, it is shown that the arguments of the function $\mathcal{L}$ are necessarily the torsion $\aleph$ and/or the curvature $\mathfrak{R}$ associated with the connection, in addition to the metric. Finally the strain energy density of a continuous medium depend on tensorial arguments, which is expected to describe some physical phenomenons. To start with, we recall some mathematical preliminaries in differential geometry, necessary for our work.

2.2 Mathematical preliminaries and framework

2.2.1 Coordinate systems

We fixe once and for all the n-dimensional vector space E (referential rigid body). An n-dimensional manifold X, embedded onto E, is a point set which is covered completely by a countable set of neighborhoods $U_1, U_2, ...$, such that each point $P \in X$ belongs to at least one of these neighborhoods. A coordinate system is defined on each U_k such that one may assign in a unique manner n real numbers $x^1, ..., x^n$ to each point $P \in U_k$. As P ranges over U_k, the corresponding numbers $x^1, ..., x^n$ range over an open domain D_k of E. Thus it exist a one-to-one mapping of each U_k onto D_k, this mapping will be assumed continuous. The numbers $x^1, ..., x^n$ are called the coordinates of P. In the case where $U_1 \cap U_2 \neq \emptyset$ there are two sets of coordinates associated to a same point $P \in U_1 \cap U_2$. Let (y^i) *(Latin indexes)* and (x^α) *(Greek indexes)* corresponding coordinate systems respectively in U_1 and U_2, Latin indexes and Greek indexes will be used to distinguish two different coordinate systems. The transformation between coordinates (y^i) and (x^α) is diffeomorphic :

$$y^i = y^i(x^\alpha), \qquad x^\alpha = x^\alpha(y^i) \tag{2.2.1}$$

$$J_i^\alpha = \frac{\partial x^\alpha}{\partial y^i}, \qquad J_{ij}^\alpha = \frac{\partial J_i^\alpha}{\partial y^j} = \frac{\partial^2 x^\alpha}{\partial y^i \partial y^j}, \qquad J_{ijk}^\alpha = \frac{\partial J_{ij}^\alpha}{\partial y^k} = \frac{\partial^3 x^\alpha}{\partial y^i \partial y^j \partial y^k} \tag{2.2.2}$$

We also have that for any coordinate system (y^i), and for any permutation $\sigma \in \mathfrak{S}_n$

$$\frac{\partial^n}{\partial y^1 ... \partial y^n} = \frac{\partial^n}{\partial y^{\sigma(1)} ... \partial y^{\sigma(n)}} \tag{2.2.3}$$

Einstein convention When a lowercase index such as j, k, l,... appears twice in a term then summation over that index is implied. The range of summation is 1,..., n, the letter n is exceptionally excluded from the summation. We have

$$\frac{\partial x^\alpha}{\partial y^i}\frac{\partial y^i}{\partial x^\beta} = J_i^\alpha A_\beta^i = \delta_\beta^\alpha, \qquad \frac{\partial y^i}{\partial x^\alpha}\frac{\partial x^\alpha}{\partial y^j} = A_\alpha^i J_j^\alpha = \delta_j^i \tag{2.2.4}$$

with respectively summation (Einstein) over i and α from 1 to n.

2.2.2 Components of tensor

We notice T_PX the tangent space of X at point P and T_PX^* its dual space. Let $\{\mathbf{e}_1, ..., \mathbf{e}_n\}$ a base of T_PX (contravariant vectors with the lower index) and the reciprocal base $\{\mathbf{f}^1, ..., \mathbf{f}^n\}$ in T_PX^* (covariant vectors with upper index) such that $\langle \mathbf{f}^i, \mathbf{e}_j \rangle = \delta_j^i$ (symbol of Kronecker).

Definition 2.2.1 *(Tensor) Let $\{\mathbf{u}_1, ..., \mathbf{u}_q\} \in T_PX$ and $\{\mathbf{v}^1, ..., \mathbf{v}^p\} \in T_PX^*$ some arbitrary vectors. A p-contravariant and q-covariant tensor field $\mathcal{T}$ on X is a multilinear form defined at each point $P \in X$ by*

$$\mathcal{T} : (\mathbf{v}^1, ..., \mathbf{v}^p, \mathbf{u}_1, ..., \mathbf{u}_q) \in (T_PX^*)^p \times (T_PX)^q \longrightarrow \mathcal{T}(\mathbf{v}^1, ..., \mathbf{v}^p, \mathbf{u}_1, ..., \mathbf{u}_q) \in \mathbb{R}$$

The sum $(p+q)$ is called the rank of the tensor field. The couple (p, q) is called its type.

Definition 2.2.2 *(Components of tensor) If $\mathcal{T}$ is a tensor field of type (p, q) then the scalars $\mathcal{T}_{l_1...l_p}^{j_1...j_q}$ are the components of $\mathcal{T}$ with respect to the base formed by $\{\mathbf{e}_{j_1}, ..., \mathbf{e}_{j_q}\}$ and $\{\mathbf{f}^{l_1}, ..., \mathbf{f}^{l_p}\}$, defined by*

$$\mathcal{T}_{j_1...j_q}^{l_1...l_p} = \mathcal{T}(\mathbf{f}^{l_1}, ..., \mathbf{f}^{l_p}, \mathbf{e}_{j_1}, ..., \mathbf{e}_{j_q})$$

In the present study, a tensor will be assimilated to its components, as soon as the vector bases are defined.

Definition 2.2.3 *If $\mathcal{T}_{k_1...k_s}^{h_1...h_r}$ constitute the components of a tensor type (r, s) then, under the transformation (2.2.1)*

$$\mathcal{T}_{l_1...l_s}^{j_1...j_r} = A_{\alpha_1}^{j_1}...A_{\alpha_r}^{j_r} J_{l_1}^{\beta_1}...J_{l_s}^{\beta_s} \mathcal{T}_{\beta_1...\beta_s}^{\alpha_1...\alpha_r} \tag{2.2.5}$$

and the corresponding inverse formulation

$$\mathcal{T}_{\beta_1...\beta_s}^{\alpha_1...\alpha_r} = J_{j_1}^{\alpha_1}...J_{j_r}^{\alpha_r} A_{\beta_1}^{l_1}...A_{\beta_s}^{l_s} \mathcal{T}_{l_1...l_s}^{j_1...j_r} \tag{2.2.6}$$

Properties 2.2.1 *According to the previous results :*

- *A scalar ψ is a tensor type $(0, 0)$ which has the same form in any coordinate system : ψ in (y^i), $\overline{\psi}$ in (x^α) and $\psi = \overline{\psi}$.*
- *If all the components of a tensor vanish in an arbitrary coordinate system then they vanish in any other coordinate system.*

Definition 2.2.4 *(Metric) A metric tensor, noted* $\mathbf{g}$*, is a tensor type* $(0,2)$*, symmetric and inversible. In base* $\{\mathbf{e}_1, ..., \mathbf{e}_n\}$*, the components of* $\mathbf{g}$ *are* g_{ij}*, the components of the inverse of* $\mathbf{g}$ *are* g^{ij} *and* $g^{ik}g_{kj} = \delta^i_j$*.*

Definition 2.2.5 *(Riemannian manifold) A differential manifold* X *endowed with a metric* $(X, \mathbf{g})$ *is a Riemannian manifold.*

In the present paper, the choice of a metric tensor components $g_{\alpha\beta}$ may be explained as follows. Locally, at any point $P \in X$ of the Riemannian manifold, it should be mentioned that in any coordinate basis, the tangent space $T_P X$ is spanned by $\{\mathbf{e}_1, \cdots, \mathbf{e}_n\}$, and the dual space $T_P X^*$ by $\{\mathbf{f}^1, \cdots, \mathbf{f}^n\}$. There is an alternative choice by taking the base defined as $\hat{\mathbf{e}}_a := \mathbf{F}^{-1}(\mathbf{e}_a)$, where $\det\mathbf{F} > 0$, and in such a way that $\mathbf{g}(\hat{\mathbf{e}}_b, \hat{\mathbf{e}}_b) := \delta_{ab}$. The quantity $\mathbf{F}$ is related to the so-called gradient of transformation in continuum mechanics e.g. [60], or also "vielbeins" in differential geometry e.g. [68]. In the present paper, $\mathbf{F}$ is not necessarily a gradient of a mapping. In continuum mechanics, it is thus possible to define the Green-Lagrange strain tensor $\mathbf{E}$ as follows :

$$E_{\alpha\beta} := (1/2)\left[\mathbf{g}(\mathbf{e}_\alpha, \mathbf{e}_\beta) - \mathbf{g}(\hat{\mathbf{e}}_\alpha, \hat{\mathbf{e}}_\beta)\right]$$

Conceptually, it is not necessary to introduce the tensor $\mathbf{E}$ as a basic strain variable, $\mathbf{g}$ being sufficient. We just remind that the arguments of any scalar field $\mathcal{L}$ may be chosen as the components of the metric $g_{\alpha\beta}$ onto a "deformed base" $\{\mathbf{e}_1, \cdots, \mathbf{e}_n\}$, according to a linear tangent transformation $\mathbf{F}$, instead of $E_{\alpha\beta}$.

Remark 2.2.1 *The definition of strain* $\mathbf{E}$ *do not require a priori the explicit introduction of displacement field and its gradient. It merely expresses the difference of shape between two configurations of a continuum. This aspect will be detailed in the following.*

2.2.3 Affine connection

A connection is an extra structure which specifies how vectors and more generally tensors are transported along a curve on the manifold. An infinite number of connections exist on a manifold X, such as affine connection, geodesic connection and crystal connection. A local tangent base is associated to a coordinate system : the contravariant base $\{\mathbf{e}_\alpha\}$ is associated to the system $\{y^\alpha\}$.

Definition 2.2.6 *(Affine connection) An affine connection* ∇ *on* X *is a map defined by*

$$\nabla : (\mathbf{u}, \mathbf{v}) \in T_P(X) \times T_P(X) \longrightarrow \nabla_{\mathbf{u}}\mathbf{v} \in T_P(X) \tag{2.2.7}$$

wich satifies the following conditions (λ *and* μ *are scalars,* ϕ *is scalar field)*

- $\nabla_{\lambda\mathbf{u}_1+\mu\mathbf{u}_2}\mathbf{v} = \lambda\nabla_{\mathbf{u}_1}\mathbf{v} + \mu\nabla_{\mathbf{u}_2}\mathbf{v}$
- $\nabla_{\mathbf{u}}(\lambda\mathbf{v}_1 + \mu\mathbf{v}_2) = \lambda\nabla_{\mathbf{u}}\mathbf{v}_1 + \mu\nabla_{\mathbf{u}}\mathbf{v}_2$
- $\nabla_{\phi\mathbf{u}}\mathbf{v} = \phi\nabla_{\mathbf{u}}\mathbf{v}$
- $\nabla_{\mathbf{u}}(\phi\mathbf{v}) = \phi\nabla_{\mathbf{u}}\mathbf{v} + \mathbf{u}(\phi)\mathbf{v}$

The coefficients of the affine connection are Γ^c_{ab} such that $\nabla_{\mathbf{e}_a}\mathbf{e}_b := \Gamma^c_{ab}\mathbf{e}_c$. The quantity $\nabla_{\mathbf{u}}$ represents a derivative along the direction $\mathbf{u}$. It is usual to define the covariant derivative, which generalizes the derivative of tensor fields defined on manifold, in the sense of the affine connection ∇. The covariant derivative of a tensor type (p,q) is a tensor type $(p,q+1)$. For example, the covariant derivative of a scalar field ϕ and a vector field $\mathbf{w}$ along the vector $\mathbf{e}_k$ (one of the vectors of the base) may be expressed in terms of their components on the local base $\{\mathbf{e}_a\}$ associated to the coordinate system (y^a)

$$\nabla_{\mathbf{e}_k}\phi = \frac{\partial\phi}{\partial y^k}, \qquad \nabla_{\mathbf{e}_k}\mathbf{w} = \left(\frac{\partial w^a}{\partial y^k} + \Gamma^a_{kc}w^c\right)\mathbf{e}_a.$$

For tensor components, we adopt the notations $\dfrac{\partial(..)}{\partial y^k} = (..)_{,k}$ and $\nabla_{\mathbf{e}_k}(..) = (..)_{|k}$.

Torsion and curvature We now consider a manifold endowed with an affine connection ∇.

Definition 2.2.7 *(Torsion) The torsion tensor $\aleph$ is a tensor type $(1,2)$*

$$\left\{\begin{array}{rcl} \aleph\left(\mathbf{f}^k,\mathbf{e}_i,\mathbf{e}_j\right) & = & \mathbf{f}^k\left(\nabla_{\mathbf{e}_i}\mathbf{e}_j - \nabla_{\mathbf{e}_j}\mathbf{e}_i\right) \\ \aleph^k_{ij} & = & \Gamma^k_{ij} - \Gamma^k_{ji} \end{array}\right. \tag{2.2.8}$$

Definition 2.2.8 *(Curvature) The curvature tensor $\mathfrak{R}$ is a tensor type $(1,3)$*

$$\left\{\begin{array}{rcl} \mathfrak{R}\left(\mathbf{f}^k,\mathbf{e}_i,\mathbf{e}_j,\mathbf{e}_l\right) & = & \mathbf{f}^k\left(\nabla_{\mathbf{e}_i}\nabla_{\mathbf{e}_j}\mathbf{e}_l - \nabla_{\mathbf{e}_j}\nabla_{\mathbf{e}_i}\mathbf{e}_l\right) \\ \mathfrak{R}^k_{ijl} & = & (\Gamma^k_{jl,i} + \Gamma^m_{jl}\Gamma^k_{im}) - (\Gamma^k_{il,j} + \Gamma^m_{il}\Gamma^k_{jm}) \end{array}\right. \tag{2.2.9}$$

Remark 2.2.2 *First, the definition of the torsion and the curvature tensors do not require the existence of a metric tensor on the manifold. Second, there exist general definitions of the torsion and the curvature, which used the Lie-Jacobi bracket e.g. [18]. The theorem of Frobenius, e.g. [68], allows to simplify the expression of the torsion and the curvature projected onto the vector base associated to a coordinate system.*

Levi-Civita connection The Levi-Civita connection is an example of Euclidean connection (derived from the metric) and introduced by the following fundamental theorem, see proof in e.g. [68] :

Theorem 2.2.1 *(Fundamental theorem of Riemannian geometry) On any Riemannian manifold $(X,\mathbf{g})$, there exists a unique connection compatible with the metric and free-torsion ($\aleph = 0$). This connection is called the Levi-Civita connection and usually denoted $\overline{\nabla}$.*

The coefficients of $\overline{\nabla}$ reduce to the symbols of Christoffel $\dfrac{\partial\mathbf{e}_b}{\partial y^a} = \overline{\Gamma}^c_{ba}\mathbf{e}_c$, calculated in terms of the metric $\mathbf{g}$ e.g. [68]

$$\overline{\Gamma}^c_{ab} = (1/2)g^{cd}(g_{ad,b} + g_{db,a} - g_{ab,d}) \tag{2.2.10}$$

For example, if $\mathbf{h}$ is a tensor type $(0,2)$ then the covariant derivative (in the sense of Levi-Civita) with respect to $\mathbf{e}_k$ (a vector of the base) is a tensor type $(0,2+1)$ for which the coordinates are noticed

$$\overline{\nabla}_{\mathbf{e}_k} h_{ij} = h_{ij|k} = \left(h_{ij,k} - \Gamma^a_{ik} h_{aj} - \Gamma^a_{jk} h_{ia}\right) \tag{2.2.11}$$

and then with respect to $\mathbf{e}_l$ (vector of the base), the second covariant derivative (in the sense of Levi-Civita) is $\overline{\nabla}_{\mathbf{e}_l}\left[\overline{\nabla}_{\mathbf{e}_k} h_{ij}\right] = h_{ij|k|l}$ with

$$\begin{aligned} h_{ij|k|l} &= h_{ij,kl} - \Gamma^a_{ik} h_{aj,l} - \Gamma^a_{jk} h_{ia,l} - \Gamma^a_{ik,l} h_{aj} - \Gamma^a_{jk,l} h_{ia} - \Gamma^b_{il} h_{bj,k} \\ &+ \Gamma^b_{il}(\Gamma^c_{bk} h_{cj} + \Gamma^c_{jk} h_{bc}) - \Gamma^b_{jl} h_{ib,k} + \Gamma^b_{jl}(\Gamma^c_{ik} h_{cb} + \Gamma^c_{bk} h_{ic}) \\ &- \Gamma^b_{kl} h_{ij,b} + \Gamma^b_{kl}(\Gamma^c_{ib} h_{cj} + \Gamma^c_{jb} h_{ic}) \end{aligned} \tag{2.2.12}$$

where we have noticed $\overline{\Gamma} = \Gamma$ for the sake of the simplicity.

Properties 2.2.2 *Let X a Riemannian manifold and $P \in X$ any point. In orthonormal base (associated to a normal coordinate system) centered on P, the symbols of Christoffel vanish : $\overline{\Gamma}^k_{ij}(P) = 0$ for $i,j,k = 1,...,n$.*

Remark 2.2.3 *A normal coordinate system on a Riemannian manifold centered at P may be also defined by local relations :*

$$g_{\alpha\beta}(P) := \delta_{\alpha\beta}, \qquad \overline{\Gamma}^{\gamma}_{\alpha\beta}(\xi)\ \xi^\alpha \xi^\beta \equiv 0$$

where $(\xi^1, \cdots, \xi^n)$ are local coordinates of points $P' := P + \xi$ about the center P. Riemannian normal coordinates are a standard tool of various differential geometry theorems, their choice to derive equations allow to simplify most problems.

No confusion will be done between the differentiation of any tensor field with respect to y^k (in the sense of Levi-Civita) and the differentiation with respect to the affine connection $\nabla_{\mathbf{e}_k}$.

2.2.4 Holonomic and nonholonomic transformations

Consider a Riemannian manifold $(X, \mathbf{g})$ embedded in a n-dimensional Euclidean space E. Let $\mathbf{X} \in X$ a point of the manifold, and let consider a mapping φ which associates $\mathbf{X}$ to a point of the Euclidean space $\mathbf{x} \in E$. We denote the mapping $\mathbf{x}(\mathbf{X})$ for simplifying. For the sake of the simplicity, we assume that the coordinates $\mathbf{X} = (X^1, \cdots, X^n)$ are Cartesian.

Holonomic mapping Let consider a smooth and single valued mapping (it is a homeomorphism and we call it holonomic mapping e.g. [74]). It is usual to define the deformation gradient also called basis triads (rigorously it is not a gradient) in components form, together with its reciprocal basis triads :

$$F^i_\alpha(\mathbf{X}) := \frac{\partial x^i}{\partial X^\alpha}(\mathbf{X}), \qquad F^\beta_j(\mathbf{x}) := \frac{\partial X^\beta}{\partial x^j}(\mathbf{x})$$

The triads satisfy the orthogonality and the completeness relationships :

$$F_\alpha^i(\mathbf{X})\ F_i^\beta[\mathbf{x}(\mathbf{X})] = \delta_\alpha^\beta, \qquad F_\alpha^i(\mathbf{X})\ F_j^\alpha[\mathbf{x}(\mathbf{X})] = \delta_j^i$$

We may write the vector transformation and the components of the metric tensor, where $\hat{\mathbf{e}}_i$ is a vector rigidly attached to the Euclidean space E :

$$\mathbf{e}_\alpha = F_\alpha^i\ \hat{\mathbf{e}}_i, \qquad g_{\alpha\beta} = \mathbf{g}(\mathbf{e}_\alpha, \mathbf{e}_\beta)$$

On the one hand, since the transformation $\mathbf{x}(\mathbf{X})$ is smooth and single valued, it is integrable, i.e. its derivative commute, by using the classic Schwarz's integrability conditions :

$$\frac{\partial F_\alpha^i}{\partial X^\beta} - \frac{\partial F_\beta^i}{\partial X^\alpha} = \frac{\partial^2 x^i}{\partial X^\beta \partial X^\alpha} - \frac{\partial^2 x^i}{\partial X^\alpha \partial X^\beta} = 0$$

On the other hand, we can differentiate the vector base, :

$$\frac{\partial \mathbf{e}_\alpha}{\partial X^\beta} := \Gamma_{\alpha\beta}^\gamma\ \mathbf{e}_\gamma = \frac{\partial F_\alpha^i}{\partial X^\beta}\ \hat{\mathbf{e}}_i = \frac{\partial F_\alpha^i}{\partial X^\beta}\ F_i^\gamma\ \mathbf{e}_\gamma \quad \Longrightarrow \quad \Gamma_{\alpha\beta}^\gamma = \frac{\partial F_\alpha^i}{\partial X^\beta}\ F_i^\gamma$$

Then it is straightforward to check that the torsion tensor is equal to zero during an holonomic transformation :

$$\aleph_{\alpha\beta}^\gamma := \left(\frac{\partial F_\alpha^i}{\partial X^\beta} - \frac{\partial F_\beta^i}{\partial X^\alpha}\right) F_i^\gamma = 0$$

Nonholonomic mapping and torsion Let consider mapping that are not smooth and/or not single valued. In such a case, the basis triads are not integrable. However, it is possible to map the points surrounding $\mathbf{X}$ defined by the tangent vector $d\mathbf{X}$ to the vector $d\mathbf{x}$ via an infinitesimal transformation defined by the triads :

$$\mathbf{e}_\alpha = F_\alpha^i\ \hat{\mathbf{e}}_i, \qquad dx^i = F_\alpha^i\ dX^\alpha$$

in which the coefficients functions $F_\alpha^i(\mathbf{X})$ are not integrable in the sense of

$$\frac{\partial F_\alpha^i}{\partial X^\beta} - \frac{\partial F_\beta^i}{\partial X^\alpha} = \frac{\partial^2 x^i}{\partial X^\beta \partial X^\alpha} - \frac{\partial^2 x^i}{\partial X^\alpha \partial X^\beta} \neq 0$$

In such a case, the mapping is called nonholonomic. It is necessary to modify slightly the previous development to give (the base $\{\hat{\mathbf{e}}_1, \cdots, \hat{\mathbf{e}}_n\}$ is assumed rigidly attached to the Euclidean space) :

$$\frac{\partial \mathbf{e}_\alpha}{\partial X^\beta} - \frac{\partial \mathbf{e}_\beta}{\partial X^\alpha} = \left(\frac{\partial F_\alpha^i}{\partial X^\beta} - \frac{\partial F_\beta^i}{\partial X^\alpha}\right) F_i^\gamma \mathbf{e}_\gamma \neq 0$$

showing that the torsion tensor $\aleph_{\beta\alpha}^\gamma\ \mathbf{e}_\gamma$ is not equal to zero for such a nonholonomic mapping. It does not lead to a single valued mapping $\mathbf{x}(\mathbf{X})$. Such a transformation may capture the translational dislocations of Volterra e.g. [61].

Nonholonomic transformation and curvature As third example, consider a transformation for which $\mathbf{x}(\mathbf{X})$ may be or not itself integrable, while the first derivatives of the vectors $\{\mathbf{e}_1, \cdots, \mathbf{e}_n\}$, where $\mathbf{e}_\alpha := F^i_\alpha \, \hat{\mathbf{e}}_i$, are not integrable. Such non integrability is captured by the non commutativity of the second-order derivatives :

$$\frac{\partial}{\partial X^\alpha}\left(\frac{\partial \mathbf{e}_\lambda}{\partial X^\beta}\right) - \frac{\partial}{\partial X^\beta}\left(\frac{\partial \mathbf{e}_\lambda}{\partial X^\alpha}\right) = \frac{\partial}{\partial X^\alpha}\left(\Gamma^\kappa_{\lambda\beta}\mathbf{e}_\kappa\right) - \frac{\partial}{\partial X^\beta}\left(\Gamma^\kappa_{\lambda\alpha}\mathbf{e}_\kappa\right)$$

From this relation, we easily deduce that the Cartan curvature is not equal to zero :

$$\mathfrak{R}^\kappa_{\alpha\beta\lambda} = \left(\Gamma^\kappa_{\beta\lambda,\alpha} + \Gamma^\xi_{\beta\lambda}\Gamma^\kappa_{\alpha\xi}\right) - \left(\Gamma^\kappa_{\alpha\lambda,\beta} + \Gamma^\xi_{\alpha\lambda}\Gamma^\kappa_{\beta\xi}\right) \neq 0$$

We can also calculate the non-commutativity by directly introducing the basis triads to give

$$\mathfrak{R}^\kappa_{\alpha\beta\lambda} = F^\kappa_i\left(\frac{\partial^2 F^i_\lambda}{\partial X^\alpha \partial X^\beta} - \frac{\partial^2 F^i_\lambda}{\partial X^\beta \partial X^\alpha}\right) \neq 0$$

Such a transformation may be related to the process of rotational dislocations e.g. [61], or some plastic deformation. This short section permits us to highlight the role of torsion and curvature tensors on the classification of continuum transformations. More general proof may be found in a previous work, devoted to the class of "weakly continuous medium" [73].

Remark 2.2.4 *Torsion tensor is associated to translational dislocations or also to the local discontinuity of any scalar field on the continuum, while curvature tensor is associated to the rotational dislocations or also to the local discontinuity of vector field on the continuum [73] .*

2.3 Quotient law

Now we remind some technical theorems in tensorial analysis [57].

Lemma 2.3.1 *Locally at point P, let the both $(n\times n)$ quantities Σ^{ij} and $\overline{\Sigma}^{ij}$ then the both $(n\times n\times n)$ quantities $\Sigma^{ij,k}$ and $\overline{\Sigma}^{ij,k}$ (the comma "," doesn't represent partial derivative). If, for any symmetric tensor type (0,2) h,*

$$\Sigma^{ij}h_{ij} + \Sigma^{ij,k}h_{ij|k} = \overline{\Sigma}^{ij}h_{ij} + \overline{\Sigma}^{ij,k}h_{ij|k} \tag{2.3.1}$$

then

$$(\Sigma^{ij} + \Sigma^{ji}) = (\overline{\Sigma}^{ij} + \overline{\Sigma}^{ji}) \tag{2.3.2}$$

and

$$(\Sigma^{ij,k} + \Sigma^{ji,k}) = (\overline{\Sigma}^{ij,k} + \overline{\Sigma}^{ji,k}) \tag{2.3.3}$$

for i, j, $k = 1, ..., n$

Proof. The equality (2.3.1) being valid for any symmetric tensor h, it is thus valid for a non null constant tensor (locally). The covariant derivative vanishes and from (2.3.1) we have the following equality $(\Sigma^{ij})h_{ij} = (\overline{\Sigma}^{ij})h_{ij}$. The term h_{ij} cannot simplify because of the summation in i and j. For i and j fixed, we choose $h_{ij} = h_{ji} = 1$ and the other components null. For i and j range over $\{1, ..., n\}$, we obtain

$$\left\{\begin{array}{rcl} \Sigma^{11} & = & \overline{\Sigma}^{11} \\ \Sigma^{12} + \Sigma^{21} & = & \overline{\Sigma}^{12} + \overline{\Sigma}^{21} \\ \Sigma^{13} + \Sigma^{31} & = & \overline{\Sigma}^{13} + \overline{\Sigma}^{31} \\ ... & & \end{array}\right. \tag{2.3.4}$$

thus we obtain (2.3.2). In the same way, locally at point P, a null tensor h with a non null constant covariant derivative can be chosen too. In this case from (2.3.1) $(\Sigma^{ij,k})h_{ij|k} = (\overline{\Sigma}^{ij,k})h_{ij|k}$. The term $h_{ij|k}$ cannot simplified because of the summation in i, j and k. For i, j and k fixed, we choose $h_{ij|k} = h_{ji|k} = 1$ and the other components null. For i, j and k range over $\{1, ..., n\}$, we obtain

$$\left\{\begin{array}{rcl} \Sigma^{11,1} & = & \overline{\Sigma}^{11,1} \\ \Sigma^{11,2} & = & \overline{\Sigma}^{11,2} \\ \Sigma^{12,1} + \Sigma^{21,1} & = & \overline{\Sigma}^{12,1} + \overline{\Sigma}^{21,1} \\ \Sigma^{12,2} + \Sigma^{21,2} & = & \overline{\Sigma}^{12,2} + \overline{\Sigma}^{21,2} \\ \Sigma^{13,1} + \Sigma^{31,1} & = & \overline{\Sigma}^{13,1} + \overline{\Sigma}^{31,1} \\ \Sigma^{13,2} + \Sigma^{31,2} & = & \overline{\Sigma}^{31,2} + \overline{\Sigma}^{31,2} \\ ... & & \end{array}\right. \tag{2.3.5}$$

thus we obtain (2.3.3).

□

We have also the version with the partial derivative :

Lemma 2.3.2 *Locally at point P, let the both $(n \times n)$ quantities Σ^{ij} and $\overline{\Sigma}^{ij}$ then the both $(n \times n \times n)$ quantities $\Sigma^{ij,k}$ and $\overline{\Sigma}^{ij,k}$ (the comma "," doesn't represent partial derivative). If, for any symmetric tensor type (0,2) h,*

$$\Sigma^{ij}h_{ij} + \Sigma^{ij,k}h_{ij,k} = \overline{\Sigma}^{ij}h_{ij} + \overline{\Sigma}^{ij,k}h_{ij,k} \tag{2.3.6}$$

then

$$(\Sigma^{ij} + \Sigma^{ji}) = (\overline{\Sigma}^{ij} + \overline{\Sigma}^{ji}) \tag{2.3.7}$$

and

$$(\Sigma^{ij,k} + \Sigma^{ji,k}) = (\overline{\Sigma}^{ij,k} + \overline{\Sigma}^{ji,k}) \tag{2.3.8}$$

for i, j, $k = 1, ..., n$

Now the following quotient theorem holds e.g. [57]

Theorem 2.3.1 *(Quotient law) Locally at point P, if the $(n \times n)$ quantities Σ^{ij} and the $(n \times n \times n)$ quantities $\Sigma^{ij,k}$ (the comma "," doesn't represent the partial derivative) are such that the quantities $\Sigma^{ij}h_{ij} + \Sigma^{ij,k}h_{ij|k}$ represent a scalar field for any symmetric tensor type (0,2) h, then the quantities $(\Sigma^{ij}+\Sigma^{ji})$ and $(\Sigma^{ij,k}+\Sigma^{ji,k})$ represent respectively the components of a tensor type (2,0) and the components of a tensor type (3,0).*

Proof. Let define the scalar $\psi = \Sigma^{ij}h_{ij} + \Sigma^{ij,k}h_{ij|k}$ and $\overline{\psi} = \Sigma^{\alpha\beta}h_{\alpha\beta} + \Sigma^{\alpha\beta,\gamma}h_{\alpha\beta|\gamma}$ in the system (y^i) and (x^α) respectively for any symmetric tensor type (0,2) h. The equality $\psi = \overline{\psi}$ becomes

$$\Sigma^{ij}h_{ij} + \Sigma^{ij,k}h_{ij|k} = \Sigma^{\alpha\beta}\frac{\partial y^i}{\partial x^\alpha}\frac{\partial y^j}{\partial x^\beta}h_{ij} + \Sigma^{\alpha\beta,\gamma}\frac{\partial y^i}{\partial x^\alpha}\frac{\partial y^j}{\partial x^\beta}\frac{\partial y^k}{\partial x^\gamma}h_{ij|k} \tag{2.3.9}$$

According to the lemma 2.3.1

$$\Sigma^{ij} + \Sigma^{ji} = \Sigma^{\alpha\beta}\frac{\partial y^i}{\partial x^\alpha}\frac{\partial y^j}{\partial x^\beta} + \Sigma^{\alpha\beta}\frac{\partial y^j}{\partial x^\alpha}\frac{\partial y^i}{\partial x^\beta} \tag{2.3.10}$$

and

$$\Sigma^{ij,k} + \Sigma^{ji,k} = \Sigma^{\alpha\beta,\gamma}\frac{\partial y^i}{\partial x^\alpha}\frac{\partial y^j}{\partial x^\beta}\frac{\partial y^k}{\partial x^\gamma} + \Sigma^{\alpha\beta,\gamma}\frac{\partial y^j}{\partial x^\alpha}\frac{\partial y^i}{\partial x^\beta}\frac{\partial y^k}{\partial x^\gamma} \tag{2.3.11}$$

then a permutation between i and j gives

$$\left\{\begin{array}{rcl} \Sigma^{ij} + \Sigma^{ji} & = & (\Sigma^{\alpha\beta} + \Sigma^{\beta\alpha})\dfrac{\partial y^i}{\partial x^\alpha}\dfrac{\partial y^j}{\partial x^\beta} \\ \\ \Sigma^{ij,k} + \Sigma^{ji,k} & = & (\Sigma^{\alpha\beta,\gamma} + \Sigma^{\beta\alpha,\gamma})\dfrac{\partial y^i}{\partial x^\alpha}\dfrac{\partial y^j}{\partial x^\beta}\dfrac{\partial y^k}{\partial x^\gamma} \end{array}\right. \tag{2.3.12}$$

Therefore $(\Sigma^{ij} + \Sigma^{ji})$ and $(\Sigma^{ij,k} + \Sigma^{ji,k})$ are respectively components of tensor type (2,0) and (3,0) according to the definitions (2.2.5) and (2.2.6).

□

2.4 Dependence with respect to the metric

In this section, we consider a scalar field $\mathcal{L}$ depending on the metric tensor and its partial derivatives $\mathcal{L} = \mathcal{L}(g_{ij}, g_{ij,k}, g_{ij,kl})$ and $\mathcal{L} = \mathcal{L}(g_{\alpha\beta}, g_{\alpha\beta,\gamma}, g_{\alpha\beta,\gamma\lambda})$ respectively in system (y^i) and (x^α). The corresponding partial derivatives are noticed

$$\Lambda^{ij} = \frac{\partial\mathcal{L}}{\partial g_{ij}}, \qquad \Lambda^{ij,k} = \frac{\partial\mathcal{L}}{\partial g_{ij,k}}, \qquad \Lambda^{ij,kl} = \frac{\partial\mathcal{L}}{\partial g_{ij,kl}}. \tag{2.4.1}$$

According to the symmetry of $\mathbf{g}$, we have the major properties of symmetry

$$\Lambda^{ij} = \Lambda^{ji}, \qquad \Lambda^{ij,k} = \Lambda^{ji,k}, \qquad \Lambda^{ij,kl} = \Lambda^{ji,kl} = \Lambda^{ij,lk}. \tag{2.4.2}$$

Minor symmetry property $\Lambda^{ij,kl} = \Lambda^{kl,ij}$ is also satisfied but they are not necessary here. The form-invariance of the Lagrangian function $\mathcal{L}$ (which could be considered as a

necessary part of the Indifference of the constitutive laws with respect to Superimposed Rigid Body Motions e.g. [7]) takes the form of

$$\mathcal{L}(g_{\alpha\beta}, g_{\alpha\beta,\gamma}, g_{\alpha\beta,\gamma\lambda}) = \mathcal{L}(g_{ij}, g_{ij,k}, g_{ij,kl}). \tag{2.4.3}$$

Remark 2.4.1 *For recall, because no observer is distinguished, laws in physics have to be observer-invariant. For our particular case about the Lagrangian function formulation, this means that the functions $\mathcal{L}$ should have the same shape for arbitrary coordinate systems : they are called form-invariant.*

2.4.1 Metric tensor

According to the definitions (2.2.5) and (2.2.6), the components of the metric and its derivatives satisfy the following transformations

$$\left\{\begin{array}{rcl} g_{ij} & = & J_i^\alpha J_j^\beta g_{\alpha\beta} \\ g_{ij,k} & = & (J_{ik}^\alpha J_j^\beta + J_i^\alpha J_{jk}^\beta) g_{\alpha\beta} + J_i^\alpha J_j^\beta J_k^\gamma g_{\alpha\beta,\gamma} \\ g_{ij,kl} & = & (J_{ikl}^\alpha J_j^\beta + J_{ik}^\alpha J_{jl}^\beta + J_{il}^\alpha J_{jk}^\beta + J_i^\alpha J_{jkl}^\beta) g_{\alpha\beta} \\ & + & (J_{ik}^\alpha J_j^\beta J_l^\gamma + J_i^\alpha J_{jk}^\beta J_l^\gamma + J_{il}^\alpha J_j^\beta J_k^\gamma + J_i^\alpha J_{jl}^\beta J_k^\gamma + J_i^\alpha J_j^\beta J_{kl}^\gamma) g_{\alpha\beta,\gamma} \\ & + & (J_i^\alpha J_j^\beta J_k^\gamma J_l^\lambda) g_{\alpha\beta,\gamma\lambda} \end{array}\right. \tag{2.4.4}$$

According to the symmetry $J_{pq}^\mu = J_{qp}^\mu$ (the transformation is assumed of class C^2), one can write $J_{pq}^\mu = (1/2)(J_{pq}^\mu + J_{qp}^\mu)$, that induces [1] $(\partial J_{ij}^\alpha / \partial J_{pq}^\mu) = (1/2)\delta_\mu^\alpha(\delta_i^q \delta_j^p + \delta_j^q \delta_i^p)$, $(\partial J_{ijk}^\alpha / \partial J_{pq}^\mu) = 0$ and $(\partial J_i^\alpha / \partial J_{pq}^\mu) = 0$. Now, introducing the expressions (2.4.4) into the equality (2.4.3), and differentiating with respect to J_{pq}^μ give

$$\begin{array}{rcl} 0 & = & \Lambda^{ij,k}\left[\delta_\mu^\alpha(\delta_k^q\delta_i^p + \delta_i^q\delta_k^p)J_j^\beta + \delta_\mu^\beta(\delta_k^q\delta_j^p + \delta_j^q\delta_k^p)J_i^\alpha\right] g_{\alpha\beta} \\ & + & \Lambda^{ij,kl}\left[J_i^\alpha J_j^\beta \delta_\mu^\gamma(\delta_k^q\delta_l^p + \delta_l^q\delta_k^p) + J_i^\alpha J_k^\gamma \delta_\mu^\beta(\delta_j^q\delta_l^p + \delta_l^q\delta_j^p)\right] g_{\alpha\beta,\gamma} \\ & + & \Lambda^{ij,kl}\left[J_j^\beta J_k^\gamma \delta_\mu^\alpha(\delta_i^q\delta_l^p + \delta_l^q\delta_i^p) + J_i^\alpha J_l^\gamma \delta_\mu^\beta(\delta_j^q\delta_k^p + \delta_k^q\delta_j^p)\right] g_{\alpha\beta,\gamma} \\ & + & \Lambda^{ij,kl}\left[J_j^\beta J_l^\gamma \delta_\mu^\alpha(\delta_i^q\delta_k^p + \delta_k^q\delta_i^p)\right] g_{\alpha\beta,\gamma} \\ & + & \Lambda^{ij,kl}\left[J_{jk}^\beta \delta_\mu^\alpha(\delta_i^q\delta_l^p + \delta_l^q\delta_i^p) + J_{il}^\alpha \delta_\mu^\beta(\delta_j^q\delta_k^p + \delta_k^q\delta_j^p)\right] g_{\alpha\beta} \\ & + & \Lambda^{ij,kl}\left[J_{jl}^\beta \delta_\mu^\alpha(\delta_i^q\delta_k^p + \delta_k^q\delta_i^p) + J_{ik}^\alpha \delta_\mu^\beta(\delta_j^q\delta_l^p + \delta_l^q\delta_j^p)\right] g_{\alpha\beta} \end{array}$$

[1] If one does not consider the symmetric part then there is a loss of some terms in the derivation.

The previous equation is valid for an arbitrary coordinate transformation, in particular for the identity transformation : $x^\alpha = y^i$, $J^\alpha_i = \delta^\alpha_i$, $J^\alpha_{ij} = 0$. In such a case, we simplify

$$\begin{aligned}
0 &= \Lambda^{ij,k}\left[\delta^\alpha_\mu(\delta^q_k\delta^p_i + \delta^q_i\delta^p_k)\delta^\beta_j + \delta^\beta_\mu(\delta^q_k\delta^p_j + \delta^q_j\delta^p_k)\delta^\alpha_i\right] g_{\alpha\beta} \\
&+ \Lambda^{ij,kl}\left[\delta^\alpha_i\delta^\beta_j\delta^\gamma_\mu(\delta^q_k\delta^p_l + \delta^t_h\delta^p_k) + \delta^\alpha_i\delta^\gamma_k\delta^\beta_\mu(\delta^q_j\delta^p_l + \delta^q_l\delta^p_j)\right] g_{\alpha\beta,\gamma} \\
&+ \Lambda^{ij,kl}\left[\delta^\beta_j\delta^\gamma_k\delta^\alpha_\mu(\delta^q_i\delta^p_l + \delta^q_l\delta^p_i) + \delta^\alpha_i\delta^\gamma_l\delta^\beta_\mu(\delta^q_j\delta^p_k + \delta^q_k\delta^p_j)\right] g_{\alpha\beta,\gamma} \\
&+ \Lambda^{ij,kl}\left[\delta^\beta_j\delta^\gamma_l\delta^\alpha_\mu(\delta^q_i\delta^p_k + \delta^q_k\delta^p_i)\right] g_{\alpha\beta,\gamma}
\end{aligned}$$

Further simplifications and symmetry of Λ induce [2]

$$2\Lambda^{q\beta,\gamma p}g_{\mu\beta,\gamma} + 2\Lambda^{p\beta,\gamma q}g_{\mu\beta,\gamma} + \Lambda^{\alpha\beta,pq}g_{\alpha\beta,\mu} + \Lambda^{p\beta,q}g_{\mu\beta} + \Lambda^{q\beta,p}g_{\mu\beta} = 0. \tag{2.4.5}$$

In the particular case of a normal coordinate system, these reduce to $\Lambda^{p\mu,q} + \Lambda^{q\mu,p} = 0$. According to the symmetry of $\Lambda^{ij,k}$, for arbitrary indexes i, j, k, we have

$$\begin{aligned}
\Lambda^{ji,k} + \Lambda^{ki,j} &= 0 \\
\Lambda^{kj,i} + \Lambda^{ki,j} &= 0 \quad (i \longleftrightarrow k) \\
\Lambda^{ji,k} + \Lambda^{kj,i} &= 0 \quad (i \longleftrightarrow j)
\end{aligned}$$

then

$$\Lambda^{ji,k} = -\Lambda^{ki,j} = \Lambda^{kj,i} = -\Lambda^{ji,k},$$

and finally

$$\Lambda^{ji,k} = \Lambda^{ij,k} = 0. \tag{2.4.6}$$

Nevertheless equations (2.4.6) are only valid in normal coordinate system.

2.4.2 Introduction of tensors

Introducing the expressions (2.4.4) into (2.4.3) and differentiating respectively with respect to $g_{\alpha\beta,\gamma\lambda}$, $g_{\alpha\beta,\gamma}$, $g_{\alpha\beta}$, allows to write

$$\left\{\begin{aligned}
\Lambda^{\alpha\beta,\gamma\lambda} &= \Lambda^{ij,kl}J^\alpha_i J^\beta_j J^\gamma_k J^\lambda_l \\
\Lambda^{\alpha\beta,\gamma} &= \Lambda^{ij,kl}\frac{\partial g_{ij,kl}}{\partial g_{\alpha\beta,\gamma}} + \Lambda^{ij,k}\frac{\partial g_{ij,k}}{\partial g_{\alpha\beta,\gamma}} \\
\Lambda^{\alpha\beta} &= \Lambda^{ij,kl}\frac{\partial g_{ij,kl}}{\partial g_{\alpha\beta}} + \Lambda^{ij,k}\frac{\partial g_{ij,k}}{\partial g_{\alpha\beta}} + \Lambda^{ij}\frac{\partial g_{ij}}{\partial g_{\alpha\beta}}
\end{aligned}\right. \tag{2.4.7}$$

The first equation shows that $\Lambda^{ij,kl}$ are components of a tensor type $(4,0)$. Conversely the two others equations show that $\Lambda^{ij,k}$ and Λ^{ij} are not components of tensor. Thus

[2] The Latin indices and Greek indices mix since the transformation is the identity.

we should introduce two tensorial quantities instead of $\Lambda^{ij,k}$ and Λ^{ij} respectively. Let $\mathbf{h}$ an arbitrary symmetric tensor type $(0,2)$ (i.e. $\mathbf{h}$ follows the same rule of transformation (2.4.4) as $\mathbf{g}$), and Π^{ij} and $\Pi^{ij,k}$ (the comma "," doesn't represent partial derivative) two unknown quantities that verify the following equation

$$\Lambda^{ij,kl}h_{ij,kl} + \Lambda^{ij,k}h_{ij,k} + \Lambda^{ij}h_{ij} = \Lambda^{ij,kl}h_{ij|k|l} + \Pi^{ij,k}h_{ij|k} + \Pi^{ij}h_{ij} \tag{2.4.8}$$

The formulations of the covariant derivative (2.2.11) and (2.2.12) are introduced into (2.4.8), that reduces to an equality without covariant derivative terms. It depends on $\{\Gamma^k_{ij}, \Gamma^k_{ij,l}\}$, $\{h_{ij}, h_{ij,k}, h_{ij,kl}\}$, $\{\Lambda^{ij}, \Lambda^{ij,k}, \Lambda^{ij,kl}\}$ and $\{\Pi^{ij}, \Pi^{ij,k}\}$. Then, the lemma 2.3.2 is applied to the equation (2.4.8) in order to identify the coefficients of $h_{ij,k}$ and h_{ij} (the coefficients of $h_{ij,kl}$ are the same in both hand sides of equation). Some adequate permutations between the indices are necessary. For the sake of the clarity, details of calculus are reported in annex. Let us recall that Λ^{ij} , $\Lambda^{ij,k}$ and $\Lambda^{ij,kl}$ have properties of symmetry but it is not necessary the case for Π^{ij} and $\Pi^{ij,k}$. Thus we obtain the following equations

$$\left\{\begin{array}{rcl}
\Pi^{ij,k}_{(S)} & = & \Lambda^{ij,k} + 2\Gamma^i_{al}\Lambda^{aj,kl} + 2\Gamma^j_{al}\Lambda^{ia,kl} + \Gamma^k_{bl}\Lambda^{ij,bl} \\
\Pi^{ij}_{(S)} & = & \Lambda^{ij} + \Gamma^i_{ak,l}\Lambda^{aj,kl} + \Gamma^j_{ak,l}\Lambda^{ia,kl} \\
 & - & \Gamma^b_{al}\Gamma^i_{bk}\Lambda^{aj,kl} - \Gamma^b_{cl}\Gamma^j_{bk}\Lambda^{ic,kl} \\
 & - & \Gamma^i_{bl}\Gamma^j_{ck}\Lambda^{bc,kl} - \Gamma^j_{bl}\Gamma^i_{ck}\Lambda^{bc,kl} \\
 & - & \Gamma^b_{kl}\Gamma^i_{cb}\Lambda^{cj,kl} - \Gamma^b_{kl}\Gamma^j_{cb}\Lambda^{ci,kl} \\
 & + & (1/2)\Gamma^i_{ak}(\Pi^{aj,k} + \Pi^{ja,k}) + (1/2)\Gamma^j_{ak}(\Pi^{ia,k} + \Pi^{ai,k})
\end{array}\right. \tag{2.4.9}$$

where $\Pi^{ij,k}_{(S)} = (1/2)(\Pi^{ij,k} + \Pi^{ji,k})$ and $\Pi^{ij}_{(S)} = (1/2)(\Pi^{ij} + \Pi^{ji})$.

Lemma 2.4.1 *$F := \Lambda^{ij,kl}h_{ij,kl} + \Lambda^{ij,k}h_{ij,k} + \Lambda^{ij}h_{ij}$ is a scalar field.*

Proof. Let us notice $F = \Lambda^{ij,kl}h_{ij,kl} + \Lambda^{ij,k}h_{ij,k} + \Lambda^{ij}h_{ij}$ and $\overline{F} = \Lambda^{\alpha\beta,\gamma\lambda}h_{\alpha\beta,\gamma\lambda} + \Lambda^{\alpha\beta,\gamma}h_{\alpha\beta,\gamma} + \Lambda^{\alpha\beta}h_{\alpha\beta}$ respectively in system (y^i) and (x^α). According to (2.4.7),

$$\begin{array}{rcl}
\Lambda^{\alpha\beta,\gamma\lambda}h_{\alpha\beta,\gamma\lambda} & = & \left[\Lambda^{ij,kl}J^\alpha_i J^\beta_j J^\gamma_k J^\lambda_l\right] h_{\alpha\beta,\gamma\lambda} \\
\Lambda^{\alpha\beta,\gamma}h_{\alpha\beta,\gamma} & = & \left[\Lambda^{ij,kl}\dfrac{\partial g_{ij,kl}}{\partial g_{\alpha\beta,\gamma}} + \Lambda^{ij,k}\dfrac{\partial g_{ij,k}}{\partial g_{\alpha\beta,\gamma}}\right] h_{\alpha\beta,\gamma} \\
\Lambda^{\alpha\beta}h_{\alpha\beta} & = & \left[\Lambda^{ij,kl}\dfrac{\partial g_{ij,kl}}{\partial g_{\alpha\beta}} + \Lambda^{ij,k}\dfrac{\partial g_{ij,k}}{\partial g_{\alpha\beta}} + \Lambda^{ij}\dfrac{\partial g_{ij}}{\partial g_{\alpha\beta}}\right] h_{\alpha\beta}
\end{array}$$

By factorization of the coefficients of $\Lambda^{ij,kl}$, $\Lambda^{ij,k}$ and Λ^{ij} we obtain $\overline{F} = (a) + (b) + (c)$ with

$$\begin{aligned}
(a) &= \Lambda^{ij,kl}\left[\frac{\partial g_{ij,kl}}{\partial g_{\alpha\beta,\gamma\lambda}}h_{\alpha\beta,\gamma\lambda} + \frac{\partial g_{ij,kl}}{\partial g_{\alpha\beta,\gamma}}h_{\alpha\beta,\gamma} + \frac{\partial g_{ij,kl}}{\partial g_{\alpha\beta}}h_{\alpha\beta}\right] \\
(b) &= \Lambda^{ij,k}\left[\frac{\partial g_{ij,k}}{\partial g_{\alpha\beta,\gamma}}h_{\alpha\beta,\gamma} + \frac{\partial g_{ij,k}}{\partial g_{\alpha\beta}}h_{\alpha\beta}\right] \\
(c) &= \Lambda^{ij}\left[\frac{\partial g_{ij}}{\partial g_{\alpha\beta}}h_{\alpha\beta}\right]
\end{aligned}$$

According to the relations (2.4.4), the quantities in square brackets are simplified, (a) $= \Lambda^{ij,kl}\,[h_{ij,kl}]$, (b) $= \Lambda^{ij,k}\,[h_{ij,k}]$, (c) $= \Lambda^{ij}\,[h_{ij}]$ and thus $\overline{F} = F$.

□

Lemma 2.4.2 *(F - $\Lambda^{ij,kl}h_{ij|k|l}$) is a scalar.*

Proof. Let us notice $G := \Lambda^{ij,kl}h_{ij|k|l}$ and $\overline{G} := \Lambda^{\alpha\beta,\gamma\lambda}h_{\alpha\beta|\gamma|\lambda}$. By (2.4.7) we have

$$\Lambda^{\alpha\beta,\gamma\lambda}h_{\alpha\beta|\gamma|\lambda} = \Lambda^{ij,kl}J_i^\alpha J_j^\beta J_k^\gamma J_l^\lambda h_{\alpha\beta|\gamma|\lambda} \tag{2.4.10}$$

h being a tensor type (0,2), the second covariant derivative $h_{\alpha\beta|\gamma|\lambda}$ form the components of a tensor type (0,4). Consequently $J_i^\alpha J_j^\beta J_k^\gamma J_l^\lambda h_{\alpha\beta|\gamma|\lambda} = h_{ij|k|l}$, thus $\overline{G} = G$. By previous lemma, we have $\overline{F} - \overline{G} = F - G$.

□

Remark 2.4.2 *A direct and simple proof may be obtained by observing that Λ^{ijkl} is in fact a tensor type $(4,0)$ and $h_{ij|k|l}$ is a tensor type $(0,4)$. Their contraction is a scalar.*

Consequently, $\Pi^{ij,k}h_{ij|k} + \Pi^{ij}h_{ij}$ is a scalar for an arbitrary tensor type (0,2) **h**. Using the quotient theorem 2.3.1, $\Pi^{ij,k}_{(S)}$ and $\Pi^{ij}_{(S)}$ are components of tensor type (3,0) and (2,0) respectively, these tensors are also symmetric.

2.4.3 Theorem

The expressions of $\Pi^{ij,k}_{(S)}$ in (2.4.9) holds in an arbitrary coordinate system. In normal coordinate system, the Christoffel symbols vanish, e.g. [68] and we have, from (2.4.9), $\Pi^{ij,k}_{(S)} = \Lambda^{ij,k}$. However, from (2.4.6) $\Lambda^{ij,k} = 0$ in normal coordinate system, thus $\Pi^{ij,k}_{(S)} = 0$ in normal coordinate system and too for any other coordinate system, because $\Pi^{ij,k}_{(S)}$ are components of tensor. The first equation in (2.4.9) is simplified in any coordinate system

$$0 = \Lambda^{ij,k} + 2\Gamma^i_{al}\Lambda^{aj,kl} + 2\Gamma^j_{al}\Lambda^{ia,kl} + \Gamma^k_{bl}\Lambda^{ij,bl}. \tag{2.4.11}$$

We can etablish the following theorem :

Theorem 2.4.1 *Let a scalar field $\mathcal{L} = \mathcal{L}\left(g_{ij}, g_{ij,k}, g_{ij,kl}\right)$ defined on a Riemannian manifold. If $\dfrac{\partial \mathcal{L}}{\partial g_{ij,kl}} = 0$ then $\dfrac{\partial \mathcal{L}}{\partial g_{ij,k}} = 0$.*

Proof. $\forall\ i, j, k, l$, the condition $\Lambda^{ij,kl} = 0$ is introduced into (2.4.11).

□

Consequently, from the second equality of (2.4.9), we deduce $\dfrac{\partial \mathcal{L}}{\partial g_{ij}} = \Pi^{ij}_{(S)}$. An equivalent formulation of theorem 2.4.1 may be found in [Lovelock and Rund, [57]].

Theorem 2.4.2 *On a Riemannian manifold, there does not exist a scalar density as $\mathcal{L} = \mathcal{L}(g_{ij}, g_{ij,k})$ that only depends on the metric g_{ij} and their first partial derivatives $g_{ij,k}$.*

2.4.4 Discussion

In any coordinate system, we have the following decomposition

$$\left\{ \begin{array}{rcl} \Pi^{ij} & = & (1/2)(\Pi^{ij} + \Pi^{ji}) + (1/2)(\Pi^{ij} - \Pi^{ji}) \\ \Pi^{ij,k} & = & (1/2)(\Pi^{ij,k} + \Pi^{ji,k}) + (1/2)(\Pi^{ij,k} - \Pi^{ji,k}) \end{array} \right. \tag{2.4.12}$$

In [57], the quantities Π^{ij} and $\Pi^{ij,k}$ are assumed to be symmetric with respect to the indices i and j : $\Pi^{ij} = \Pi^{ji}$, $\Pi^{ij,k} = \Pi^{ji,k}$ and it is proven that the quantities $\Pi^{ij,k}$ are always null. In the present study it has been proven that only the symmetric part $\Pi^{ij,k}_{(S)}$ is null : the quantities $\Pi^{ij,k}$ are skew-symmetric $\Pi^{ij,k} = -\Pi^{ji,k}$. The present study is slightly more general than the result presented in [57]. The metric is a tensor and consequently the Lagrangian $\mathcal{L}(\mathbf{g})$ depends on a tensor. To extend the arguments of $\mathcal{L}$, defined on Riemannian manifold endowed with an affine connection ∇, the new form is then $\mathcal{L}(\mathbf{g}, \nabla\mathbf{g}, \nabla^2\mathbf{g})$ where all the arguments are tensors. The corresponding form in the coordinate system (x^α) is $\mathcal{L}(g_{\alpha\beta}, g_{\alpha\beta|\gamma}, g_{\alpha\beta|\gamma|\lambda})$. If the connection is Euclidean (derived from the metric) then we have $g_{\alpha\beta|\gamma} \equiv g_{\alpha\beta,\gamma}$ since $\Gamma^\gamma_{\alpha\beta} \sim g_{\alpha\beta,\gamma}$. In [57], the used connection is implicitly that of Levi-Civita, this is the reason why we studied the form with partial derivatives $\mathcal{L}(g_{\alpha\beta}, g_{\alpha\beta,\gamma}, g_{\alpha\beta,\gamma\lambda})$. Another motivation is that, according to the Lemma of Ricci e.g. [18], the covariant derivative of the metric tensor $\mathbf{g}$, in the sense of Levi-Civita connection, is identically equal to zero.

2.5 Invariance with respect to the connection

The metric is imposed by the ambient space (Euclidean space) and there exist many possibilities for the affine connection. It is possible to impose restrictions on the possible form of connections. We demand that the metric be covariantly constant : $\nabla\mathbf{g} \equiv 0$. In such a case the connection is said compatible with the metric. The choice of the connection is arbitrary but it is worth to use a connection compatible with the metric. This implies that $\nabla\mathbf{g}$ cannot be an explicit argument of the Lagrangian $\mathcal{L}$. This is the

reason why we consider ∇ as argument rather than $\nabla\mathbf{g}$. We labeled the biconnection $\nabla^2 = \nabla\circ\nabla$. In order to extend the list of arguments of $\mathcal{L}$, we consider the following forms : $\mathcal{L}(\mathbf{g},\nabla)$, $\mathcal{L}(\mathbf{g},\nabla^2)$ and $\mathcal{L}(\mathbf{g},\nabla,\nabla^2)$. However it should be stressed that the connection is not tensor conversely to the metric, thus we aim to obtain tensorial arguments instead of the connection and/or the bi-connection.

2.5.1 Preliminary

We define the invariance of any scalar field (more precisely the form-invariance) : $\mathcal{L}(X,Y) = \mathcal{L}(X',Y')$ with both formal arguments X and Y defined in any two coordinate systems (with and without ').

Lemma 2.5.1 *Let us consider arbitrary constants K_1, K_2, C_1, C_2, C_3 and the variables x, x', y, y', p, p', q, q' which follow the transformations*

$$\left\{\begin{array}{lcl} x' & = & K_1\ x + K_2 \\ y' & = & K_1\ y \\ p' & = & C_1\ p + C_2\ (x+y) + C_3 \\ q' & = & C_1\ q \end{array}\right. \tag{2.5.1}$$

Now let us consider a scalar function $\mathcal{L}$ which satisfies the equations (form-invariance)

1. $\mathcal{L}(x,y) = \mathcal{L}(x',y')$
2. $\mathcal{L}(p,q) = \mathcal{L}(p',q')$
3. $\mathcal{L}(x,y,p,q) = \mathcal{L}(x',y',p',q')$.

If $(\partial K_1/\partial K_2) = 0$, $(\partial K_1/\partial C_3) = 0$, $(\partial K_2/\partial C_3) = 0$, $(\partial C_1/\partial C_3) = 0$ then, from equation (1.) we have $\mathcal{L}(y) = \mathcal{L}(y')$, from equation (2.) we have $\mathcal{L}(q) = \mathcal{L}(q')$, from equation (3.) we have $\mathcal{L}(y,q) = \mathcal{L}(y',q')$.

Proof.

Equation 1 According to (2.5.1) we have $\mathcal{L}(x,y) = \mathcal{L}(K_1\ x + K_2, K_1\ y)$. We differentiate this equation with respect to K_2, to find

$$\begin{array}{lcl} 0 & = & \dfrac{\partial\mathcal{L}}{\partial x'}\dfrac{\partial x'}{\partial K_2} + \dfrac{\partial\mathcal{L}}{\partial y'}\dfrac{\partial y'}{\partial K_2} \\ 0 & = & \dfrac{\partial\mathcal{L}}{\partial x'}\left[\dfrac{\partial K_1}{\partial K_2}\ x + 1\right] + \dfrac{\partial\mathcal{L}}{\partial y'}\dfrac{\partial K_1}{\partial K_2}\ y \end{array}$$

which involves that $\partial\mathcal{L}/\partial x' = 0$ if $\partial K_1/\partial K_2 = 0$. Then, according to $(\partial\mathcal{L}/\partial x) = (\partial\mathcal{L}/\partial x')(\partial x'/\partial x)$, we prove that $\partial\mathcal{L}/\partial x = 0$.

Equation 2 According to (2.5.1) we have $\mathcal{L}(p,q) = \mathcal{L}(C_1\ p + C_2\ (x+y) + C_3, C_1\ q)$. We differentiate this equation with respect to C_3, to find

$$\begin{aligned} 0 &= \frac{\partial \mathcal{L}}{\partial p'}\frac{\partial p'}{\partial C_3} + \frac{\partial \mathcal{L}}{\partial q'}\frac{\partial q'}{\partial C_3} \\ 0 &= \frac{\partial \mathcal{L}}{\partial p'}\left[\frac{\partial C_1}{\partial C_3}\ p + \frac{\partial C_2}{\partial C_3}\ (x+y) + 1\right] + \frac{\partial \mathcal{L}}{\partial q'}\frac{\partial C_1}{\partial C_3}\ q \end{aligned}$$

which involves that $\partial\mathcal{L}/\partial p' = 0$ if $\partial C_1/\partial C_3 = 0$, the term in square brackets not vanishing. Then, according to $(\partial\mathcal{L}/\partial p) = (\partial\mathcal{L}/\partial p')(\partial p'/\partial p)$, we prove that $\partial\mathcal{L}/\partial p = 0$. Finally we obtain $\mathcal{L}(q) = \mathcal{L}(q')$.

Equation 3 According to (2.5.1) we have $\mathcal{L}(x,y,p,q) = \mathcal{L}(K_1\ x + K_2, K_1\ y, C_1\ p + C_2\ (x+y) + C_3, C_1\ q)$. We differentiate this equation with respect to C_3, to find

$$\begin{aligned} 0 &= \frac{\partial \mathcal{L}}{\partial x'}\frac{\partial x'}{\partial C_3} + \frac{\partial \mathcal{L}}{\partial y'}\frac{\partial y'}{\partial C_3} + \frac{\partial \mathcal{L}}{\partial p'}\frac{\partial p'}{\partial C_3} + \frac{\partial \mathcal{L}}{\partial q'}\frac{\partial q'}{\partial C_3} \\ 0 &= \frac{\partial \mathcal{L}}{\partial x'}\left[\frac{\partial K_1}{\partial C_3}\ x + \frac{\partial K_2}{\partial C_3}\right] + \frac{\partial \mathcal{L}}{\partial y'}\frac{\partial K_1}{\partial C_3}\ y + \frac{\partial \mathcal{L}}{\partial p'}\left[\frac{\partial C_1}{\partial C_3}\ p + \frac{\partial C_2}{\partial C_3}\ (x+y) + 1\right] \\ &+ \frac{\partial \mathcal{L}}{\partial q'}\frac{\partial C_1}{\partial C_3}\ q \end{aligned}$$

which involves that $\partial\mathcal{L}/\partial p' = 0$ if $\partial K_1/\partial C_3 = 0$, $\partial K_2/\partial C_3 = 0$, $\partial C_1/\partial C_3 = 0$. Then we have too $\partial\mathcal{L}/\partial p = 0$. According to $(\partial\mathcal{L}/\partial x) = (\partial\mathcal{L}/\partial p')(\partial p'/\partial x)$, we prove that $\partial\mathcal{L}/\partial x = 0$. To finish, according to $(\partial\mathcal{L}/\partial x) = (\partial\mathcal{L}/\partial x')(\partial x'/\partial x) = (\partial\mathcal{L}/\partial x')\ K_1$, we prove that $\partial\mathcal{L}/\partial x' = 0$. Finally we obtain $\mathcal{L}(y,q) = \mathcal{L}(y',q')$.

□

Remark 2.5.1 *The previous proof is based on the principle of fields invariance introduced by Lovelock and Rund [57]. It is equivalent to the form-invariance, a term borrowed from [79].*

In an arbitrary coordinate system (y^i), the components of the metric, the connection and the bi-connection are respectively g_{ij}, Γ^k_{ij} and $\Gamma^k_{ij,l} + \Gamma^m_{ij}\Gamma^k_{lm}$. The forms $\mathcal{L}(g,\nabla)$, $\mathcal{L}(g,\nabla^2)$ and $\mathcal{L}(g,\nabla,\nabla^2)$ are then explicitly written as $\mathcal{L}(g_{ij},\Gamma^k_{ij})$, $\mathcal{L}\left(g_{ij},\Gamma^k_{ij,l} + \Gamma^m_{ij}\Gamma^k_{lm}\right)$ and $\mathcal{L}\left(g_{ij},\Gamma^k_{ij},\Gamma^k_{ij,l} + \Gamma^m_{ij}\Gamma^k_{lm}\right)$, respectively. Let (x^α) an other coordinate system, let us assume the form-invariance of the scalar field $\mathcal{L}$ (three cases) :

$$\left\{\begin{aligned} \mathcal{L}(\Gamma^k_{ij}) &= \mathcal{L}(\Gamma^\gamma_{\alpha\beta}) \\ \mathcal{L}(\Gamma^k_{ij,l} + \Gamma^m_{ij}\Gamma^k_{lm}) &= \mathcal{L}(\Gamma^\gamma_{\alpha\beta,\lambda} + \Gamma^\mu_{\alpha\beta}\Gamma^\gamma_{\lambda\mu}) \\ \mathcal{L}(\Gamma^k_{ij},\Gamma^k_{ij,l} + \Gamma^m_{ij}\Gamma^k_{lm}) &= \mathcal{L}(\Gamma^\gamma_{\alpha\beta},\Gamma^\gamma_{\alpha\beta,\lambda} + \Gamma^\mu_{\alpha\beta}\Gamma^\gamma_{\lambda\mu}) \end{aligned}\right. \tag{2.5.2}$$

where the components of the metric will be omitted for the sake of simplicity. For further applications, let us introduce the following components

$$\left\{\begin{array}{rcl} \mathbb{T}^k_{ij} & = & (1/2)\left(\Gamma^k_{ij}-\Gamma^k_{ji}\right) \\ \mathbb{S}^k_{ij} & = & (1/2)\left(\Gamma^k_{ij}+\Gamma^k_{ji}\right) \\ \mathbb{B}^k_{lij} & = & (1/2)\left(\Gamma^k_{ij,l}+\Gamma^m_{ij}\Gamma^k_{lm}-\Gamma^k_{lj,i}-\Gamma^m_{lj}\Gamma^k_{im}\right) \\ \mathbb{A}^k_{lij} & = & (1/2)\left(\Gamma^k_{ij,l}+\Gamma^m_{ij}\Gamma^k_{lm}+\Gamma^k_{lj,i}+\Gamma^m_{lj}\Gamma^k_{im}\right) \end{array}\right. \tag{2.5.3}$$

According to (2.5.3), a permutation between i and j allows the decomposition $\Gamma^k_{ij}=\mathbb{S}^k_{ij}+\mathbb{T}^k_{ij}$. A permutation between i and l allows the decomposition $\Gamma^k_{ij,l}+\Gamma^m_{ij}\Gamma^k_{lm}=\mathbb{A}^k_{lij}+\mathbb{B}^k_{lij}$. A first permutation between i and j then an other successive permutation between i and l allow simultaneous decompositions $\Gamma^k_{ij}=\mathbb{S}^k_{ij}+\mathbb{T}^k_{ij}$ and $\Gamma^k_{ij,l}+\Gamma^m_{ij}\Gamma^k_{lm}=\mathbb{A}^k_{lij}+\mathbb{B}^k_{lij}$. Details of calculus are given in annex. Thanks to these decompositions, the form-invariance of $\mathcal{L}$ (2.5.2) becomes

$$\left\{\begin{array}{rcl} \mathcal{L}(\mathbb{S}^k_{ij},\mathbb{T}^k_{ij}) & = & \mathcal{L}(\mathbb{S}^\gamma_{\alpha\beta},\mathbb{T}^\gamma_{\alpha\beta}) \\ \mathcal{L}(\mathbb{A}^k_{lij},\mathbb{B}^k_{lij}) & = & \mathcal{L}(\mathbb{A}^\gamma_{\lambda\alpha\beta},\mathbb{B}^\gamma_{\lambda\alpha\beta}) \\ \mathcal{L}(\mathbb{S}^k_{ij},\mathbb{T}^k_{ij},\mathbb{A}^k_{lij},\mathbb{B}^k_{lij}) & = & \mathcal{L}(\mathbb{S}^\gamma_{\alpha\beta},\mathbb{T}^\gamma_{\alpha\beta},\mathbb{A}^\gamma_{\lambda\alpha\beta},\mathbb{B}^\gamma_{\lambda\alpha\beta}) \end{array}\right. \tag{2.5.4}$$

2.5.2 Application

Let us consider the following identification of variables x, x', y, y', p, p', q, q' :

$$x=\mathbb{S}^k_{ij},\quad y=\mathbb{T}^k_{ij},\quad p=\mathbb{A}^k_{lij},\quad q=\mathbb{B}^k_{lij}, \tag{2.5.5}$$

$$x'=\mathbb{S}^\gamma_{\alpha\beta},\quad y'=\mathbb{T}^\gamma_{\alpha\beta},\quad p'=\mathbb{A}^\gamma_{\lambda\alpha\beta},\quad q'=\mathbb{B}^\gamma_{\lambda\alpha\beta}. \tag{2.5.6}$$

The transformation laws between the above variables take the form of (2.5.1) with (see annex)

$$\left\{\begin{array}{rcl} K_1 & = & J^i_\alpha J^j_\beta A^\gamma_k \\ K_2 & = & J^j_{\alpha\beta}A^\gamma_j \\ C_1 & = & J^i_\alpha J^j_\beta J^l_\lambda A^\gamma_k \\ C_2 & = & J^i_{\alpha\lambda}J^j_\beta A^\gamma_k+J^i_\lambda J^j_{\alpha\beta}A^\gamma_k+J^i_\alpha J^j_{\beta\lambda}A^\gamma_k \\ C_3 & = & J^i_\mu J^l_\lambda J^j_{\alpha\beta}A^\gamma_j A^\mu_{il}+J^i_{\mu\lambda}J^j_{\alpha\beta}A^\mu_i A^\gamma_j \end{array}\right. \tag{2.5.7}$$

We have $\partial K_1/\partial K_2=0$, $\partial K_1/\partial C_3=0$, $\partial K_2/\partial C_3=0$, $\partial C_1/\partial C_3=0$. According to lemma 2.5.1, the invariance of $\mathcal{L}$ (2.5.4) means

$$\left\{\begin{array}{rcl} \mathcal{L}(\mathbb{T}^k_{ij}) & = & \mathcal{L}(\mathbb{T}^\gamma_{\alpha\beta}) \\ \mathcal{L}(\mathbb{B}^k_{lij}) & = & \mathcal{L}(\mathbb{B}^\gamma_{\lambda\alpha\beta}) \\ \mathcal{L}(\mathbb{T}^k_{ij},\mathbb{B}^k_{lij}) & = & \mathcal{L}(\mathbb{T}^\gamma_{\alpha\beta},\mathbb{B}^\gamma_{\lambda\alpha\beta}) \end{array}\right. \tag{2.5.8}$$

We now identify the components of torsion tensor by $\aleph^k_{ij} = 2\mathbb{T}^k_{ij}$ and the components of curvature tensor by $\mathfrak{R}^k_{lij} = 2\mathbb{B}^k_{lij}$. From (2.5.8) we have

$$\left\{\begin{array}{rcl} \mathcal{L}(\aleph^k_{ij}) & = & \mathcal{L}(\aleph^\gamma_{\alpha\beta}) \\ \mathcal{L}(\mathfrak{R}^k_{lij}) & = & \mathcal{L}(\mathfrak{R}^\gamma_{\lambda\alpha\beta}) \\ \mathcal{L}(\aleph^k_{ij}, \mathfrak{R}^k_{lij}) & = & \mathcal{L}(\aleph^\gamma_{\alpha\beta}, \mathfrak{R}^\gamma_{\lambda\alpha\beta}) \end{array}\right. \tag{2.5.9}$$

2.5.3 Synthesis

For the sake of the simplicity we have previously omitted the argument g_{ij}. Adding this argument does not change the proof. The overall result then includes the metric, the connection, and the bi-connection as arguments of the Lagrangian function $\mathcal{L}$. We also have the following Form-Invariance :

$$\left\{\begin{array}{rcl} \mathcal{L}(g_{ij}, \aleph^k_{ij}) & = & \mathcal{L}(g_{\alpha\beta}, \aleph^\gamma_{\alpha\beta}) \\ \mathcal{L}(g_{ij}, \mathfrak{R}^k_{lij}) & = & \mathcal{L}(g_{\alpha\beta}, \mathfrak{R}^\gamma_{\lambda\alpha\beta}) \\ \mathcal{L}(g_{ij}, \aleph^k_{ij}, \mathfrak{R}^k_{lij}) & = & \mathcal{L}(g_{\alpha\beta}, \aleph^\gamma_{\alpha\beta}, \mathfrak{R}^\gamma_{\lambda\alpha\beta}) \end{array}\right. \tag{2.5.10}$$

All the arguments of $\mathcal{L}$ are components of tensors, they are invariant under the action of the diffeomorphism (in the sense that they transform covariantly according to usual tensor transformations depending of their type). Therefore, the Lagrangian function is form-invariant. The components of torsion are explicitly defined according to the coefficients of connection and the components of curvature are explicitly defined according to the coefficients of biconnection. From (2.5.10) we have

$$\left\{\begin{array}{rcl} \mathcal{L}(g_{ij}, \Gamma^k_{ij}) & = & \mathcal{L}(g_{\alpha\beta}, \Gamma^\gamma_{\alpha\beta}) \\ \mathcal{L}(g_{ij}, \Gamma^k_{ij,l} + \Gamma^m_{ij}\Gamma^k_{lm}) & = & \mathcal{L}(g_{\alpha\beta}, \Gamma^\gamma_{\alpha\beta,\lambda} + \Gamma^\mu_{\alpha\beta}\Gamma^\gamma_{\lambda\mu}) \\ \mathcal{L}(g_{ij}, \Gamma^k_{ij}, \Gamma^k_{ij,l} + \Gamma^m_{ij}\Gamma^k_{lm}) & = & \mathcal{L}(g_{\alpha\beta}, \Gamma^\gamma_{\alpha\beta}, \Gamma^\gamma_{\alpha\beta,\lambda} + \Gamma^\mu_{\alpha\beta}\Gamma^\gamma_{\lambda\mu}) \end{array}\right. \tag{2.5.11}$$

The results are summarized in the following theorem :

Theorem 2.5.1 *Let a Riemannian manifold $(X, \mathbf{g})$ embedded into an Euclidean space and endowed with an affine connection ∇ compatible with the metric ($\nabla\mathbf{g} = 0$). To the connection are associated the torsion tensor $\aleph$ and the curvature tensor $\mathfrak{R}$. For any scalar field $\mathcal{L}$ defined on X, the form-invariance induces*

$$\mathcal{L}(\mathbf{g}, \nabla) = \mathcal{L}(\mathbf{g}, \aleph), \quad \mathcal{L}(\mathbf{g}, \nabla^2) = \mathcal{L}(\mathbf{g}, \mathfrak{R}), \quad \mathcal{L}(\mathbf{g}, \nabla, \nabla^2) = \mathcal{L}(\mathbf{g}, \aleph, \mathfrak{R}) \tag{2.5.12}$$

The equations (2.5.12) can be read in the two directions :
- *$\mathcal{L} = \mathcal{L}(\mathbf{g}, \nabla)$ is form-invariant if and only if $\mathcal{L} = \mathcal{L}(\mathbf{g}, \aleph)$*
- *$\mathcal{L} = \mathcal{L}(\mathbf{g}, \nabla^2)$ is form-invariant if and only if $\mathcal{L} = \mathcal{L}(\mathbf{g}, \mathfrak{R})$*
- *$\mathcal{L} = \mathcal{L}(\mathbf{g}, \nabla, \nabla^2)$ is form-invariant if and only if $\mathcal{L} = \mathcal{L}(\mathbf{g}, \aleph, \mathfrak{R})$*

Under the same hypothesis as for the theorem 2.5.1, we have the corollary :

Corollary 2.5.2 *On Riemannian manifold, there does not exist a scalar field $\mathcal{L}$ (form-invariant) which depends on the metric* $\mathbf{g}$ *and the Levi-Civita connection* $\overline{\nabla}$.

Proof. According to the theorem 2.2.1 and theorem 2.5.1 : $\mathcal{L}(\mathbf{g}, \overline{\nabla}) = \mathcal{L}(\mathbf{g}, \aleph = 0) = \mathcal{L}(\mathbf{g})$.

□

Remark 2.5.2 *The corollary 2.5.2 can be proven by using the components formulation. Indeed, the coefficients of the Levi-Civita connection are the Christoffel symbols labeled* $\overline{\Gamma}^k_{ij}$ *(2.2.10) which depend on the components of the metric and its first partial derivatives e.g. [68]. According to the theorem 2.4.2 :* $\mathcal{L}(g_{ij}, \overline{\Gamma}^k_{ij}) = \mathcal{L}(g_{ij}, g_{ij,k}) = \mathcal{L}(g_{ij})$.

Remark 2.5.3 *The extension consists in using an affine connection which does not derive from a metric although compatible with the metric, and thus to introduce the torsion and/or the curvature to describe the dislocations and the disclinations field e.g. [61], [74]. However the connection of Levi-Civita is compatible, is derived from the metric and especially the associated torsion necessary vanishes (theorem 2.2.1). Although essential and used for models of continuous medium, the use of Levi-Civita connection seems limited and is not adapted in this framework.*

2.6 Strain gradient continuum

2.6.1 Interpretation

According to the form of the strain energy potential (part of the Lagrangian function), the potential energy of a system depends on the strain tensor $\mathbf{E}$ and possibly on other arguments. In Riemannian geometry, the metric $\mathbf{g}$ and the affine connection ∇ are fundamental tools to describe the tensor fields and their derivatives defined on manifold. The torsion $\aleph$ and the curvature $\mathfrak{R}$ are tensors which are associated to the affine connection. This geometrical approach is applied in the study of defects through continuous media e.g. [50], [61], [74], [85] and more generally in physics, e.g. [18], [46]. For continuum mechanics, the metric tensor $\mathbf{g}$ is related with the strain tensor $\mathbf{E}$, by the following relation [75] :

$$\mathbf{g} = \mathbf{I} + 2\mathbf{E}, \qquad g_{ij} = \delta_{ij} + 2E_{ij} \tag{2.6.1}$$

where $\mathbf{I}$ is the identity tensor type $(0, 2)$. It should be also stressed that the relation (2.6.1) implicitly assumes that material coordinates within the continuum are used for describing the continuum transformation (i.e. we use Lagrangian description with convected vector base e.g. [74]). Consequently the first type of the scalar field (Lagrangian) $\mathcal{L}$ we would like to analyze, takes the form of (by abuse of notation)

$$\mathcal{L}(g_{ij}, g_{ij,k}, g_{ij,kl}) \equiv \mathcal{L}(E_{ij}, E_{ij,k}, E_{ij,kl}). \tag{2.6.2}$$

In the framework of strain gradient continuum, the forms of Lagrangian functions are $\mathcal{L}(E_{ij}, E_{ij|k})$ for first or $\mathcal{L}(E_{ij}, E_{ij|k}, E_{ij|k|l})$ for second strain gradient model. Many strain

gradient models use an affine connection which derives from the metric. Consequently, the Lagrangian is respectively reformulated by $\mathcal{L}(E_{ij}, E_{ij,k})$ and $\mathcal{L}(E_{ij}, E_{ij,k}, E_{ij,kl})$. According to the theorem 2.4.2 [57], the form $\mathcal{L}(E_{ij}, E_{ij,k})$ does not exist. Consequently the possible forms are e.g. [1] :

- $\mathcal{L}(E_{ij})$ which is used in classical elasticity theory.
- $\mathcal{L}(E_{ij}, E_{ij,kl})$ and $\mathcal{L}(E_{ij}, E_{ij,k}, E_{ij,kl})$ which are used in strain gradient theory.

In the case where the affine connection is Euclidean[3], among the Lagrangian arguments we find necessarily the second order of the derivative of the strain. Thus the strain gradient theory is more rigorously named the second strain gradient theory, also called continuum of grade three e.g. [1]. But the partial derivatives of tensor components are not necessary the components of tensor, therefore the quantities $E_{ij,k}$ and $E_{ij,kl}$ may not represent physical quantities, in general. Indeed, according to the equation between the strain and the metric (2.6.1), we observe that the components $g_{ij,k}$ and $g_{ij,kl}$ are not components of tensor by (2.4.4). We choice then a non Euclidean connection but compatible with the metric. The affine connection is not a tensor however, the studied forms $\mathcal{L}(\mathbf{g}, \nabla)$, $\mathcal{L}(\mathbf{g}, \nabla^2)$ and $\mathcal{L}(\mathbf{g}, \nabla, \nabla^2)$ are respectively equivalent to $\mathcal{L}(\mathbf{g}, \aleph)$, $\mathcal{L}(\mathbf{g}, \mathfrak{R})$ and $\mathcal{L}(\mathbf{g}, \aleph, \mathfrak{R})$. All the arguments are tensors and can represent physical quantities. The proof is based on the invariance principle, essential criterium in study of fields in physics.

Let us consider a continuous medium (continuum) modelled by a Riemannian manifold endowed with an affine connection (compatible with the metric). The choice of the continuum comes owing to the fact that torsion is null (Riemannian approach) or not (Cartan approach). By the way, the introduction of torsion and curvature was done in previous works as tensorial measures of Volterra dislocations and disclinations e.g. [61], [74].

- $\mathcal{L}(\mathbf{g}, \aleph = 0, \mathfrak{R} = 0)$ corresponds to an elastic energy strain function.
- $\mathcal{L}(\mathbf{g}, \aleph)$ is associated to an elastic continuum with dislocation.
- $\mathcal{L}(\mathbf{g}, \aleph, \mathfrak{R})$ is associated to an elastic continuum with dislocation and disclination.

The elasticity of the continuum refers to the metric as argument of the Lagrangian whereas the dislocations and disclinations are described by the torsion and the curvature tensors associated to the affine connection ∇ e.g. [61], [73].

Remark 2.6.1 *For establishing the form-invariance requirement we are searching for constitutive laws of higher gradient continuum mechanics. We do not take all applicable arbitrary coordinate systems. We limit to coordinate systems x^α and y^i that are all diffeomorphically equivalent to each other. This is obviously a larger class than the orthogonal transformations (rotation and translation of coordinates) and even much larger than the class of coordinate systems related by linear transformations, but it should be again reminded that still just a small fraction of all possible coordinate systems e.g. [74]. Further studies in this direction still hold as great challenge, by considering the concept of path-dependent integration method e.g. [46].*

[3]The Euclidean connection derived from the metric tensor of a referential body was mostly the connection used in mechanics for over two centuries, e.g. [74].

2.6.2 Comparison

In this subsection we aim to compare the model previously introduced (with metric, torsion and curvature as arguments of $\mathcal{L}$) and the model of second strain gradient elasticity initially introduced by Mindlin in [65]. The main difference concerns the arguments of the Lagrangean function or elastic potential energy.

What order gradient for the elastic continuum ? According to [65] the potential energy-density $\mathcal{W}$, that we can also label $\mathcal{L}$, takes the form of $\mathcal{L}(\varepsilon, \nabla\varepsilon, \nabla\nabla\varepsilon)$ where the symbol ∇ is the gradient operator and $\varepsilon := (1/2)(\nabla\mathbf{u} + \nabla^T\mathbf{u})$ with $\mathbf{u}$ the displacement. For sake of simplicity we label $\nabla\nabla\varepsilon := \nabla^2\varepsilon$. We notice that

- ε corresponds to first gradient of displacement
- $\nabla\varepsilon$ corresponds to first strain gradient, or second gradient of displacement
- $\nabla^2\varepsilon$ corresponds to second gradient of strain, or third gradient of displacement.

Thus the terminology adopted for the models $\mathcal{L}(\varepsilon, \nabla\varepsilon)$ (see [66]) and $\mathcal{L}(\varepsilon, \nabla\varepsilon, \nabla^2\varepsilon)$ (see [65]) is associated with the order of derivation in space of the argument strain ε. For the general form $\mathcal{L}(\mathbf{g}, \aleph, \mathfrak{R})$, we adopt the terminology borrowed in [65] according to the dimension[4] of variables $\nabla\varepsilon$ and $\nabla^2\varepsilon$. The ranks (see definition 2.2.1) of the different arguments of $\mathcal{L}$ are : the metric $\mathbf{g}$ is a second-order tensor, the torsion $\aleph$ is a third-order tensor and the curvature $\mathfrak{R}$ is a four-order tensor. Associating the dimensions of $\nabla\varepsilon$ and $\nabla^2\varepsilon$ with the ranks of $\aleph$ and $\mathfrak{R}$, we may define :

- $\mathcal{L}(\mathbf{g}, \aleph)$ is a contribution in the so-called first strain gradient elasticity, or second gradient of displacement
- $\mathcal{L}(\mathbf{g}, \mathfrak{R})$ is a contribution in the so-called second strain gradient elasticity, or third gradient of displacement
- $\mathcal{L}(\mathbf{g}, \aleph, \mathfrak{R})$ is also a contribution in the so-called second strain gradient elasticity, or third gradient of displacement

It is important to know if the gradient concerns the strain or the displacement. In all the cases the term "second gradient" appears. This chapter may then be relabelled : "On the Form-Invariance of Lagrangian Function for Second Gradient Continuum" [4].

How can we interpret the arguments of the energy ? The main different between this present model with the one of Mindlin [65] is that all the arguments $\mathbf{g}$, $\aleph$ and $\mathfrak{R}$ are tensors, while, in general, $\nabla\varepsilon$ and $\nabla^2\varepsilon$ are not tensors. In the form $\mathcal{L}(\varepsilon, \nabla\varepsilon, \nabla^2\varepsilon)$, all the arguments are defined in terms of the displacement $\mathbf{u}$ and the gradient operator ∇. In the form $\mathcal{L}(\mathbf{g}, \aleph, \mathfrak{R})$, all the arguments are defined in terms of the metric $\mathbf{g}$ (similar to the strain ε) or an affine connection, also labelled ∇, which is compatible with the metric ($\nabla\mathbf{g} = 0$). The notion of derivation in the model $\mathcal{L}(\mathbf{g}, \aleph, \mathfrak{R})$ is more general than in the model $\mathcal{L}(\varepsilon, \nabla\varepsilon, \nabla^2\varepsilon)$, due to the presence of the covariant derivative induced by the affine connection. In the study of fields in physics, the tensors are adapted to describe the physical phenomena. According to e.g. [61], [44], the physical interpretation of the torsion and the curvature is given in terms of dislocations and disclinations of Volterra. More

[4] ε : dimension 2 ; $\nabla\varepsilon$: dimension 3 ; $\nabla^2\varepsilon$: dimension 4.

precisely in [73] and also [74], the arguments $\aleph$ and $\mathfrak{R}$ are given in terms of discontinuity fields : the torsion is used to describe the discontinuity fields of scalar fields like dislocations, and the curvature is used to describe the discontinuity fields of vectorial fields like disclinations. Consequently, if we study an elastic continuum with dislocations we will use the form of $\mathcal{L}(\mathbf{g}, \aleph)$. If we study an elastic continumm with disclinations without dislocation we use the form of $\mathcal{L}(\mathbf{g}, \mathfrak{R})$, and if we study an elastic continuum with disclinations and dislocations we use the form of $\mathcal{L}(\mathbf{g}, \aleph, \mathfrak{R})$. These three forms then permit to capture the dislocations and/or the disclinations in an elastic material, and in particular the torsion and the curvature are considered like independent variables : we have successively introduce forms with either only $\aleph$, either only $\mathfrak{R}$, or $\aleph$ and $\mathfrak{R}$, in addition to the metric. Our model permits then to distinghuish the Riemannian geometry (without torsion) to the non-Riemannian geometry, e.g. [44]. The model initially introduced by Mindlin [65] is a more completed form of the potential energy-density which includes the form in [66]. This is a generalization of linear elasticity which includes higher-order terms to account for micro-structures or couple stress effects in materials. But many works have also emphasized the link with the disclocations and disclinations e.g. [54]. In addition to Cauchy-like stress tensors, hyperstresses (double stresses and triple stresses) occur in such a framework. But in this chapter we have not introduced this type of variable. Indeed we have not derived the Lagrangean function with respect to its arguments (torsion and curvature) in order to write the corresponding constitutive equations. The present comparison is not been finished yet, the investigations on our model must continue (see perspectives).

2.7 Concluding remarks

Most of the materials may be regarded as Noll's simple materials [69]. Reduced form of their constitutive laws are therefore determined through both the Euclidean-Frame Indifference and the Form-Indifference that ensure the Indifference with respect to Superimposed Rigid Body Motions (rigid translation and rigid rotation) [79]. Elastic simple material is therefore well defined by a strain energy density function depending on the metric tensor components as arguments. Strain Gradient continuum does not belong to the Noll's simple materials class, strain energy density also depend on higher space derivatives of the metric tensor. The goal of the present paper was to analyze the form-invariance of second strain gradient, or also named third grade continuum. The ratio supporting the interest of such a third grade continuum may be found initially in [64] and recently in e.g. [27], [54]. In a previous work, we were also leaded to third grade models however from a differential geometry point of view, when accounting for discontinuity of scalar and vector fields within the continuum [73]. We do not pay attention to the inertial terms in the present paper, reducing the Lagrangian function to the strain energy density function.

According to a method borrowed from [57], the present investigations have shown, on the one hand, the necessary dependence of the Lagrangian function on the second order derivative of the metric, or the strain (main argument). On the other hand, the form-

invariance method applied to a Lagrangian function that depends on both the metric and the (compatible) connection involves the necessary dependence of the Lagrangian with respect to the torsion and/or the curvature associated to the connection. It is observed that the introduction of the affine connection as arguments of any physical quantity, such as the Lagrangian function, has its roots in basic physics of spacetime. Connection was already introduced in the earlier works of Einstein, Weyl, and Cartan to describe the concept of gravity e.g. [21], in which the both metric and connection are considered as two of the fundamentals tools for mechanics and physics. The Lagrangian function is reduced to an elastic potential energy function and the dimension of its arguments inform on the character of higher order of gradient. The form $\mathcal{L}(\mathbf{g}, \aleph)$ is associated to a second strain gradient elastic continuum with the argument torsion, whereas the form $\mathcal{L}(\mathbf{g}, \aleph, \mathfrak{R})$ is associated to an elastic continuum of third grade with the curvature also as additional argument.

Chapitre 3

Propagation d'onde dans un corps hétérogène

Ce chapitre sera consacré à l'étude des propagations d'ondes élastiques dans un milieu qualifié d'hétérogène, où la distribution de la matière est supposée continue mais des discontinuités de champs scalaires et vectoriels (hétérogénéités) peuvent apparaître. Nous considérons une densité de masse variable suivant une loi exponentielle qui nous permet d'obtenir les équations du mouvement perturbées. Le paramètre perturbateur intervient dans la forme originale de l'équation de Navier. Puis nous traitons des exemples d'application en résolvant analytiquement les équations du mouvement. L'analyse modale des solutions met en évidence une atténuation en espace de l'onde et le phénomène de fréquence de coupure pour l'onde. Ce travail constitue la référence [5] : le lecteur est donc invité à substituer éventuellement l'expression "in this paper" par "in this chapter".

In this chapter we deal with the elastic wave propagation through a heterogeneous medium, where the matter is assumed continuous with some discontinuity fields of scalar fields or vector fields (heterogeneities). We introduce an exponential variation of mass density which implies a disturbed wave propagation equation. We give with two examples : a modal analysis highlights the space attenuation of the wave and the stop pass frequency for the wave. This work is associated to the reference [5] : the reader can thus replace the expression "in this paper" by "in this chapter".

3.1 Introduction

During the last decades, measurement of the velocity and attenuation of waves has been the basis of quantitative non-destructive evaluation of engineering material properties e.g. [41], [70]. Non destructive evaluation of materials combines wave propagation theory and technology as ultrasonic, x-ray diffraction and other methods of investigations. The basic theory behind the more and more sophisticated technology remains the wave propagation within heterogeneous media. Strain gradient models e.g. [28] have been used to describe heterogeneity in continua and the wave dispersion which is experimentally observed e.g. [35], [41]. Particularly, gradient-enriched elasticity models have been used to investigate the attenuation of high-frequency waves. They involve not only first gradient of the displacement (strain) but also account for the gradient of strain e.g. [86]. The dispersive character of waves experimentally observed can be analyzed with a higher accuracy but often empirically. It is usual to a fortiori multiply the wave results of homogeneous continuum by an attenuation of the exponential type to fit theory with experiments. Additionally, the experimental eigenfrequencies of heterogeneous medium are in general slightly higher than for homogeneous medium e.g. [41]. Then, developing heterogeneous continuum models is not only motivated by theoretical point of view. Experimental analysis of wave characteristics with fractured solid, geophysical material, defected material also constitutes an active research field in the domain of non destructive testing and needs support of rigorous underlying concept. Namely the existence of stop-pass band behavior waves which propagate through some heterogeneous material is an important help in monitoring the in situ degradation of material e.g. [67]. The present paper can be related to the modelling of "weakly continuous medium" (WCM), previously developed in [73]. This work aims to develop a particular non homogeneous continuum model similar to WCM, for analyzing the propagation of wave within an heterogeneous medium.

3.2 Wave propagation equation

This section focuses on the Hamilton's formulation of a particular class of non homogeneous continuum. We consider in the present paper a finite (bounded) continuum $\mathcal{B}$, a closure of a open set of $\mathbb{R}^3$ with its piecewise smooth boundary $\partial\mathcal{B}$. We assume a linearized theory of elastic continuum. The transformation of such a continuum is defined by its displacement field $\mathbf{u}(\mathbf{x}, t)$ where $\mathbf{x}$ is the position of any point of the continuum and t the instant. The non homogeneity of the elastic continuum is defined by variable density $\rho := \rho(\mathbf{x})$ depending on space (vector $\mathbf{x}$). In this framework, we remind the Cauchy small strain $\varepsilon = (1/2)\left(\nabla\mathbf{u} + \nabla^{\mathrm{T}}\mathbf{u}\right)$. We limit ourself to elastic material and one can thus write a phenomenological expression of the Lagrangian density function of the continuum. For an elastic material, the density of Lagrangian function per unit volume takes the form of (the explicit dependence on t and $\mathbf{x}$ is omitted for the sake of simplicity) e.g. [60]

$$\mathcal{L}(\mathbf{u}_t, \nabla\mathbf{u}) := \frac{1}{2}\,\rho\,\|\mathbf{u}_t\|^2 - \rho\,\psi(\nabla\mathbf{u})$$

The first term is the kinetic energy and the second one the potential energy (strain energy density). From now and hereafter, $\mathbf{u}_t$ denotes the partial derivative of the displacement with respect to time t, and $\nabla\mathbf{u}$ the space gradient of the displacement field.

Remark 3.2.1 *Conforming the classical mechanics, it should be stressed that* $\mathbf{x}$ *is not a generalized coordinate. It serves as a continuous label for each material point of the continuum e.g. [33]. The variation* δ *applies only on the displacement field* $\mathbf{u}$ *and its derivatives.*

To derive the local equation of the wave propagation from the Lagrangian $\mathcal{L}$, consider the Hamiltonian functional action given by

$$\mathcal{S}\left[\mathbf{u}_t, \nabla\mathbf{u}\right] := \int_{t_i}^{t_f} \left\{ \int_{\mathcal{B}} \mathcal{L}\left(\mathbf{u}_t, \nabla\mathbf{u}\right) dv \right\} dt.$$

In order to apply the Principle of Least Action $\delta\mathcal{S} \equiv 0$, the directional derivative of the Hamiltonian action holds

$$\delta\mathcal{S} = \int_{t_i}^{t_f} \left\{ \int_{\mathcal{B}} \left[\frac{\partial\mathcal{L}}{\partial\mathbf{u}_t} \cdot \delta\left(\mathbf{u}_t\right) + \frac{\partial\mathcal{L}}{\partial\nabla\mathbf{u}} : \delta\left(\nabla\mathbf{u}\right) \right] dv \right\} dt$$

For convenience, we define the generalized momenta

$$\mathbf{p}_t := \frac{\partial\mathcal{L}}{\partial\mathbf{u}_t}, \qquad \mathbf{P}_{\nabla\mathbf{u}} := \frac{\partial\mathcal{L}}{\partial\nabla\mathbf{u}}.$$

Consider the two relationships

$$\begin{aligned} \mathbf{p}_t \cdot \delta\left(\mathbf{u}_t\right) &= \mathbf{p}_t \cdot \left(\frac{\partial\delta\mathbf{u}}{\partial t}\right) = \frac{\partial}{\partial t}\left(\mathbf{p}_t \cdot \delta\mathbf{u}\right) - \frac{\partial}{\partial t}\left(\mathbf{p}_t\right) \cdot \delta\mathbf{u} \\ \mathbf{P}_{\nabla\mathbf{u}} : \delta\left(\nabla\mathbf{u}\right) &= \mathbf{P}_{\nabla\mathbf{u}} : \nabla\left(\delta\mathbf{u}\right) = \mathrm{div}\left(\mathbf{P}_{\nabla\mathbf{u}}^{\mathrm{T}}\delta\mathbf{u}\right) - \delta\mathbf{u} \cdot \mathrm{div}\mathbf{P}_{\nabla\mathbf{u}} \end{aligned}$$

Introducing these two relations in the expression of directional derivative allows to write

$$\begin{aligned} \delta\mathcal{S} &= \int_{t_i}^{t_f} \left\{ \int_{\mathcal{B}} \left[\frac{\partial}{\partial t}\left(\mathbf{p}_t \cdot \delta\mathbf{u}\right) - \frac{\partial}{\partial t}\left(\mathbf{p}_t\right) \cdot \delta\mathbf{u} \right] dv \right\} dt \\ &+ \int_{t_i}^{t_f} \left\{ \int_{\mathcal{B}} \left[\mathrm{div}\left(\mathbf{P}_{\nabla\mathbf{u}}^{\mathrm{T}}\delta\mathbf{u}\right) - \delta\mathbf{u} \cdot \mathrm{div}\mathbf{P}_{\nabla\mathbf{u}} \right] dv \right\} dt \end{aligned}$$

Factorization, arrangement and Stokes' theorem may be used to rewrite this equation in the following form

$$\begin{aligned} \delta\mathcal{S} = &- \int_{t_i}^{t_f} \left\{ \int_{\mathcal{B}} \left[\frac{\partial}{\partial t}\left(\mathbf{p}_t\right) + \mathrm{div}\mathbf{P}_{\nabla\mathbf{u}} \right] \cdot \delta\mathbf{u}\, dv \right\} dt \\ &+ \left[\int_{\mathcal{B}} \mathbf{p}_t \cdot \delta\mathbf{u}\, dv \right]_{t_i}^{t_f} + \int_{t_i}^{t_f} \left\{ \int_{\partial\mathcal{B}} \mathbf{P}_{\nabla\mathbf{u}}\left(\mathbf{n}\right) \cdot \delta\mathbf{u}\, da \right\} dt \end{aligned}$$

where we respectively point out two terms for the boundary and for the initial and final instants. Natural limit assumption as

$$\delta \mathbf{u}\left(\mathbf{x}, t_i\right) = \delta \mathbf{u}\left(\mathbf{x}, t_f\right) \equiv 0 \tag{3.2.1}$$

allows to eliminate the second term e.g. [60]. This conforms to classical Hamiltonian mechanics. On the other hand, the conditions at the continuum boundary $\partial\mathcal{B}$ allow to eliminate the third term. For the sake of the simplicity, only Dirichlet and / or Neumann boundary conditions are considered in the present paper, without loss of the generality. The arbitrary nature of the variation $\delta\mathbf{u}$ (kinematically admissible) means that the stationarity of the action $\mathcal{S}$ is satisfied only when the term in square brackets of the first integral vanishes. Then the Principle of Least Action gives us the linear momentum equation e.g. [33], [60]

$$\frac{\partial}{\partial t}\left(\mathbf{p}_t\right) + \mathrm{div}\mathbf{P}_{\nabla\mathbf{u}} = 0 \tag{3.2.2}$$

We are interested in the present work in the case of variable density field obtained with the so-called conformal transformations e.g. [46]. From now and hereafter, we then consider a particular non homogeneous (bounded) continuum with variable density as

$$\rho := \rho_0 \ \exp(\tilde{\aleph}_0 \cdot \mathbf{x}) \tag{3.2.3}$$

where $\tilde{\aleph}_0$ denotes an uniform and constant 1-form field on $\mathcal{B}$ (isomorph with a vector in an Euclidean ambient space). For the material under investigation, the following relations hold

$$\mathbf{p}_t = \rho_0 \ \frac{\partial \mathbf{u}}{\partial t} \ \exp(\tilde{\aleph}_0 \cdot \mathbf{x}), \qquad \mathbf{P}_{\nabla\mathbf{u}} = -\rho_0 \ \frac{\partial \psi}{\partial \nabla\mathbf{u}} \ \exp(\tilde{\aleph}_0 \cdot \mathbf{x})$$

Remark 3.2.2 *The strain energy density $\rho\ \psi$ should be invariant under a rigid translation and rigid rotation of the continuum. For linearized elasticity without initial stress, the (scalar) energy takes the form of*

$$\psi\left(\nabla\mathbf{u}\right) = (1/2)\varepsilon : \mathbb{E}\left[\varepsilon\right]$$

where $\mathbb{E}_{ijkl}$ are the components of the elasticity tensor of the material.

For the sake of the simplicity, we only consider an isotropic non homogeneous continuum with

$$\rho_0 \ \mathbb{E}_{ijkl} = \lambda_0 \ \delta_{ij}\delta_{kl} + \mu_0 \left(\delta_{ik}\delta_{jl} + \delta_{il}\delta_{jk}\right) \tag{3.2.4}$$

Introducing the expression of the energy density into the linear momentum equation (3.2.2) leads to the local wave propagation equation :

$$\left(\lambda_0 + \mu_0\right) \nabla\left(\mathrm{div}\mathbf{u}\right) + \mu_0 \ \Delta\mathbf{u} + \lambda_0 \mathrm{Tr}\varepsilon \ \mathbb{I}(\tilde{\aleph}_0) + 2\mu_0 \ \varepsilon(\tilde{\aleph}_0) = \rho_0 \ \mathbf{u}_{tt} \tag{3.2.5}$$

The precisions and details of calculus are in annex.

Remark 3.2.3 *The wave propagation equation is disturbed by the introduction of the parameter* $\tilde{\aleph}_0$*. For* $\tilde{\aleph}_0 = 0$*, we obtain classical Navier's equation. We aim to define the role played by* $\tilde{\aleph}_0$ *in the resolution of equation. The obtained local equation (3.2.5) is exactly the same as the wave equation for weakly continuous medium developed in [74] where* $\tilde{\aleph}_0$ *is defined by means of the constants of structure of Cartan e.g. [14]. Presence of the torsion tensor in the Euler-Lagrange equations is also observed for classical and quantum particle mechanics [46]. The torsion tensor* $\aleph$ *is introduced by means of the space connection whenever nonholonomic path is followed by particles in the configurational space.*

3.3 Classification of waves in this non homogeneous continuum

First of all, plane wave solutions of the linear momentum conservation equation may be written as follows $\mathbf{u} = \mathbf{u}_0 \exp\left[i\left(\mathbf{k}\cdot\mathbf{x} + \omega t\right)\right]$ with $i^2 = -1$. Introducing this solution into the motion equation gives :

$$\begin{aligned} & \left[\left(\rho_0\omega^2 - \mu_0 k^2\right)\mathbb{I} - \left(\lambda_0 + \mu_0\right)k^2\ \mathbf{n}\otimes\mathbf{n}\right]\mathbf{u}_0 \\ + \quad & ik\ \aleph_0\left[\left(\lambda_0\ \mathbf{m}\otimes\mathbf{n} + \mu_0\ \mathbf{n}\otimes\mathbf{m}\right) + \mu_0\ \mathbf{n}\cdot\mathbf{m}\ \mathbb{I}\right]\mathbf{u}_0 = 0 \end{aligned}$$

where we have defined the wave vector and the nonhomogeneity vector parameter as $\mathbf{k} := k\ \mathbf{n}$ and $\tilde{\aleph}_0 := \aleph_0\ \mathbf{m}$ respectively. $\mathbf{m}$ and $\mathbf{n}$ are unit vectors, where $\mathbf{m}$ is associated to matter whereas $\mathbf{n}$ to the wave propagation direction. For the plane wave analysis, it suffices to consider two situations.

3.3.1 Wave orthogonal to non homogeneity

The wave direction $\mathbf{n}$ is orthogonal to the material vector $\mathbf{m}$, say $\mathbf{n}\cdot\mathbf{m} = 0$. Let $(\mathbf{m}, \mathbf{n})$ be an orthonormal base in the plane generated by these two vectors. The eigenvalues problem takes the form of

$$\begin{bmatrix} \rho_0\omega^2 - \mu_0 k^2 & i\lambda_0\ k\ \aleph_0 \\ i\mu_0\ k\ \aleph_0 & \rho_0\omega^2 - \left(\lambda_0 + 2\mu_0\right)k^2 \end{bmatrix}\begin{pmatrix} u_{0m} \\ u_{0n} \end{pmatrix} = \begin{pmatrix} 0 \\ 0 \end{pmatrix}$$

From this equation, we can clearly observe the classical longitudinal wave and the shearing wave if the scalar $\aleph_0 = 0$. Otherwise, the frequency equation holds :

$$\left(\rho_0\omega^2 - \mu_0 k^2\right)\left[\rho_0\omega^2 - \left(\lambda_0 + 2\mu_0\right)k^2\right] + \lambda_0\ \mu_0\ k^2\ \aleph_0^2 = 0$$

The non homogeneity, characterized by the scalar $\aleph_0$, obviously couples the longitudinal and shearing waves. In other words, some part of volumic energy is transformed into shearing energy and vice versa for nonhomogeneous continuum by means of this non homogeneity parameter. Let define three wave numbers and the celerities ratio as follows :

$$k_T^2 := \frac{\omega^2}{c_T^2}, \quad k_\ell^2 := \frac{\omega^2}{c_\ell^2}, \quad k_\aleph^2 := \frac{\lambda_0}{\lambda_0 + 2\mu_0}\ \aleph_0^2, \quad c^2 := \frac{c_T^2}{c_\ell^2}$$

where c_T and c_ℓ are respectively the celerity of volumic and shear wave within the homogeneous continuum with uniform density ρ_0. The dispersion equation reduces to

$$k^4 - \left(k_T^2 + k_\ell^2 - k_\aleph^2\right) k^2 + k_T^2\, k_\ell^2 = 0$$

The discriminant of this second-degree can be rewritten as follows :

$$\Delta := \left(k_T - k_\ell - k_\aleph\right)\left(k_T - k_\ell + k_\aleph\right)\left(k_T + k_\ell - k_\aleph\right)\left(k_T + k_\ell + k_\aleph\right)$$

Owing that $k_\ell < k_T$, the sign of the discriminant is the same as the sign of

$$\Delta^*(\omega) := \left(\frac{\omega}{c_T} - \frac{\omega}{c_\ell} - k_\aleph\right)\left(\frac{\omega}{c_T} + \frac{\omega}{c_\ell} - k_\aleph\right)$$

For convenience, we introduce the following quantities expressed in terms of waves celerity : $\lambda_0 + 2\mu_0 := \rho_0\, c_\ell^2$, $\mu_0 := \rho_0\, c_T^2$, and $k_\aleph = \sqrt{1-2c^2}\,\aleph_0$. Then, we can analyze the sign of Δ depending on the frequency ω.

Case 1(Low frequency)

$$\omega < \frac{c_\ell\, c_T}{c_\ell + c_T}\sqrt{1-2\,c^2}\,\aleph_0 \quad \Longrightarrow \quad \Delta > 0$$

The expression of the square of the wave number is given by

$$k^2 = \frac{1}{2}\left[\left(k_T^2 + k_\ell^2 - k_\aleph^2\right) \pm \sqrt{\left(k_T^2 + k_\ell^2 - k_\aleph^2\right)^2 - 4\, k_T^2\, k_\ell^2}\right]$$

and owing that $k_T^2 + k_\ell^2 - k_\aleph^2 < 0$. This ensures that $k^2 < 0$ in any case. The wave number is therefore a pure imaginary number $k \in i\,\mathbb{R}$. In principle, for such a case, there is only an attenuated exponential solution in space. It is similar to a stop-pass frequency ω_c phenomenon empeaching the wave to propagate e.g. [67] :

$$\omega_c := \frac{c_\ell\, c_T}{c_\ell + c_T}\sqrt{1-2\,c^2}\,\aleph_0$$

Case 2 (Intermediate frequency)

$$\frac{c_\ell\, c_T}{c_\ell + c_T}\sqrt{1-2\,c^2}\,\aleph_0 < \omega < \frac{c_\ell\, c_T}{c_\ell - c_T}\sqrt{1-2\,c^2}\,\aleph_0 \quad \Longrightarrow \quad \Delta < 0$$

The expression of the square of the wave number is given by

$$k^2 = \frac{1}{2}\left[\left(k_T^2 + k_\ell^2 - k_\aleph^2\right) \pm i\,\sqrt{4\, k_T^2\, k_\ell^2 - \left(k_T^2 + k_\ell^2 - k_\aleph^2\right)^2}\right]$$

In this case, the solutions are complex $k = k_R + i\, k_J \in \mathbb{C}$ assessing that solutions have space attenuated wave forms provided that $k_J > 0$.

Case 3 (High frequency)

$$\frac{c_\ell\, c_T}{c_\ell - c_T}\,\sqrt{1-2\,c^2}\,\aleph_0 < \omega \quad \Longrightarrow \quad \Delta > 0$$

The expression of the square of the wave number is given by

$$k^2 = \frac{1}{2}\left[\left(k_T^2 + k_\ell^2 - k_\aleph^2\right) \pm \sqrt{\left(k_T^2 + k_\ell^2 - k_\aleph^2\right)^2 - 4\,k_T^2\,k_\ell^2}\right]$$

and owing that $k_T^2 + k_\ell^2 - k_\aleph^2 > 0$. Conversely to low frequency, we observe that $k^2 > 0$. This means a non attenuated wave solution since $k \in \mathbb{R}$.

Remark 3.3.1 *It is observed that the values of the corresponding phase velocity for very large values of the wave number $k \to \infty$ remain bounded, meaning that the model is physically acceptable at least concerning this aspect e.g. [71].*

3.3.2 Wave parallel to non homogeneity

The wave direction $\mathbf{n}$ is parallel with the material vector $\mathbf{m}$. We use the vector $\mathbf{m}$ and its direct orthogonal counterpart $\mathbf{m}^\perp$ to form a base in the $\left(\mathbf{m}, \mathbf{m}^\perp\right)$ plane. The eigenvalues problem takes the form of

$$\begin{bmatrix} \rho_0\omega^2 - (\lambda_0 + 2\mu_0)\left(k^2 - ik\,\aleph_0\right) & 0 \\ 0 & \rho_0\omega^2 - \mu_0\left(k^2 - i\,k\,\aleph_0\right) \end{bmatrix} \begin{pmatrix} u_{0m} \\ u_{0m^\perp} \end{pmatrix} = \begin{pmatrix} 0 \\ 0 \end{pmatrix}$$

The existence of two distinct waves is straightforward in this formulation. We remind here below the concept of stop-pass frequency by analyzing this longitudinal parallel wave. All the examples we deal with belong to this class of "parallel" wave. Extension to the "orthogonal" wave does not present conceptual difficulties. A short discussion on this topic will be given at the end of the thick-walled tube example.

Adimensionalisation. In this paper, the variable t represents the time (dimensioned), the variables x and r represent the space (dimensioned) and the heterogeneity of the media is represented by $\aleph_0$ (dimensioned). Let us introduce the time $t = T\,\overline{t}$ and the space variables

$$x = L\,\overline{x} \Rightarrow \aleph_0 = 2\overline{\aleph_0}\,L^{-1}, \quad r = R\,\overline{r} \Rightarrow \aleph_0 = 2\overline{\aleph_0}\,R^{-1} \tag{3.3.1}$$

where L and R represent length and radius in the next examples. The scales being T, L and R, the symbols with an over-line are non-dimensioned variables. But for convenience we will choose to write without over-line :

$$\overline{t} \to t, \qquad \overline{r} \to r, \qquad \overline{\aleph}_0 \to \aleph_0 \tag{3.3.2}$$

etc from now and hereafter. λ_0 and μ_0 are the constants of Lame and ρ_0 is the mass density then we respectively notice the longitudinal velocity and the transversal velocity

$$c_L^2 := \frac{\lambda_0 + 2\mu_0}{\rho_0}, \qquad c_T^2 := \frac{\mu_0}{\rho_0}, \qquad c^2 := \frac{c_T^2}{c_L^2} < 1 \tag{3.3.3}$$

where c_L^2 represents the longitudinal velocity and c_T^2 represents the transversal velocity. Depending on the examples, we choose the time scales

$$T = \frac{L}{c_L}, \qquad T = \frac{R}{c_L} \tag{3.3.4}$$

Stop-pass frequency. For waves parallel to the non homogeneity. It is easier to define the concept of stop-pass frequency. Stop-pass frequency originates from 1-D wave propagation through a medium with micro-fracture distribution, perpendicular to the wave direction, that presents a sound basis for determining the micro-fracture characteristics as geophysics and mining engineering e.g. [67]. For further simplification, let us consider a fixed-fixed beam of length ℓ. The kinematics is assumed to be described by a displacement vector $\mathbf{u} := u(x,t)\ \mathbf{e}_1$ and an uniform field $\tilde{\aleph}_0 := \aleph_0\ \mathbf{e}_1$ which is similar to the distribution of "scalar discontinuity" (heterogeneity of material) developed in e.g. [74]. Without going into details (choice $L = \ell$) the non dimensionnal 1-D wave propagation equation takes the form of

$$\frac{\partial^2 u}{\partial x^2} + 2\aleph_0\ \frac{\partial u}{\partial x} - \frac{\partial^2 u}{\partial t^2} = 0. \tag{3.3.5}$$

The dynamic equation includes then an additional term which represents the influence of non homogeneity. The equation (3.3.5) can be solved by applying the integral Fourier transform over the dimensionless time t. Assuming $u(x,.) \in H^1(\mathbb{R})\ \forall x \in [0,1]$ and multiplying equation (3.3.5) by $e^{-i\omega t}$ (ω being an arbitrary parameter) and integrating it by $\int_{\mathbb{R}}\ dt$, we obtain

$$U^{''}(x) + 2\aleph_0\ U^{'}(x) + \omega^2\ U(x) = 0 \tag{3.3.6}$$

where $U(x) := \int_{\mathbb{R}}\ u(x,t)\ e^{-i\omega t}\ dt$ is the Fourier transform of $u(x,.)$. Searching for solutions of the type $U = e^{kx}$, with $k \in \mathbb{C}$ (eigenvalues problem), equation (3.3.6) leads to the dispersion equation

$$k^2 + 2\aleph_0 k + \omega^2 = 0 \tag{3.3.7}$$

Three types of solution k are possible according to the sign of the discriminant $\Delta := \aleph_0^2 - \omega^2$. In each case the solution depends on parameters ω and $\aleph_0$. Given $\omega = \omega_n \in \mathbb{R}_+$, $n = 0, ..., \infty$ (discret spectrum), we have a discret family of solutions k_n. Consequently the solution of (3.3.6) takes the form of $U_n(x) = e^{k_n x}$, which finally depends on the parameter $\aleph_0$. The general solution $u(x,t)$ of wave propagation equation (3.3.5) is the decomposition in Fourier series

$$u(x,t) = \sum_{n\in\mathbb{N}}\ U_n(x)\ e^{i\omega_n t} \tag{3.3.8}$$

We henceforth seek solutions of the type $u(x,t) = U(x)\ e^{i\omega t}$ in the next examples. We call stop-pass frequency (or cut-off frequency) the frequency ω which is defined by $\Delta = 0$ e.g. [67], $\omega_n \in \mathbb{R}_+$ represents the nth eigenfrequency of the wave, k_n represents the wave number and U_n is the wave function. Let us consider a preliminary example treated in [74] with exactly the same equation as equation (3.3.5) : a fixed-fixed beam of length L with an homogeneous distribution of "scalar discontinuity" and the boundary conditions are then $U(0) = U(1) = 0$. We should assume $\omega > \aleph_0$ since no non trivial solutions are possible when $\Delta \geq 0$. Indeed when the frequency reaches $\omega \leq \aleph_0$, the boundary conditions induce $U_1 = U_2 = 0$, meaning that no waves are allowed to propagate through the heterogeneous beam. Finally the stop-pass frequency is equal to $\aleph_0$ e.g. [67]. To comply with Einstein's causality, a partial differential equation that governs dynamic behaviour of a 1-D model must be of the same order with respect to the spatial coordinate and with respect to time. This necessary condition of causality has been proven for the second-order partial differential equations. The modal (3.3.5) is causal and the resolution allows to describe some space attenuation of elastic wave, [74].

3.4 Thick-walled cylinder

3.4.1 Kinematics and equation of motion

Let us consider a thick-walled cylinder of infinite length, with inner radius p and outer radius q $(0 < p < q)$ in an axisymmetric problem $(\partial_\theta \equiv 0)$. The displacement is assumed radial : $\mathbf{u} = u\,(r,t)\,\mathbf{e}_r$. From the strain energy density, we remind the components of the

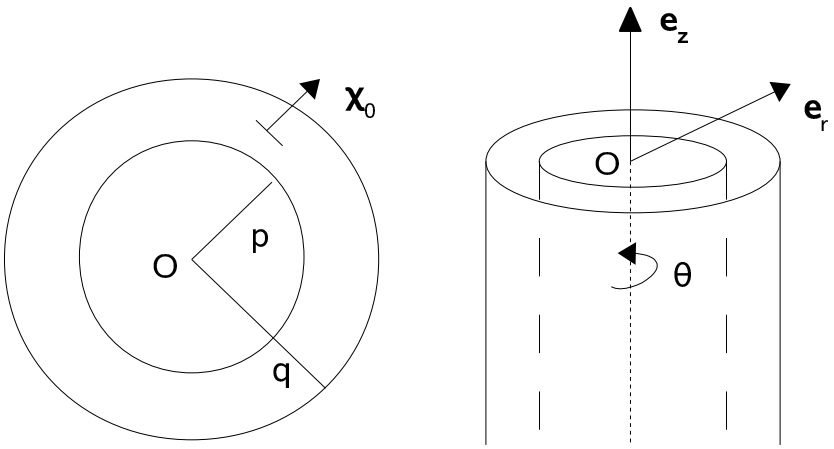

FIG. 3.4.1 – Thick-walled cylinder with inner radius p and outer radius q.

stress

$$\begin{cases} \sigma_{rr} &= (\lambda_0 + 2\mu_0)\,\dfrac{\partial u}{\partial r} + \lambda_0\,\dfrac{u}{r} \\ \sigma_{\theta\theta} &= \lambda_0\,\dfrac{\partial u}{\partial r} + (\lambda_0 + 2\mu_0)\,\dfrac{u}{r} \\ \sigma_{zz} &= \lambda_0\left[\dfrac{\partial u}{\partial r} + \dfrac{u}{r}\right] \end{cases} \tag{3.4.1}$$

With $\tilde{\aleph}_0 = \aleph_0\,\mathbf{e}_r$, the equation of motion (3.2.5) reduces to

$$c_L^2\,\frac{\partial^2 u}{\partial r^2} + c_L^2\left[\aleph_0 + \frac{1}{r}\right]\frac{\partial u}{\partial r} + \left[\frac{\left(c_L^2 - 2c_T^2\right)\aleph_0}{r} - \frac{c_L^2}{r^2}\right]u = \frac{\partial^2 u}{\partial t^2}.$$

Then the corresponding non dimensional equation holds

$$\frac{\partial^2 u}{\partial r^2} + \left[2\aleph_0 + \frac{1}{r}\right]\frac{\partial u}{\partial r} + \left[\frac{2\left(1 - 2c^2\right)\aleph_0}{r} - \frac{1}{r^2}\right]u = \frac{\partial^2 u}{\partial t^2}. \tag{3.4.2}$$

Solutions of (3.4.2) take the form of $u\,(r,t) = U\,(r)\,e^{i\omega t}$, $\omega \in \mathbb{R}_+$ for $r \in [p/R; q/R]$ and $t \in [0; +\infty]$. Introducing such a solution into (3.4.2) gives

$$U''(r) + \left(A_0 + \frac{B_0}{r}\right)\,U'(r) + \left(A_1 + \frac{B_1}{r} + \frac{C_1}{r^2}\right)U(r) = 0 \tag{3.4.3}$$

where $A_0 = 2\aleph_0,\ B_0 = 1,\ A_1 = \omega^2,\ B_1 = 2\left(1 - 2c^2\right)\aleph_0,\ C_1 = -1$. Equation (3.4.3) is particular case of confluent hypergeometric equation e.g. [2]. The general solution of (3.4.3) takes the form of

$$U\,(r) = r^{-A}\,e^{-f(r)}\,\left[K_1\,\mathcal{M}\,(a,b;h(r)) + K_2\,\mathcal{U}\,(a,b;f(r))\right] \tag{3.4.4}$$

where $\mathcal{M}\,(..,..;..)$ and $\mathcal{U}\,(..,..;..)$ are respectively the Kummer's functions of first and second kind, where $f(r) = a_1 r$, $h(r) = a_2 r$ and $a_1, a_2 \in \mathbb{C}$ and $A, a, b \in \mathbb{C}$. In this section, we henceforth consider the discriminant

$$\Delta := \aleph_0^2 - \omega^2 \tag{3.4.5}$$

Note. Depending on the sign of the discriminant Δ there are four possible systems according to the values of A, b, a_1, a_2 and a. Each system corresponds to one base of the solutions (see the details in annex).

3.4.2 Resolution for $\Delta \neq 0$

For negative discriminant $\Delta < 0$, one solution (3.4.4) may be constructed with

$$\begin{cases} A &= -1 \\ b &= 3 \\ a &= -\left[2\left(1-2c^2\right)\aleph_0 - a_1 - a_2\right]/a_2 \\ a_1 &= \aleph_0 + i\sqrt{-\Delta} \\ a_2 &= 2i\sqrt{-\Delta} \end{cases} \tag{3.4.6}$$

For positive discriminant $\Delta > 0$, one solution (3.4.4) may be constructed with

$$\begin{cases} A &= -1 \\ b &= 3 \\ a &= -\left[2\left(1-2c^2\right)\aleph_0 - a_1 - a_2\right]/a_2 \\ a_1 &= \aleph_0 + \sqrt{\Delta} \\ a_2 &= 2\sqrt{\Delta} \end{cases} \tag{3.4.7}$$

The solution takes the form of

$$U(r) = r\ e^{-a_1 r}\left[K_1\mathcal{M}(a,3;a_2 r) + K_2\mathcal{U}(a,3;a_2 r)\right] \tag{3.4.8}$$

It is formulated with the help of the parameters ω, c and $\aleph_0$.

Discussion about $\aleph_0$. For $\aleph_0 \in \mathbb{R}_+$, the previous solution has spatial exponential attenuation according to the factor $e^{-\aleph_0 r}$. If $\aleph_0 = 0$ into (3.4.3) then we have the classical wave propagation equation

$$r^2\ U''(r) + r\ U'(r) + (r^2\omega^2 - 1)U(r) = 0 \tag{3.4.9}$$

One solution of base is the Bessel function $\mathcal{J}_1(\omega r)$ of first kind e.g. [2]. If $\aleph_0 = 0$ is introduced directly in the confluent hypergeometric solution of first kind from (3.4.4), then, for $\Delta < 0$ and according to (3.4.6), we obtain

$$U(r) = r\ e^{-i\omega r}\ \mathcal{M}\left(3/2, 3, 2i\omega r\right)$$

And according to the relation between Bessel and Kummer's functions e.g. [2], we have

$$U(r) = (2/\omega)\ \mathcal{J}_1(\omega r)$$

For $\omega > 2$, the solution disturbed by $\aleph_0$ is attenuated, compared to classical one. Finally the solution we obtain is slightly different since the introduction of parameter $\aleph_0$ as uniform variable involves confluent hypergeometric functions, which are more general than the Bessel functions.

Choice of parameters. For both cases negative and positive discriminant Δ, the general form of the solutions of (3.4.3) is formulated with the help of the Kummer's functions (3.4.4). If $\Re(b) > \Re(a) > 0$ then the integral representations of Kummer's functions are convergent (see annex) e.g. [2]. The choice of the value of parameter b ($b = 3$) is then justified. For the value of parameter a, we have $\Re(a) = 3/2$ in the case $\Delta < 0$, thus the convergence is ensured. But in the case $\Delta > 0$, we have $a \in \mathbb{R}$ and the condition $a > 0$ depends on the values of ω, c and $\aleph_0$. Then the convergence is not ensured at first sight. Consequently in this paper our investigation deals with only the case $\Delta < 0$ (and later with the case $\Delta = 0$).

Application for $\Delta < 0$. As illustration, let us consider the breathing wave of fixed-fixed cylinder : for an imposed displacement at the two radii $r = p/R$ and $r = q/R$, we have two boundary conditions

$$U(p/R) = 0, \qquad U(q/R) = 0 \tag{3.4.10}$$

The dimensional radii of the thick-walled cylinder are

$$R = p = 50[\mu m], \qquad q = 100[\mu m] \tag{3.4.11}$$

For the convenience of physical interpretation of the singularities in the cylinder, we define the characteristic defect length, e.g. [74]

$$d_\aleph = 2/\aleph_0 \tag{3.4.12}$$

We choose $d_\aleph = 1[\mu m]$, consequently the dimensional norm $\aleph_0 = 2[(\mu m)^{-1}]$. The chosen material is aluminium, e.g. [74] :

$$c_L = 3040[ms^{-1}], \qquad c_T = 6420\ [ms^{-1}] \tag{3.4.13}$$

The non dimensional parameters then become

$$\aleph_0 = 50, \qquad c = 152/321, \qquad p/R = 1, \qquad q/R = 2 \tag{3.4.14}$$

and for negative discriminant ($\aleph_0 < \omega$)

$$\begin{cases} a_1 &= 50 + i\sqrt{\omega^2 - 2500} \\ a_2 &= 2i\sqrt{\omega^2 - 2500} \\ a &= (3/2) + i\left(265625/(103041\sqrt{\omega^2 - 2500})\right) \end{cases}$$

Since the terms e^{-a_1} and e^{-2a_1} may be factorized, the constants K_1 and K_2 in (3.4.4) are solutions of

$$\begin{cases} K_1\ \mathcal{M}(a, 3; a_2) + K_2\ \mathcal{U}(a, 3; a_2) &= 0 \\ K_1\ \mathcal{M}(a, 3; 2a_2) + K_2\ \mathcal{U}(a, 3; 2a_2) &= 0 \end{cases} \tag{3.4.15}$$

Non trivial solutions exist if and only if the determinant is equal to zero. The necessary and sufficient condition reduces to the dispersion equation

$$\mathcal{M}\left(a,3;a_2\right)\ \mathcal{U}\left(a,3;2a_2\right)-\mathcal{M}\left(a,3;2a_2\right)\ \mathcal{U}\left(a,3;a_2\right)=0 \tag{3.4.16}$$

which relates the non dimensional frequency ω, the material properties c, the dimensions of cylinder (ratio q/R) of the problem and the non dimensional constant $\aleph_0$.

Eigenfrequencies. Again, a stop-pass frequency (cut-off frequency) is reached whenever the discriminant $\Delta := \aleph_0^2 - \omega^2$ is equal to zero, i.e. $\omega = 50$. The non dimensional eigenfrequencies are noted ω_n and represent the values of ω for which both the imaginary and real parts of the determinant (3.4.16) are equal to zero. In such a case, eigenfrequencies ω_n are such that $\omega_n > \aleph_0 = 50$. The figure 3.4.2 permits to capture the eigenfrequencies ($n = 1, ..., 5$) where the module of the determinant is equal to zero.

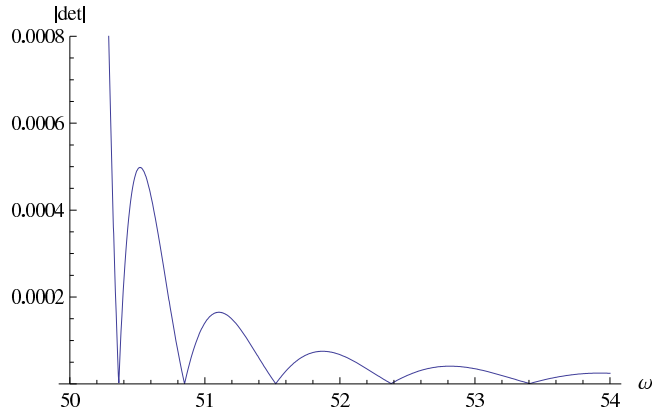

FIG. 3.4.2 – Norm of the determinant $|det(\omega, c, r_1)|$ vs. real frequency ω of the inhomogeneous aluminium cylinder.

Attenuation of the wave. We aim to determine a radius from which the wave can be neglected (within heterogenous cylinder with $d_\aleph = 1$). According to the eigenfrequencies $\omega_n,\ n = 1, ..., 5$, the wave displacement is

$$u(r,t) = \sum_{n=1}^{5} U_n(r) e^{i\omega_n t} \tag{3.4.17}$$

Let us consider arbitrary $\epsilon = 10^{-24}$. For $r > 1.1$ we have

$$|u(r,t)| \leq \sum_{n=1}^{5} |U_n(r)| < \epsilon \tag{3.4.18}$$

Finally the amplitude of the wave is approximately equal to zero within the cylinder for $r > 55[\mu m]$ (corresponding dimensional radius). This short analysis shows that beyond the radius $r = 1 + 10\%$ the wave is strongly attenuated. Therefore the analysis of wave for unbounded continuum is not necessary for such a model.

3.4.3 Resolution for $\Delta = 0$

The equation of the motion (3.4.3) is

$$U^{''}(r) + \left(2\aleph_0 + \frac{1}{r}\right) U^{'}(r) + \left(\frac{2\left(1-2c^2\right)\aleph_0}{r} - \frac{1}{r^2} + \aleph_0^2\right) U(r) = 0 \tag{3.4.19}$$

Let us seek solution in the form of $U(r) = e^{-\aleph_0 r}\alpha(r)$. We obtain

$$r^2\ \alpha^{''}(r) + r\ \alpha^{'}(r) + \left(\left(1-4c^2\right)\aleph_0 r - 1\right)\ \alpha(r) = 0 \tag{3.4.20}$$

The variable change $x = 2\sqrt{(1-4c^2)\aleph_0 r}$ is introduced into (3.4.20). We obtain (see details in annex)

$$x^2\ \alpha^{''}(x) + x\ \alpha^{'}(x) + (x^2 - 4)\alpha(x) = 0 \tag{3.4.21}$$

which is a Bessel type equation of second order e.g. [2]. The general solution of (3.4.20) takes the form of

$$\alpha(r) = K_1\ \mathcal{J}_2(2\sqrt{(1-4c^2)\aleph_0 r}) + K_2\ \mathcal{Y}_2(2\sqrt{(1-4c^2)\aleph_0 r})$$

Finally, the general solution of (3.4.19) is

$$U(r) = e^{-\aleph_0 r}\left[K_1\ \mathcal{J}_2(2\sqrt{(1-4c^2)\aleph_0 r}) + K_2\ \mathcal{Y}_2(2\sqrt{(1-4c^2)\aleph_0 r})\right]$$

Remark 3.4.1 *For the case $\Delta = 0$ the Kummer's series are defined through the Bessel functions which are more classical. And if $\aleph_0 > 0$ then we have spatial exponential attenuation of the wave.*

3.4.4 Discussion on the direction of wave

We assume that the displacement $\mathbf{u}$ and the parameter $\tilde{\aleph}_0$ are one-dimensional (with respect to $\mathbf{e}_r$ or $\mathbf{e}_\theta$). We assume that $\tilde{\aleph}_0$ is uniform and $\mathbf{u}$ only depends on r. We notice either $u_r = u(r,t)$ or $u_\theta = u(r,t)$. We now investigate the four following cases

- Case 1 : $\{\mathbf{u} = u(r)\mathbf{e}_r, \tilde{\aleph}_0 = \aleph_0\mathbf{e}_r\}$
- Case 2 : $\{\mathbf{u} = u(r)\mathbf{e}_\theta, \tilde{\aleph}_0 = \aleph_0\mathbf{e}_\theta\}$
- Case 3 : $\{\mathbf{u} = u(r)\mathbf{e}_r, \tilde{\aleph}_0 = \aleph_0\mathbf{e}_\theta\}$
- Case 4 : $\{\mathbf{u} = u(r)\mathbf{e}_\theta, \tilde{\aleph}_0 = \aleph_0\mathbf{e}_r\}$

Case 1. The case 1 has been previously developed in details. For the other possible axisymmetric cases, let us remind the non homogeneous wave propagation equation with $\tilde{\aleph}_0 \neq 0$:

$$(\lambda_0 + \mu_0)\,\nabla\,(\mathrm{div}\mathbf{u}) + \mu_0\ \Delta\mathbf{u} + \lambda_0 \mathrm{Tr}\varepsilon\ \mathbb{I}(\tilde{\aleph}_0) + 2\mu_0\ \varepsilon(\tilde{\aleph}_0) = \rho_0\ \mathbf{u}_{tt}.$$

The seeking solutions take the form of $u(r,t) = U(r)\ e^{i\omega t}$, $\omega \in \mathbb{R}_+$.

Case 2. From (3.2.5), the non-dimensional wave propagation equation within the thick tube is

$$\frac{\partial^2 u}{\partial r^2} + \left[2\aleph_0 + \frac{1}{r}\right]\frac{\partial u}{\partial r} - \left[\frac{2\aleph_0}{r} + \frac{1}{r^2}\right] u = c^{-2}\ \frac{\partial^2 u}{\partial t^2} \tag{3.4.22}$$

which leads to

$$U^{''}(r) + \left(2\aleph_0 + \frac{1}{r}\right)\ U^{'}(r) + \left(\frac{\omega^2}{c^2} - \frac{2\aleph_0}{r} - \frac{1}{r^2}\right)\ U(r) = 0. \tag{3.4.23}$$

Again, the solutions of this equation take the form of linear combination of confluent hypergeometric functions, previously developed in the case 1. We remark the same form of equation as for the breathing wave within the cylinder. Indeed, such a situation is a particular case of the section on the general aspect of wave classification.

Case 3. From (3.2.5), the non-dimensional wave propagation equation is

$$\left\{\begin{array}{rcl} \dfrac{\partial^2 u}{\partial r^2} + \dfrac{1}{r}\dfrac{\partial u}{\partial r} - \dfrac{u}{r^2} & = & \dfrac{\partial^2 u}{\partial t^2} \\ 2(1-2c^2)\aleph_0\ \dfrac{\partial u}{\partial r} + \dfrac{2\aleph_0}{r}\ u & = & 0 \end{array}\right. \tag{3.4.24}$$

leading to

$$\left\{\begin{array}{rcl} r^2\ U^{''}(r) + r\ U^{'}(r) - (\omega^2 r^2 - 1)U(r) & = & 0 \\ 2(1-2c^2)\aleph_0\ U^{'}(r) + \dfrac{2\aleph_0}{r}\ U(r) & = & 0 \end{array}\right. \tag{3.4.25}$$

The first-order Bessel functions (first and second kind) are solutions of the first equation of (3.4.25) : $U(r) = K_2\mathcal{J}_1(\omega r) + K_2\mathcal{Y}_1(\omega r)$. However these Bessel functions do not necessarily satisfy the second equation of (3.4.25). Therefore, there may not exist non trival solution.

Case 4. From (3.2.5), the non-dimensional wave propagation equation holds

$$\left\{\begin{array}{rcl} 2c^2\aleph_0\left(\dfrac{\partial u}{\partial r} - \dfrac{u}{r}\right) & = & 0 \\ c^2\left(\dfrac{\partial^2 u}{\partial r^2} + \dfrac{1}{r}\dfrac{\partial u}{\partial r} - \dfrac{u}{r^2}\right) & = & \dfrac{\partial^2 u}{\partial t^2} \end{array}\right. \tag{3.4.26}$$

Introduction of the first equation into the second one leads to a classical wave equation

$$\frac{\partial^2 u}{\partial r^2} - \frac{1}{c^2}\frac{\partial^2 u}{\partial t^2} = 0. \tag{3.4.27}$$

In such a case, we have a shearing wave that is not space attenuated. This confirms again the results predicted by the previous wave classification section.

Summary. Without accounting for the boundary conditions, the following table summarizes the general spatial solution of the wave propagation equation (3.2.5), according to the wave $\mathbf{u}$ is parallel (case 1 and case 2) or orthogonal (case 3 and case 4) to non homogeneity represented by the scalar $\tilde{\aleph}_0$.

$\mathbf{u}$ / $\tilde{\aleph}_0$	$\mathbf{e}_r$	$\mathbf{e}_\theta$
$\mathbf{e}_r$	Case 1 : Confluent Hypergeometric functions	Case 3 : Bessel first-order + compatibility condition
$\mathbf{e}_\theta$	Case 4 : base of solutions : $\{exp[i(\omega/c)^2\ r], exp[-i(\omega/c)^2\ r]\}$	Case 2 : Confluent Hypergeometric functions

3.5 Bending of beams

3.5.1 Kinematics and equation of motion

We investigate a Timoshenko beam, which may be considered as a Cosserat model e.g. [75], with a variable density. We will not take into account the slip $\gamma = 0$ and we will note the displacement $\mathbf{u} = y$ (Figure 3.5.1). The deformation includes thus a transversal displacement $\mathbf{u}$ and an angular rotation θ of a section. Let M a geometric point on the section of the beam and A the centre of the section. The displacement vector in M is (e.g. [75])

$$\mathbf{u}(M) := \mathbf{u}(A) + \overrightarrow{\Omega} \times \mathbf{AM} \tag{3.5.1}$$

Projection onto the base $\{\mathbf{e}_1, \mathbf{e}_2, \mathbf{e}_3\}$ associated with the coordinates system (x_1, x_2, x_3), we have

$$\mathbf{u}(A) = (0, u_2, 0), \qquad \overrightarrow{\Omega} = (0, 0, \theta), \qquad \mathbf{AM} = (0, x_2, x_3) \tag{3.5.2}$$

We obtain then

$$\mathbf{u}(M) = (-x_2\theta, u_2, 0) \tag{3.5.3}$$

We assume that $\theta = \theta(x_1)$ and $u_2 = u_2(x_1)$. Next we will note $u_2 = u$ and $x_1 = x$. Let us introduce the uniform vector $\aleph$ for capturing the non homogeneity of the material :

$$\aleph = \aleph_1\ \mathbf{e}_1 + \aleph_2\ \mathbf{e}_2 \tag{3.5.4}$$

The beam kinematics involves three local fields $(\mathbf{u}, \theta, \aleph)$ at each point $\mathbf{x}$. Let us note

$$(..)_{tt} := \partial^2(..)/\partial t^2, \qquad (..)_x := \partial(..)/\partial x, \qquad (..)_{xx} := \partial^2(..)/\partial x^2 \tag{3.5.5}$$

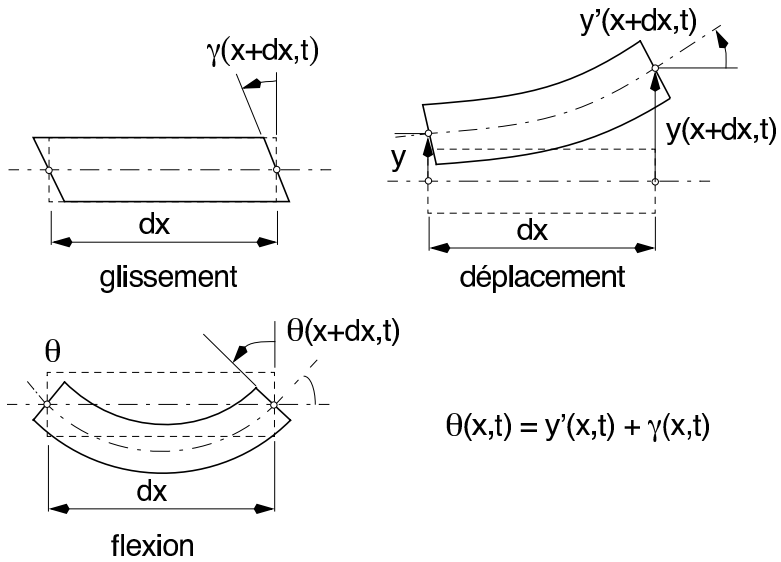

FIG. 3.5.1 – Deformation of an element of Timoshenko beam : the figure is extracted of [75].

For beam undergoing small strain, the equation of the motion (3.2.5) projected onto $\{\mathbf{e}_1, \mathbf{e}_2, \mathbf{e}_3\}$ takes the form of

$$\left\{\begin{array}{rcl} c_L^2 x_2\ \theta_{xx} + c_L^2 x_2 \aleph_1\ \theta_x + c_T^2 \aleph_2\ \theta - c_T^2 \aleph_2\ u_x - x_2\ \theta_{tt} & = & 0 \\ -\left[c_L^2 - c_T^2 + (\lambda_0/\rho_0) x_2 \aleph_2\right]\ \theta_x - c_T^2 \aleph_1\ \theta + c_T^2\ u_{xx} + c_T^2 \aleph_1\ u_x - u_{tt} & = & 0 \\ 0 & = & 0 \end{array}\right. \tag{3.5.6}$$

We note $\mathcal{S}$ the area of the beam cross-section (surface of equation $x_1 = 0$) and we define a scalar product

$$\langle u, v\rangle := \frac{1}{\mathcal{S}} \int u\ v\ dx_2 dx_3 \tag{3.5.7}$$

consequently

$$\langle 1, x_2\rangle = 0, \qquad \langle 1, 1\rangle = 1, \qquad \langle x_2, x_2\rangle = \mathbb{I}/\mathcal{S} \tag{3.5.8}$$

where $\mathbb{I}$ is the quadratic moment in respect with x_3. We integrate the system (3.5.6) to obtain $(1/\mathcal{S}) \int dx_2 dx_3$ and $(1/\mathcal{S}) \int x_2\ dx_2 dx_3$. Since the angle θ and the displacement u

depend on neither x_2 nor x_3, according to (3.5.8) we get

$$\left\{\begin{array}{rcl} c_T^2 \aleph_2\ \theta - c_T^2 \aleph_2\ u_x & = & 0 \\ c_L^2 \mathbb{I}\ \theta_{xx} + c_L^2 \mathbb{I} \aleph_1\ \theta_x - \mathbb{I}\ \theta_{tt} & = & 0 \\ -\left(c_L^2 - c_T^2\right)\ \theta_x - c_T^2 \aleph_1\ \theta + c_T^2\ u_{xx} + c_T^2 \aleph_1\ u_x - u_{tt} & = & 0 \\ (\lambda_0/\rho_0)\aleph_2 \mathbb{I}\ \theta_x & = & 0 \end{array}\right. \tag{3.5.9}$$

The corresponding non dimensional system holds

$$\left\{\begin{array}{rcl} 2c^2 \aleph_2\ \theta - 2c^2 \aleph_2\ u_x & = & 0 \\ \theta_{xx} + 2\aleph_1\ \theta_x - \theta_{tt} & = & 0 \\ -\left(1 - c^2\right)\ \theta_x - 2c^2 \aleph_1\ \theta + c^2\ u_{xx} + 2c^2 \aleph_1\ u_x - u_{tt} & = & 0 \\ 2(1 - 2c^2)\aleph_2\ \theta_x & = & 0 \end{array}\right. \tag{3.5.10}$$

There are four possible cases :

1. $\{\aleph_1 = 0, \aleph_2 = 0\}$
2. $\{\aleph_1 = 0, \aleph_2 \neq 0\}$
3. $\{\aleph_1 \neq 0, \aleph_2 \neq 0\}$
4. $\{\aleph_1 \neq 0, \aleph_2 = 0\}$

Case (1) corresponds to a homogeneous beam e.g. [75]. Cases (2) and (3) are mentionned in annex. Here we deal with the case (4) : $\aleph_1 \neq 0$ and $\aleph_2 = 0$. In such a case system (3.5.10) reduces to

$$\left\{\begin{array}{rcl} \theta_{xx} + 2\aleph_1 \theta_x - \theta_{tt} & = & 0 \\ -\left(1 - c^2\right)\ \theta_x + 2c^2 \aleph_1 \left(u_x - \theta\right) + c^2\ u_{xx} - u_{tt} & = & 0 \end{array}\right. \tag{3.5.11}$$

in which the first equation is uncoupled from u. The other cases will be discussed later since they do not present any particular difficulty. The chosen example is a particular case in which the vector parameter $\aleph = \aleph_0\ \mathbf{e}_1$, [14]. In fact, this a particular case of Cosserat continuum model, as for micropolar continuum, rotation θ may occur alone without displacement (as illustration, a set of aligned dominos falling - with the same motion - on a horizontal table, they relatively slip each other, but the line of mass center remains horizontal) e.g. [63]. In this particular case, the coupling in the first equation disappears. This is not the case when the 1-form has a component along $\mathbf{e}_2$ in which coupling terms appear for the two equations constituting the system. It is interesting that this second case, with $\aleph = \aleph_0\ \mathbf{e}_2$ resembles more to the classical Timoshenko beam

e.g. [75]. In such a situation, the transverse shear is strongly coupled with the bending as for classical Timoshenko beam. For the analytical solutions, we again introduce into (3.5.11) the type of function

$$\theta\left(x,t\right)=\Theta\left(x\right)e^{i\omega t},\qquad u\left(x,t\right)=U\left(x\right)e^{i\omega t} \tag{3.5.12}$$

and we obtain

$$\left\{\begin{array}{rcl}\Theta''(x)+2\aleph_1\ \Theta'(x)+\omega^2\ \Theta(x) & = & 0\\ U''(x)+2\aleph_1\ U'(x)+(\omega^2/c^2)\ U(x) & = & (c^{-2}-1)\ \Theta'(x)+2\aleph_1\ \Theta(x)\end{array}\right. \tag{3.5.13}$$

We henceforth consider the both discriminants

$$\Delta_\Theta:=\aleph_1^2-\omega^2,\qquad \Delta_U:=\aleph_1^2-(\omega^2/c^2) \tag{3.5.14}$$

Since $0<c^2<1$, we have $\Delta_U<\Delta_\Theta$.

3.5.2 Resolution for $\Delta_\Theta<0$

For $\Delta_\Theta<0$, the general solution of (3.5.13) for angle is

$$\Theta(x)=\left[C_1\ e^{i\sqrt{\omega^2-\aleph_1^2}x}+C_2\ e^{-i\sqrt{\omega^2-\aleph_1^2}x}\right]e^{-\aleph_1 x}. \tag{3.5.15}$$

Consequently $\Delta_U<0$, the general solution of (3.5.13) for transversal displacement is

$$\left\{\begin{array}{rcl}U\left(x\right) & = & U^{hom}\left(x\right)+U^{part}\left(x\right)\\ U^{hom}\left(x\right) & = & e^{-\aleph_1 x}\left[K_1\ e^{i\sqrt{(\omega/c)^2-\aleph_1^2}x}+K_2\ e^{-i\sqrt{(\omega/c)^2-\aleph_1^2}x}\right]\\ U^{part}\left(x\right) & = & \left[\left(1-c^2\right)\ \Theta'+2c^2\aleph_1\ \Theta\right]/\left[-\left(1-c^2\right)\omega^2\right]\end{array}\right. \tag{3.5.16}$$

where the angle Θ refers to (3.5.15), U^{hom} represents the general solution of homogeneous equation associated with

$$U''(x)+2\aleph_1\ U'(x)+(\omega^2/c^2)\ U(x)=(c^{-2}-1)\ \Theta'(x)+2\aleph_1\ \Theta(x) \tag{3.5.17}$$

and U^{part} is a particular solution of it (see annex). The angle and transversal displacement depend on the non dimensional parameters ω, c and $\aleph_1$. If $\aleph_1\in\mathbb{R}_+$, solution (angle and transversal) has spatial exponential attenuation, according to the factor $e^{-\aleph_1 x}$.

Application. We consider bending and transversal wave within a clamped-clamped beam. The boundary conditions are then

$$\Theta(0)=\Theta(1)=0,\qquad U(0)=U(1)=0 \tag{3.5.18}$$

According to (3.5.15), the constants C_1 and C_2 are solutions of

$$\left\{\begin{array}{rcl} C_1 + C_2 & = & 0 \\ C_1 e^{i\sqrt{\omega^2-\aleph_1^2}} + C_2 e^{-i\sqrt{\omega^2-\aleph_1^2}} & = & 0 \end{array}\right. \tag{3.5.19}$$

Non trivial solutions exist if and only if the determinant of system (3.5.19) is equal to zero i.e. $\sin(\sqrt{\omega^2-\aleph_1^2}) = 0$. The eigenfrequencies are then, e.g. [74]

$$\omega_n = \sqrt{n^2\pi^2 + \aleph_1^2}, \qquad n = 1, ..., \infty \tag{3.5.20}$$

The angle is then noticed $\Theta = \Theta_n$. Without going into details of calculus, according to (3.5.16), the constants K_1 and K_2 are

$$\left\{\begin{array}{rcl} K_2 & = & -\dfrac{n\pi C_1}{\omega_n^2} \\ K_1 & = & \dfrac{n\pi C_1}{\omega_n^2 \sin(\sqrt{(\omega_n^2/c^2)-\aleph_1^2})}\left[\cos(\sqrt{(\omega_n^2/c^2)-\aleph_1^2}) + (-1)^{n+1}\right] \end{array}\right. \tag{3.5.21}$$

and the displacement is noticed $U = U_n$. We noticed L the beam length and $d_\aleph$ represents the characteristic non homogeneity length of the beam e.g. [74]. For numerical application we choose

$$n = 1, \quad C_1 = 1, \quad L = 100[\mu m], \quad d_\aleph = 1[\mu m] \tag{3.5.22}$$

and the material is aluminium

$$c_T = 3040[ms^{-1}], \quad c_L = 6420[ms^{-1}] \tag{3.5.23}$$

The corresponding non dimensional parameters are then

$$c = 152/321, \qquad \omega_1 = \sqrt{10^4 + \pi^2}, \qquad \aleph_1 = 100 \tag{3.5.24}$$

They lead to the results represented on the figures in the next subsection. The wave consists in a low frequency wave which supports a higher frequency wave. For convenience, curves display only the oscillating aspects of the wave.

Attenuation of wave. We aim to determine a length of beam from which the wave can be neglected (within heterogeneous beam with $d_\aleph = 1$). According to the eigenfrequencies ω_n, $n = 1, ..., 5$, the wave angle is

$$\theta(x,t) = \sum_{n=1}^{5} \Theta_n(x) e^{i\omega_n t} \tag{3.5.25}$$

and the transversal wave is

$$u(x,t) = \sum_{n=1}^{5} U_n(x) e^{i\omega_n t} \tag{3.5.26}$$

Let us consider arbitrary $\epsilon = 10^{-2}$. For $x > 0.06$ we have

$$|\theta(x,t)| \leq \sum_{n=1}^{5} |\Theta_n(x)| < \epsilon, \qquad |u(x,t)| \leq \sum_{n=1}^{5} |U_n(x)| < \epsilon \tag{3.5.27}$$

Finally the amplitude of the total wave (angle and transversal) is approximately equal to zero within the beam for $x > 6[\mu m]$ (corresponding dimensional length). Here again, we find that it is not necessary to consider unbounded (infinite length) continuum $\mathcal{B}$ since beyond some characteristic lentgh, the wave is strongly space attenuated. For this example, the wave amplitude is reduced to 10% of its initial amplitude at a length of $x = 6\%$.

3.5.3 Figures

We present the oscillating aspects of the wave (angle Θ and displacement U) through the beam. On the one hand we plot the non-attenuated form $\Theta_n(x)/e^{-\aleph_1 x}$, and on the other hand the attenuated form $\Theta_n(x)$. Then we compare the non-attenuated forms $U_n(x)/\exp(-\aleph_1 x)$ with the attenuated forms $U_n(x)$ of the transversal displacement, according to the values of $d_\aleph = 0.1, 1, 10$.

Remark 3.5.1 *The angular solution (3.5.15) takes the form of*

$$\Theta_n(x) = e^{-\aleph_1 x} \ \sin(n\pi \ x)$$

We note that the non-attenuated form $\Theta_n(x)/e^{-\aleph_1 x}$ does not depend on $\aleph_1$ and consequently the oscillating aspects of the wave (angle) are the same for any value of $d_\aleph$. But the forms $\Theta_n(x)$, attenuated by $e^{-\aleph_1 x}$ are different according to the value of $d_\aleph$.

3.6 Discussion

For the examples mentioned in this paper, the wave amplitude decays with respect to the space location and there exists a stop-pass frequency. Attenuation of waves depends on the amount of heterogeneity assuming that this heterogeneity can be represented by an uniform field $\aleph_0$. The present work aims to calculate the eigenfrequencies ω_n of non homogeneous continuum. We find that the discriminant $\Delta := \aleph_0^2 - \omega^2$ represents a key-parameter to distinct the different cases. According to [73], when $\aleph_0 \geq \omega$ that corresponds to high density of singularity distribution, it is equivalent to the situation where the excitation frequency is greater than the defect circular frequency. And when $\aleph_0 < \omega$ that corresponds to low density of singularity and this is the more interesting case (for the other case see summary in annex). Indeed the stop-pass frequency is reached for $\aleph_0 = \omega$ and for any eigenfrequencies smaller than $\aleph_0$ no wave can propagate. The possibility of determining the $\aleph_0$ field becomes a keystone to assess the pertinence of the present model. When the characteristic length of a sample to be tested are of the same order as $\aleph_0$, its effects are no longer negligeable. In $3D$, $\aleph_0$ has three components which could

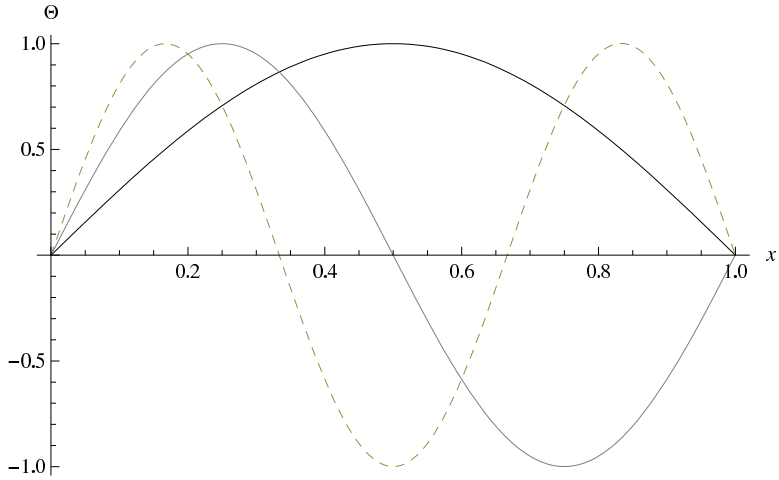

FIG. 3.5.2 – Three first modal angle $\Theta_n/\exp(-\aleph_1 x)$ for heterogeneous beam with $d_\aleph = 0.1$, 1, or 10 (plain thick Θ_1, plain thin Θ_2, dotted Θ_3).

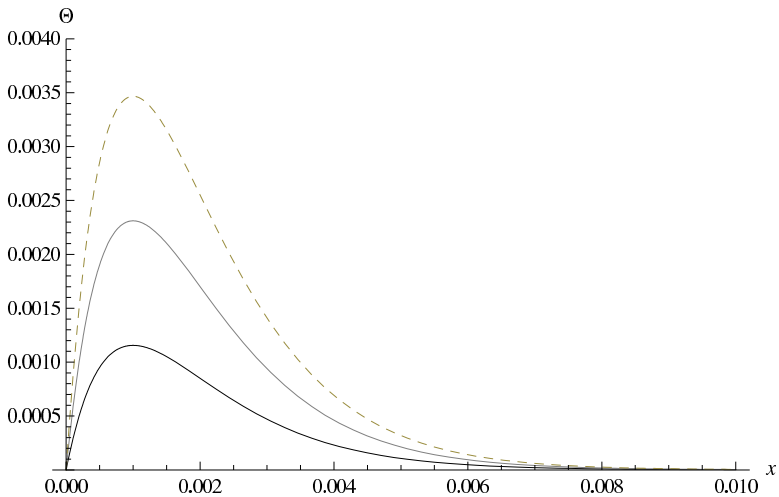

FIG. 3.5.3 – Three first modal angle Θ_n (attenuated) for heterogeneous beam with $d_\aleph = 0.1$ (plain thick Θ_1, plain thin Θ_2, dotted Θ_3).

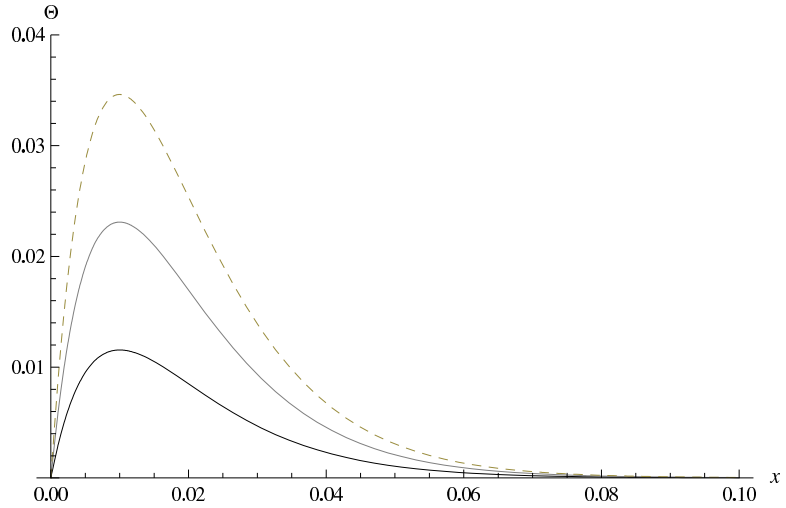

FIG. 3.5.4 – Three first modal angle Θ_n (attenuated) for heterogeneous beam with $d_\aleph = 1$ (plain thick Θ_1, plain thin Θ_2, dotted Θ_3).

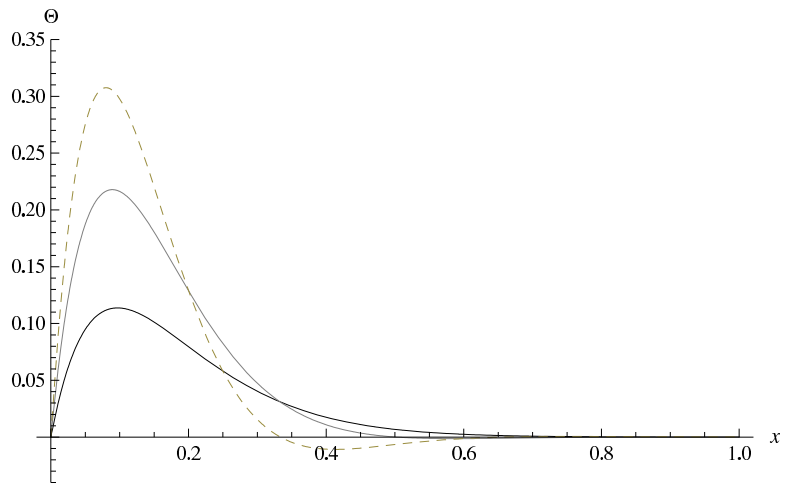

FIG. 3.5.5 – Three first modal angle Θ_n (attenuated) for heterogeneous beam with $d_\aleph = 10$ (plain thick Θ_1, plain thin Θ_2, dotted Θ_3).

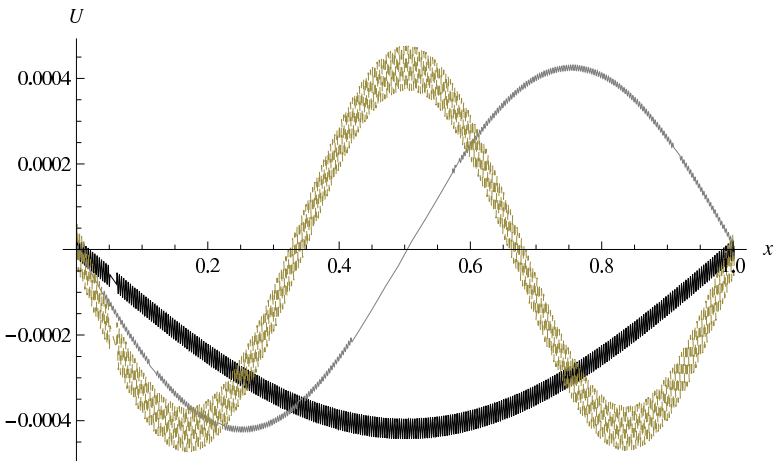

FIG. 3.5.6 – Three first modal displacement $U_n/\exp(-\aleph_1 x)$ for heterogeneous beam with $d_\aleph = 0.1$ (plain thick U_1, plan thin U_2, dotted U_3).

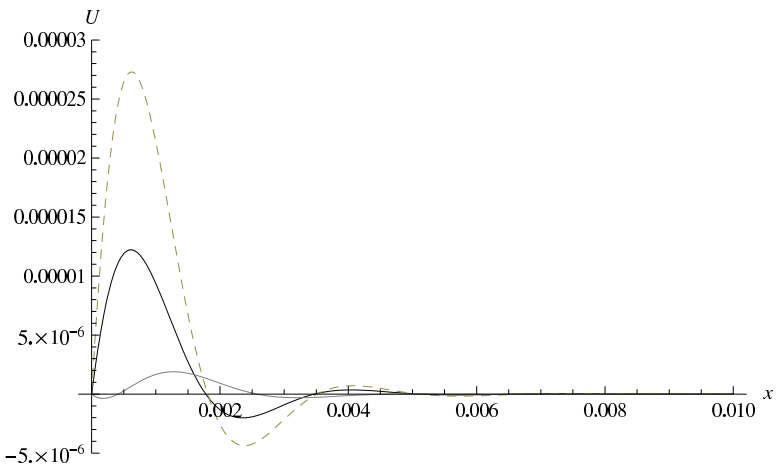

FIG. 3.5.7 – Three first modal attenuated displacement U_n (attenuated) for heterogeneous beam with $d_\aleph = 0.1$ (plain thick U_1, plan thin U_2, dotted U_3).

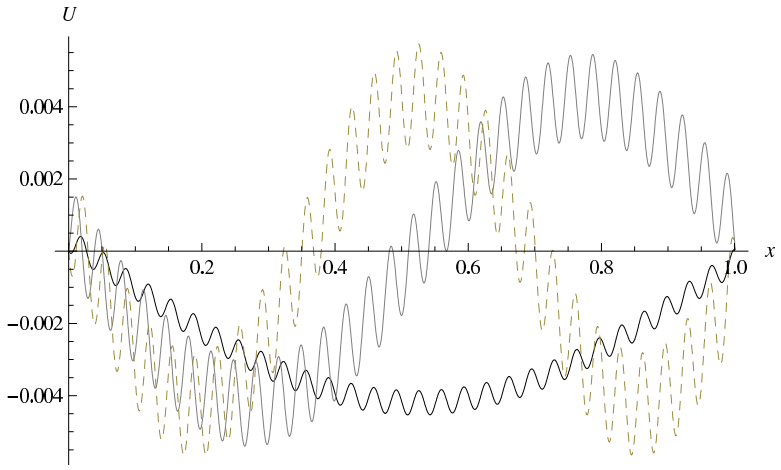

FIG. 3.5.8 – Three first modal displacement $U_n/\exp(-\aleph_1 x)$ for heterogeneous beam with $d_\aleph = 1$ (plain thick U_1, plan thin U_2, dotted U_3).

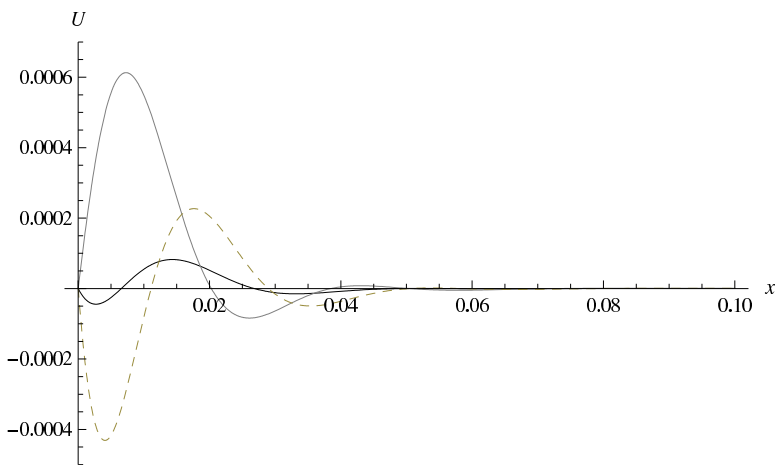

FIG. 3.5.9 – Three first modal displacement U_n (attenuated) for heterogeneous beam with $d_\aleph = 1$ (plain thick U_1, plan thin U_2, dotted U_3).

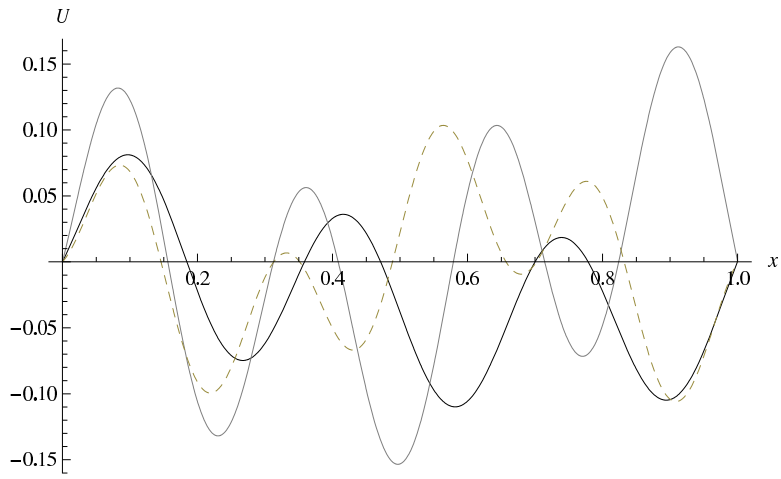

FIG. 3.5.10 – Three first modal displacement $U_n/\exp(-\aleph_1 x)$ for heterogeneous beam with $d_\aleph = 10$ (plain thick U_1, plan thin U_2, dotted U_3).

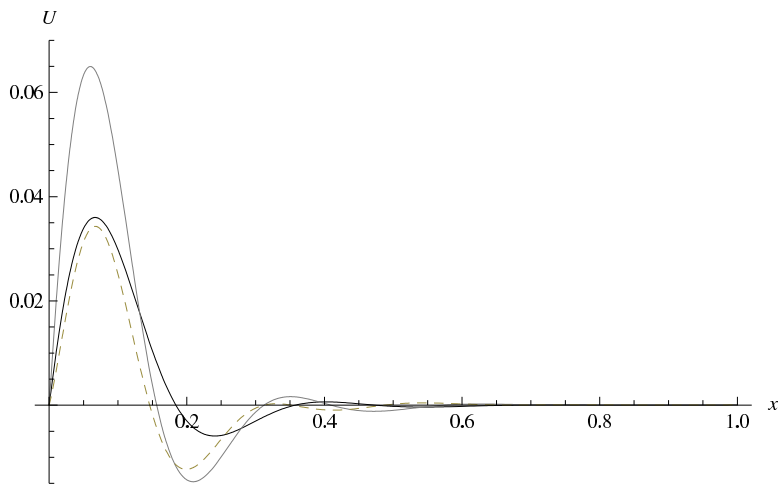

FIG. 3.5.11 – Three first modal displacement $U_n/$ (attenuated) for heterogeneous beam with $d_\aleph = 10$ (plain thick U_1, plan thin U_2, dotted U_3).

be associated to three values of length scales [74]. The model could find its applications in the measuring of ultrasonic signal loss due to propagation through a heterogeneous material sample. It is observed that the heterogeneity may also come from the presence of defects in the material, for which a geometrical approach is attempted e.g. [50], when comparing wave propagation equation obtained in [73]. This provides new motivations for investigating the material inhomogeneities from a theoretical point of view, e.g. [61], [69], [85]. But this concerns a more general approach in manifold framework.

3.7 Concluding remarks

The present paper deals with the wave propagation within non homogeneous continuum. Non homogeneity is here described by a density field depending on the space location. An exponential variation of density with a parameter $\aleph_0$ is chosen. It was shown that this particular density distribution induces a special form of linear momentum equation, that is strikingly similar to the motion equation of continuum with singularity previously developed in mechanics e.g. [69], [73], or more generally in classical and quantum physics [46]. In fact, both of them are connected by the concept of nonholonomic path in the configurational space. Examples are analytically solved for highlighting the attenuation of wave with respect to space, and the occuring of at least two scales for the waves, a higher frequency wave superimposed on a lower frequency wave one. There still remain a number of open questions in connection with the modeling of inhomogeneities in continua, the use of nonlocal continuum theories and the strain gradient elastic formulations which require resolution e.g. [17], [71]. Among these numerous questions, a central focus is the issues of whether a higher order formulation is always necessary, and the problem of the most effective way to combine strain and strain gradients in the phenomenological macroscopic theory. In this paper, the applications are chosen deliberately simple in order to obtain a series of explicit analytical solutions. Further extension of the model should include the moment stress dual of the torsion and derive the balance of equations for moment of momentum.

Chapitre 4

Une étude analytique de l'indentation du verre

Dans ce chapitre nous inroduisons une modélisation du processus de charge d'un indenteur de forme conique sur le matériau verre. L'empreinte sur le verre crée par l'indenteur est modélisée à partir d'un modèle analytique de Yoffe (1982) et fait appel à la notion d'inclusion de Eshelby. Les calculs sont semi-analytiques, comparés aux données expérimentales et nous nous focalisons sur l'influence du coefficient de Poisson comme paramètre du modèle. Ce travail compose les références [11], [12], [3] : le lecteur est donc invité a substituer éventuellement l'expression "in this paper" par "in this chapter".

In this chapter we introduce the indentation of glass with a conical shape. The print beneath the indenter is calculated according to an analytical model of Yoffe (1982) and we introduce the notion of the inclusion of Eshelby. Calculus are semi-analytic, compared to experimental data and we focus on the influence of Poisson' ratio. This work contains the references [11], [12], [3] : the reader can thus replace the expression "in this paper" by "in this chapter".

4.1 Présentation

4.1.1 Indentation du verre

Le verre est un matériau de plus en plus répandu dans la vie courante. Connu depuis l'antiquité, il est utilisé dans de nombreuses applications récentes de hautes technologies : optique, éclairage, architecture, pare-brise, vitres blindées, stockage des déchets nucléaires. Ces usages demandent des progrès constants dans l'amélioration des propriétés chimiques et mécaniques. Les études actuelles nécessitent une meilleure connaissance du comportement mécanique complexe du matériau verre et s'inscrivent dans une convergence d'approches expérimentales et théoriques. Le verre est un matériau au comportement élastique macroscopique non résistant aux chocs à température ambiante. L'essai d'indentation est ainsi mis en oeuvre pour étudier le comportement réhologique du verre. L'indentation est un procédé expérimental qui consiste à enfoncer dans un matériau, en ce qui nous concerne il s'agit du verre, un élément, applé indenteur, qui a une forme géométrique précise (pyramide, cône, sphère). L'origine de cet essai, vers 1900, est attribuée à l'ingénieur suédois Johan August Brinell (1849-1925). Après un processus de charge puis de décharge, l'indenteur laisse une empreinte visible sur la surface du verre : l'analyse expérimentale, par observation en microscope à force atomique (AFM) et numérique de cette empreinte peut fournir des caractéristiques sur le type de verre indenté, notamment en ce qui concerne sa dureté. La mise en forme par abrasion et l'usinage du verre mettent en jeu des problèmes de contacts mécaniques et de tribologie qui nécessitent la compréhension des endommagements de surface du verre, [77], [84]. Dans ce contexte, l'étude de la réponse de la surface d'un verre à une indentation constitue un moyen très efficace pour approfondir le comportement du matériau : c'est un paramètre clé pour comprendre la stabilité de la structure du verre, dépendante de la fiabilité de la surface. Nous parlerons dans ce chapitre de l'indentation avec un indenteur conique (voir figure C.0.1 en annexe).

4.1.2 Inclusion de type Eshelby

Nous considérons un milieu infini homogène élastique et isotrope, que l'on appelle "matrice". Nous considérons ensuite une région incluse dans cette matrice, que l'on appelle tout simplement "inclusion". Cette inclusion subit des changements de forme et de taille qui induirait en elle un champ de déformation homogène, dans le cas où la matrice n'interagit pas avec l'inclusion : l'interaction inclusion-matrice crée un champ de contrainte dans l'inclusion et aussi en dehors de celle-ci. Dans [24], les investigations portent alors sur l'état élastique du système, en effet ils mettent en evidence les champs de contrainte élastique et les champs de déplacements associés, dans l'inclusion et dans la matrice. La problématique est résolue par un processus imaginaire de sectionnement, d'extraction, de déformation et de réinsertion (schéma de pensée "cutting and welding" selon Eshelby [24]) :

1. Sectionnement (fin) au niveau de l'interface située entre l'inclusion et la matrice
2. Extraction de l'inclusion

3. Modification de forme et de taille de l'inclusion, via la présence de la transformation sans contrainte
4. Application de forces nécessaires sur la surface de l'inclusion afin de reconstituer la forme inclusion en état d'insertion
5. Réinsertion de l'inclusion dans la matrice au niveau de l'espace libéré précédemment
6. L'inclusion est réinsérée et la transformation sans contrainte génére les contraintes internes

La partie qui suit présente un projet mené avec Manuel Buisson (IRMAR) et Jean-Christophe Sangleboeuf (LARMAUR) : [11] puis [12] puis [3].

4.2 Densification of glass beneath an indenter

The Vickers indentation test, developped for metals, can measure the apparent hardness of glass. This hardness is qualified as apparent, indeed it does not shed light on the mechanism of irreversible deformation of glass under sharp contact loading. There are mainly two modes of mechanism of irreversible deformation [84], [42] :

- The shear flow within the mean of the irreversible isovolumic deformation also met for polycrystalline metals, called plasticity.
- The densification within the mean of the transformation by contracted volume.

Thus, two glasses may have the same apparent hardness but with different behaviours during rupture tests, damage, machining or scratching according to the respective eigenmodes of starting of plasticity or densification. To classify the problems and to avoid some unexpected craks which can cause the rupture of the glass, low indentation of glass is practiced with loads $< 100[mN]$. These experiments focus only on the co-existence of the plastic deformation and the densification localized beneath the indenter [42]. The study presented in this paper is "pragmatic" : the objective is to give some analytical results by making a simple model but which must be physically pertinent. Indeed, on the one hand, the physical mechanisms at the origin of the transformations are complex and thus the analytical behaviour law of glass is hard to develop. On the other hand, the shape of the indenter, for example a pyramid for the Vickers test, must be carefully modeled with the 3D finite element method for the contact conditions between the indenter and the material [25], [45]. Let a flat surface of a semi-infinite space, this represents the material (in fact glass). The indentation test, which consists in the one hand to apply a load onto the material, can be represented by a force locally distributed onto the flat surface of the semi-infinite space. The area of the force action is a disc with a center noted O and a fixed radius. Finally the applied load is a pressure disc, this force produces beneath this surface a stress field which creates deformations in two zones :

- The first zone called *zepd* (elastic-plastic-densification zone) is near the active zones of the indenter. It is where plasticity, densification [84], [42], and elasticity coexist.
- The second, far from the indenter, surrounds the first zone and only elastic deformation takes place in.

The stress fields used in this case are those of Yoffe [83], the *zepd* is like a blister shape inclusion [25]. The analytical calculus presented here [10], [11], are inspired by the mechanics of Eshelby [59], also called *the mechanics of the defects*. The *zepd* is considered as a semi-inclusion embedded into an elastic semi-infinite matrix. We have the same motivation as [82] in considering an inhomogeneity at the free surface of an elastic half-space and we aim also deduce analytical results.

4.3 Models of Yoffe and mechanics of Eshelby

Let us consider a flat surface of a semi-infinite space. A pressure disc of center O is applied and the spherical coordinate $\{r, \theta, \phi\}$ is associated to the base $\{O, \mathbf{e}_r, \mathbf{e}_\theta, \mathbf{e}_\phi\}$.

4.3.1 Preliminaries

The problem is assumed axisymmetric with respect to ϕ. Equations depend with variables $\{r, \theta\}$. The parameters are labeled p, q, B, P, a and ν. The Poisson ratio ν is the only parameter which is associated with the material (glass) and we will introduce also the Young modulus E and the shear modulus G. The indenter is described by a uniform pressure disc : the vertical load is P and the radius of the disc is a. The other parameters p, q (uniform pressures) and B (will be defined later) are exclusively related to the present model. The fixed parameters of the model are the force P, the radius a and the Poisson ratio ν (the Young modulus E or the shear modulus G). The unknown parameters are the constant B and the uniform pressures p, q. The unknown parameters $\{B, p, q\}$ depend on the fixed parameters $\{P, a, \nu, E\}$. The units are :

$$\begin{cases} P & \rightarrow & [mN] \\ a & \rightarrow & [\mu m] \\ B & \rightarrow & [mN][\mu m] \\ p, q & \rightarrow & [mN]/[\mu m^2] \end{cases} \tag{4.3.1}$$

The Poisson ratio will be the key-parameter of the studied model.

4.3.2 Definition of defect

When the indenter is applied to the glass, it generates a sufficiently high stress induce elastic, plastic and/or densification. The plastic deformation and the densification are related to small-distances stress, near to the indenter action zone. The elastic deformation is related to more long distance. The stress field into the *zepd* is built with its elastic equivalent by using the elastic stress models of Yoffe, the elastic equivalent is valid as long as the unload does not take place. The following pragmatic construction uses a schematic presented in [83], where the elastic part is represented by the stress field of Boussinesq and the set plasticity-densification by the blister stress field. The whole is integrated into the semi-inclusion schematic of Eshelby type.

4.3.3 Elasticity

The indenter applies a total force P distributed on the pressing faces of the pyramid. According to the Saint Venant's principle, it is showed in [25] that far from the indenter the elastic stress merges with a stress induced by a force-point. The stress field related to this point force is the so-called stress field of Boussinesq. The latter stress field is used to describe the elasticity and it is notable that it is function of r^{-2}. Thus near the indenter, it is assumed that the difference between the stress field of Boussinesq and the elastic stress field created by the pyramid shape of the indenter strongly decreases, due to the local accommodating plasticity and densification. This adaptation is not negligible, indeed the level of the stress generated by a only elastic stress field of Boussinesq near the origine O would cause the rupture of the material [12]. The rupture would take place even with a low load but it is not observed in experiments [84], [42]. Then one must note the importance of the accommoding plasticity/densification : the plastic adaptation is well known for metals and, more specifically for glasses, the densification manifests itself by a local irreversible contraction. According to its vitreous nature, the glass is less dense than crystallin structure and so the glass energy configuration can decrease by this densification.

4.3.4 Plasticity and densification

In [83] plasticity and densification are taken into account by mentioning a plasticity within the mean of a irreversible but non isovolumic deformation. This model of pseudo-plasticity, so-called blister field does not separate plasticity and densification ; the both latter are immediately combined near the indenter and it is then a function of r^{-3} which is used to describe this local stress related to plasticity-densification [25].

4.3.5 Bilan of defect

The *zepd* is a defect (a semi-inclusion) at the surface of the glass. Its elastic equivalent is due to the superposition of the stress field of Boussinesq and a blister field described in [83]. It is notable that the blister field is function of r^{-3}, so it is near the indenter and consequently the stress related to plasticity-densification acts locally. The stress field of Boussinesq related to elasticity is function of r^{-2} and then it acts in a more large volume.

4.3.6 Definition of the matrix

In [25] one speaks about the Saint Venant's principle and the finite element results. In [83] one speaks about the accommodating pseudo-plasticity. According to the arguments of [25] and [83] one can substitute, to simplify, the load P of the indenter by a vertical pressure p uniformly distributed onto a disc of center O and radius a such that $P = p\pi a^2$. This disc is called disc of average pressure with a and p specified thereafter. The material would sink and also spread laterally under the action of the pressure : a system of stresses based on the uniform pressures p (sinking) and q (spreading) is introduced. How does the pressure p onto the disc spread into the material ? The schematic reported to hereafter

and the model in [83] give some elements of response. It is notable that the pressure p is represented by vertical arrow out of the semi-infinite space and into this one the composition of the previous pressures, respectively p for sinking and q for spreading, is represented by the divergent distribution of the arrows. The orange zone symbolizes the semi-inclusion *zepd*, which is included into the elastic semi-infinite matrix, represented by the yellow zone (Figure 4.3.1, [12]). The matrix is thus defined as the surrounded elastic semi-infinite space. This matrix and the embedded inclusion confront each other and is the support of the two pressures $(-p, -q)$ previously mentionned, reacting thus to the indentation process. According to the schematic of Eshelby, one can put out the orange inclusion by cutting without some supplementary stresses but by simultaneous distributing of the pressure system (p, q) onto the cutting zone. This substitution will not affect mechanically the matrix because the inclusion is replaced by a stress system which it exerts onto this same matrix. The cutted zone is not necessary a half-sphere : an hemispherical contour with a center which does not coincide with O but placed on the revolution axe.

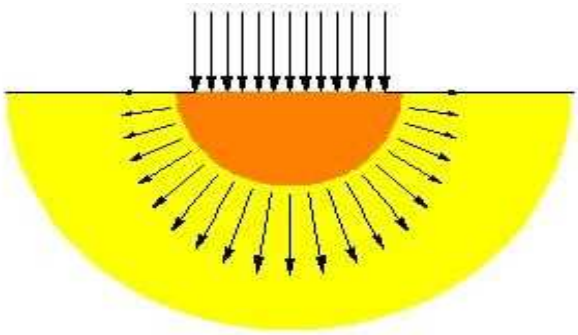

FIG. 4.3.1 – Semi-inclusion embedded to the semi-infinite matrix, pressure p in vertical arrow, pressure q the other. Cf [12].

With the models of Yoffe and the schematic of Eshelby some analytical results for the stress under the action of a micro-indenter can be obtained.

4.4 Analytical results

The equations are derived in spherical coordinates $\{r, \theta, \phi\}$: θ is the angle between the axe of revolution and the vector **OM**, M being the calculus point of the force. Some components of Cauchy stress respectively for Boussinesq and blister fields, and uniform pressures (p, q) will be reported below, [83].

4.4.1 Stress field

With the symmetry of the load and the assumed homogeneity of the material, the equations given by the models of Yoffe use a vertical axisymmetry passing by O : the displacement vector $\mathbf{u}$ includes one component u_r and one component u_θ, the component u_ϕ being null by axisymmetry.

– **Boussinesq (Bo) :** The displacement components are

$$\left\{\begin{array}{lcl} u_r^{Bo} & = & \dfrac{P}{4\pi G r}[4(1-\nu)\cos\theta-(1-2\nu)] \\ u_\theta^{Bo} & = & \dfrac{P}{4\pi G r}\left[\dfrac{(1-2\nu)\sin\theta}{1+\cos\theta}-(3-4\nu)\sin\theta\right] \end{array}\right. \tag{4.4.1}$$

the elastic stress field of Boussinesq is derived from the displacement (4.4.1)

$$\left\{\begin{array}{lcl} \sigma_{Bo}^{rr} & = & \dfrac{P}{2\pi r^2}[1-2\nu-2(2-\nu)\cos\theta] \\ \sigma_{Bo}^{\theta\theta} & = & \dfrac{P}{2\pi r^2}\dfrac{(1-2\nu)\cos^2\theta}{1+\cos\theta} \\ \sigma_{Bo}^{\phi\phi} & = & \dfrac{P(1-2\nu)}{2\pi r^2}[\cos\theta-\dfrac{1}{1+\cos\theta}] \\ \sigma_{Bo}^{r\theta} & = & \dfrac{P(1-2\nu)}{2\pi r^2}\dfrac{\sin\theta\cos\theta}{(1+\cos\theta)} \end{array}\right. \tag{4.4.2}$$

– **Blister (bl) :** The constant B measures the magnitude of the stress field induced by the plasticity and the densification. The components of the displacement are

$$\left\{\begin{array}{lcl} u_r^{bl} & = & \dfrac{B}{Gr^2}[2(1-\nu)-(5-4\nu)\cos^2\theta] \\ u_\theta^{bl} & = & \dfrac{B}{Gr^2}2(1-2\nu)\sin\theta\cos\theta \end{array}\right. \tag{4.4.3}$$

The corresponding elastic stress field is

$$\left\{\begin{array}{lcl} \sigma_{bl}^{rr} & = & \dfrac{B}{r^3}4[(5-\nu)\cos^2\theta-(2-\nu)] \\ \sigma_{bl}^{\theta\theta} & = & \dfrac{-B}{r^3}2(1-2\nu)\cos^2\theta \\ \sigma_{bl}^{\phi\phi} & = & \dfrac{B}{r^3}2(1-2\nu)(2-3\cos^2\theta) \\ \sigma_{bl}^{r\theta} & = & \dfrac{B}{r^3}4(1+\nu)\sin\theta\cos\theta \end{array}\right. \tag{4.4.4}$$

– **Uniform pressures (U) :** The uniform and anisotropic pressures p and q are used to introduce the third stress

$$\begin{cases} \sigma_U^{rr} &= -p\cos^2\theta - q\sin^2\theta \\ \sigma_U^{\theta\theta} &= -p\sin^2\theta - q\cos^2\theta \\ \sigma_U^{\phi\phi} &= -q \\ \sigma_U^{r\theta} &= (p-q)\sin\theta\cos\theta \end{cases} \tag{4.4.5}$$

According to Yoffe [83], the three previous stress fields are sufficient to describe many of the observed features of elasto-plastic indentation of glass.

4.4.2 Inclusion-matrix interface

The elastic equivalent of stress field into the semi-inclusion (*zepd*) is the sum of the Boussinesq field and the blister field $\sigma_{Bo} + \sigma_{bl}$. According to the schema of Eshelby, the semi-inclusion will be perfectly included into the matrix if one can write on the opened inclusion/matrix interface that the total elastic equivalent coincides with the stress system defined by the uniform σ_U. The substitution zone is conditionned with the continuity of the field at inclusion-matrix interface, the continuity is valid for the stress components rr and $r\theta$

$$\begin{cases} \sigma_U &= \sigma_{Bo} + \sigma_{bl} \\ \sigma_U^{rr} &= \sigma_{Bo}^{rr} + \sigma_{bl}^{rr} \\ \sigma_U^{r\theta} &= \sigma_{Bo}^{r\theta} + \sigma_{bl}^{r\theta} \end{cases} \tag{4.4.6}$$

The continuity of the other stress components is not necessary for a first investigation. The left hand side of (4.4.6) concerns what must happen inside *zepd* and the right hand side concerns what must happen outside *zepd*. Now the equality (4.4.6) will be used to estimate the radius of the affected zone by the elasticity-plasticity-densification phenomen, this radius will be noted R.

4.4.3 Fourier's series method

The equality (4.4.6) is approximed with an identification technics using the Fourier's series [10], [11], [12]. Details of the calculus is found in annex. According to Yoffe the indentification has been done with the radial component σ_{rr} and tangential $\sigma_{r\theta}$, assuming perfect bonding along the interface [83], also the extended calculus [82]. The form of the semi-inclusion is truncated spherical : the center does not necessary take place on the surface of the glass.

Results : We obtain the radius, labeled R, which is related to the interface inclusion/matrix. The non-dimensionnal radius depends only on the Poisson ratio [10], [11], [12] :

$$R = a\,\frac{\sqrt{8 + \pi(3-6\nu) + 20\nu}}{6\pi} \tag{4.4.7}$$

the coefficient B, characteristic of the plasticity-densification described by the blister field

$$B = Pa\,\frac{(16-20\nu+\pi(-3+6\nu))\sqrt{8+\pi(3-6\nu)+20\nu}}{36\sqrt{6\pi^5}} \tag{4.4.8}$$

the horizontal pressure q

$$q = (P/a^2)\,\frac{(-88+124\nu-40\nu^2+3\pi(7-16\nu+4\nu^2))}{3\pi(-8-3\pi-20\nu+6\pi\nu)} \tag{4.4.9}$$

If the truncated shape for the semi-inclusion is left free, the perfect bending conditions of stresses onto inclusion/matrix interface led us to propose polar equations of this interface. The radius $r[\theta]$, divided by the length scale a, is non dimensional. Details of the calculus is found in annex :

$$r_1[\theta] = \frac{3(-1+\nu)[1+\nu+2(1+\nu)\cos\theta-3(-1+\nu)\cos 2\theta]\sec^2[\theta/2]}{8(-1+\nu^2+(-3+6\nu)\cos 2\theta)} \tag{4.4.10}$$

where $\sec\theta = 1/\cos\theta$. And the second form

$$r_2[\theta] = -\frac{N}{D} \tag{4.4.11}$$

with the numerator

$$\begin{aligned} N &= \sqrt{8+\pi(3-6\nu)+20\nu}(-8-3\pi-20\nu+6\pi\nu) \\ &\times (16-20\nu+\pi(-3+6\nu))(1+\nu+2(1+\nu)\cos\theta-3(-1+\nu)\cos 2\theta) \end{aligned}$$

and the denominator

$$\begin{aligned} D &= 6\sqrt{6\pi^3}(-40+12\pi+88\nu-21\pi\nu+20\nu^2-6\pi\nu^2 \\ &+ (6\pi(5-11\nu+2\nu^2)-8(8-23\nu+5\nu^2))\cos\theta \\ &+ (-32+15\pi+92\nu-33\pi\nu-20\nu^2+6\pi\nu^2)) \end{aligned}$$

These results express the intensity of B and estimate the blister shape by an explicit function of Poisson's ratio ν of the glass, [11].

4.5 Comparison with the experimental

With different types of glass, AFM observations of micro-indentation print and sophisticated technics of annealing, it is showed in [84] and [42] that a decreasing function describes the relation between the capacity of densification and the Poisson's ratio.

4.5.1 Densification capacity

This experimental result is confirmed by the developped model in this paper. Indeed u_r^{bl} being the radial displacement related to the blister field, the following integral calculus used in [83]

$$\int_0^{\pi/2} 2\pi r^2 u_r^{bl}[r,\theta]\sin\theta \; d\theta \tag{4.5.1}$$

gives the variation of the volume $\Delta V = [2B\pi(1-2\nu)]/3G$ of the hemisphere with a radius r and one plasticity-densification increment. By substitution of B by its expression depending of the Poisson's ratio and the shear modulus by the Young's modulus $E = 2G(1+\nu)$, the following non-dimensional number

$$\frac{E\ \Delta V}{Pa} = \frac{(1-2\nu)(1+\nu)(16-20\nu+\pi(-3+6\nu))\sqrt{8+\pi(3-6\nu)+20\nu}}{27\sqrt{6\pi^3}} \tag{4.5.2}$$

characterizes the non elastic volume affected to the load P and the disc of average pressure p and radius a. This expression is well a decreasing function with respect to the Poisson's ratio ν, [11], [12].

4.5.2 Densification volume according to the load

To quantify the volume ΔV in function of the load P, let us consider the adapted relation for a Vickers test [43], [26] : $\pi a^2 = 24.5\ h^2$ where πa^2 is the area of the disc of average pressure surface and h is the displacement of the indenter in loading configuration. This h is approximed as the elastic equivalent total displacement calculated onto the vertical axe : $h = u_r^{Bo}[R,0] + u_r^{bl}[R,0]$. One can deduce the expression of the uniform average pressure (see annex for the details) [12]

$$p = E\sqrt{-\frac{27\pi^2(-8-3\pi-20\nu+6\pi\nu)}{49[(8+3\pi(-2+\nu)-10\nu)(3+\nu-2\nu^2)]^2}} \tag{4.5.3}$$

and the plot of the densification volume with respect to the load for different types of glass (Figure 4.5.1). The experimental data come from [43] *tableau II.7.*

In the table 4.5.2, the function $f(E,\nu)$ appears in the expressions of $\Delta V = f(E,\nu)\ P^{3/2}$. The power (3/2) is a consequence of the auto-similar characteristic of the indenter[1]. The results in [12] are comparable and coherent with the Ji's study [43]. To go further, let us give analytical expressions of the divergence[2] of the associated displacement fields respectively for Boussinesq Bo and blister bl fields below, $\mathrm{div}(\mathbf{u}^{Bo})$ and $\mathrm{div}(\mathbf{u}^{bl})$:

$$\mathrm{div}(\mathbf{u}^{Bo}) =$$

$$\frac{3a^2\pi(1+\nu)(-1+2\nu)}{7r^2}\sqrt{\frac{24\pi(9-18\nu)+60\nu}{[(8+3\pi(-2+\nu)-10\nu)(3+\nu-2\nu^2)]^2}}\cos\theta \tag{4.5.4}$$

[1]Information suggested by reviewer for publication in journal "Matériaux et Techniques" (2008).

[2]The divergence in spherical coordinate system is $\mathrm{div}(u) = \partial_r u_r + (2/r)u_r + (1/r)\partial_\theta u_\theta + (1/r tan\theta)u_\theta$, with $\partial_\phi = 0$.

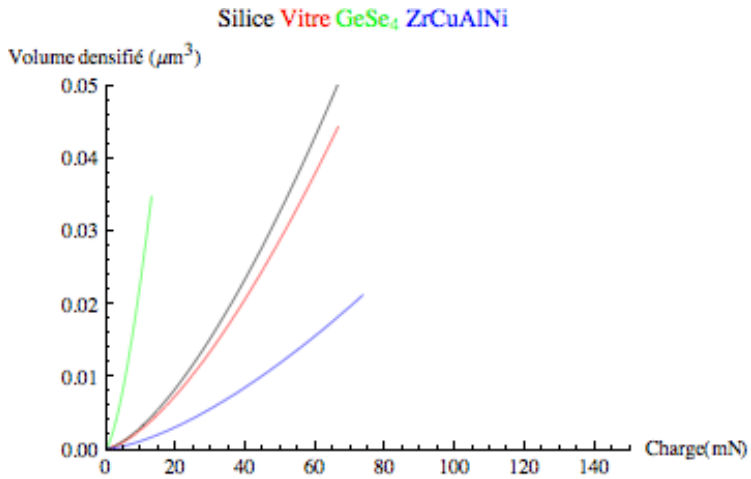

FIG. 4.5.1 – Densification volume $[\mu m]$ with respect to the load $[mN]$ for 4 types of glass. According to [12].

Type of glass	E $[GPa]$	ν	$f(E,\nu) * 10^4$ $[(\mu m)^3$ $(mN)^{-3/2}]$
Silice	74.5	0.17	0.92
Vitre	74.4	0.22	0.81
GeSe4	14.8	0.29	7.2
ZrCuAlNi	81.6	0.38	0.33

FIG. 4.5.2 – Data for 4 types of glass. According to [43] and [12].

$$\mathrm{div}(\mathbf{u}^{bl}) =$$
$$\frac{a^3(-8-\pi(3-6\nu)-20\nu)(-1+\nu+2\nu^2)(16-20\nu+\pi(-3+6\nu))(1+3\cos 2\theta)}{42\sqrt{2\pi}r^3(8+3\pi(-2+\nu)-10\nu)(3+\nu-2\nu^2)} \quad (4.5.5)$$

Let us recall that the divergence of the displacement field corresponds to the relative variation (dv/v) of the local volume v. These two formula give us access to the respective contributions of Boussinesq and blister fields related to the densification process. These results depend on the actual radius of the average pressure disc and the Poisson's ratio, the results are local values in terms of r and θ. As an example, we calculate the mean value of the total divergence for $r = R$. Let

$$(2/\pi)\int_0^{\pi/2} \mathrm{div}(\mathbf{u}^{Bo}+\mathbf{u}^{bl})\, d\theta =$$
$$\frac{-\sqrt{3\pi^2}}{\sqrt{49(8+3\pi+20\nu-6\pi\nu)}}\frac{(-1+\nu+2\nu^2)(-20(1+\nu)+\pi(-3+6\nu))}{(8+3\pi(-2+\nu)+10\nu)(3+\nu-2\nu^2)} \quad (4.5.6)$$

with the associated plot (Figure (4.5.3))

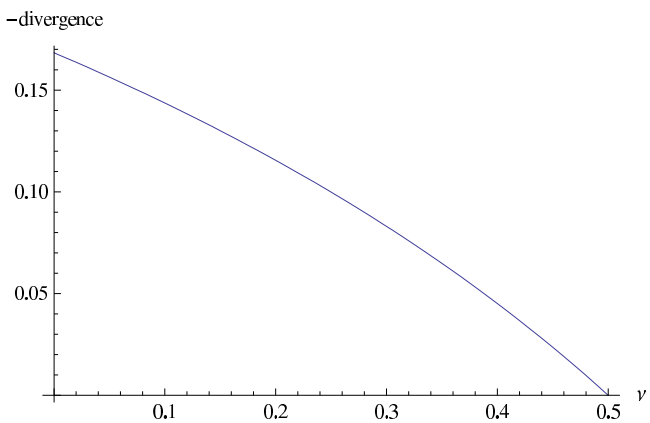

FIG. 4.5.3 – Global densification -(4.5.6) with respect to the Poisson's ratio ν.

4.5.3 Development of the blister shape

For the silica glass the polar form $r_2[\theta]$ gives for example the schematic for the blister shape represented in Figure 4.5.4 [11], [12]. The diameter of the disc of average pressure is $a = 2.5[\mu m]$ for a total load $P = p\pi a^2$ of value $500[mN]$. The *zepd* spreads on $2[\mu m]$, results also comparable with [43]. Let us note two symmetric localisations which are more noticeable if the discretisation is more precise. A study to better detail this phenomenon of localization is in hand. To have more details one can plot the director angular θ of the localization, possible precursor of the fracture, in function of the Poisson's ratio. For sake of simplicity, the figure 4.5.5 has been plotted with the first polar form of the radius

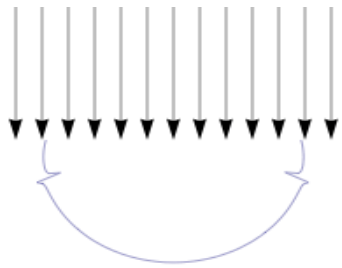

FIG. 4.5.4 – Blister shape for the silica glass with a beginning of defect. Cf [11], [12].

$r_1[\theta]$: we solve the equation $Den(r_1[\theta]) = 0$ (denominator), to determine θ with respect to ν.

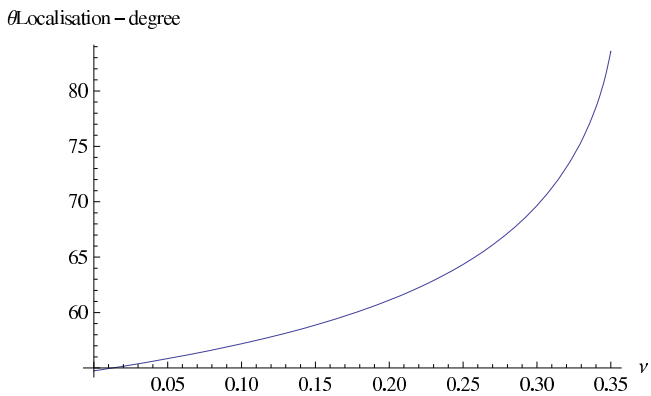

FIG. 4.5.5 – The angular localization with respect to the Poisson's ratio.

4.6 Conclusion

The analytical models of Yoffe associated with a semi-inclusion schema of Eshelby provide some quantitative and qualitative results about the densification of glasses during the micro-indentation. For a loading configuration and a given Young's modulus, the densification decreases in respect to the Poisson's ratio. This is coherent with experimental studies. The first observations of the densification zones are similar with the first trials to analyse the geometric blister shape. However the present study is simplified due to the choice of the models. Some developments are necessary in particular about the presence of localizations leading often to cracks in glass. The calculus technics of stress and strain field for the semi-inclusion problem and for the local surface forces.

Conclusion générale

Le chapitre 2 établit une contribution à la théorie du gradient en elasticité, en introduisant les tenseurs de torsion et de courbure en plus du tenseur métrique. Si (avec la métrique) nous utilisons seulement la torsion, nous sommes dans le cadre de "first strain gradient elasticity". De même si nous utilisons la courbure (avec ou sans torsion), nous sommes dans le cadre de "second strain gradient elasticity". Dans les deux cas le présent modèle n'est pas remis en cause par la propriété fondamentale démontrée par Lovelock et Rund (1975) [57], contrairement à celui proposé initialement dans [66]. D'une manière générale, le modèle proposé dans ce mémoire s'insère dans la théorie de "second strain gradient elasticity" de Mindlin (1965) [65] plutôt que dans celle de "first strain gradient elasticity" de Mindlin et Eshel (1968) [66]. Cependant, si nous voulons utiliser une terminologie en fonction du vecteur déplacement, nous présentons alors le modèle avec torsion comme un modèle de second gradient (de déplacement) et celui avec courbure (avec ou sans torsion) comme un modèle de troisième gradient (de déplacement). Le lecteur pourra à sa guise interpréter le terme "second gradient" qui est mentionné dans le titre de ce mémoire.

Le chapitre 3 est consacré à la propagation d'onde dans un milieu faiblement continu, rebaptisé ici milieu hétérogène avec une densité de masse variable. L'analyse modale pour deux exemples choisis permet de mettre en évidence une atténuation de l'onde en espace, à priori observée de manière empirique, et une fréquence de coupure. Nous confirmons la pertinence du modèle mathématique introduit par Rakotomanana (1997) [73].

Le chapitre 2 et le chapitre 3 s'intéressent à la modélisation des milieux faiblement continus par une approche géométrique non-riemannienne qui fait intervenir les tenseurs de torsion et de courbure. Dans le chapitre 2 nous avons manipulé la torsion $\aleph$ et la courbure $\mathfrak{R}$, et dans le chapitre 3 nous avons uniquement manipulé le vecteur covariant de Cartan $\tilde{\aleph}_0$ qui est plus directement lié à la torsion. En effet, la torsion projetée dans une base non holonome donne $\aleph^c_{ab} + \aleph^c_{0ab} = \Gamma^c_{ab} - \Gamma^c_{ba}$. Dans le chapitre 2, les tenseurs sont projetés dans une base tangente locale associée à un système de coordonnées (base holonome). En citant le Théorème de Frobenius, nous ne faisons pas intervenir le vecteur covariant de Cartan $\tilde{\aleph}_0$. Dans le chapitre 3, le milieu hétérogène est décrit par un vecteur uniforme noté $\aleph_0$ inséré dans la densité de masse variable. La forme particulière de l'équation du mouvement obtenue nous permet de faire l'analogie avec le vecteur covariant de Cartan, qui s'exprime en terme des coefficients de structure de Cartan $\aleph^c_{0ab}$. L'énergie potentielle $\psi = \psi(\varepsilon)$ a été choisie sans terme à gradient de déformation pour

décrire un comportement purement élastique (sans dislocation) des microcosmes. Nous avons finalement étudié un cas simple et original de la propagation d'ondes élastiques dans un milieu défectueux (voir perspectives). Le chapitre 3 est une application dans un cadre particulier d'un modèle adapté pour les milieux faiblement continus. Il n'est pas une application directe de la théorie énoncée dans le chapitre 2, qui nécessite un approfondissement (voir perspectives). Nous pouvons cependant citer l'utilisation de la torsion dans ces deux chapitres sous différentes formes.

Le chapitre 4 se consacre à une modélisation analytique du processus de charge de l'indentation du verre. Nous avons justifié un développement en séries trigonométriques de Fourier pour les équations reliant les contraintes à l'interface. Pour le calcul des paramètres du modèle analytique précédemment introduit par Yoffe (1982), nous n'avons pris en compte que les coefficients de Fourier d'ordre au plus 1. Par conséquent l'étude est restreinte à une approche semi-analytique. Les résultats semi-analytiques concordent avec des données expérimentales qui mettent en valeur l'influence du coefficient de Poisson. Cela constituait d'une part notre principal objectif, et les figures soulignent d'autre part l'amorce de localisations dans le verre qui constitue une source de motivation supplémentaire pour une étude fine via un cadre second gradient. Dans ce mémoire, le chapitre 4 est éloigné des préoccupations scientifiques des chapitres 2 et 3. En effet, la modélisation ne fait pas appel à la notion de second gradient. Elle ne fait pas non plus appel à la mécanique d'Eshelby au sens large, riche et variée dont les contributions figurent dans le recueil [24]. D'après D. M. Barnett, auteur d'avant-propos dans [24], le schéma de pensée "cutting and welding" selon Eshelby est un argument pertinent pour aborder la solution des problèmes aux bords, d'où les équations à l'interface que nous avons écrites. Nos calculs portent sur le modèle pragmatique de Yoffe et la notion de tenseur d'Eshelby (souvent assimilé directement à la mécanique d'Eshelby) n'intervient pas. Le lien avec la mécanique d'Eshelby se situe dans le schéma de pensée bien connu d'inclusion d'Eshelby qui idéalise le dispositif d'essai réel de l'indentation.

Perspectives

Modèle de second gradient. (*chapitre 2*)

Les variables primales qui sont utilisées pour décrire la déformation généralisée du continuum sont le déplacement $\mathbf{u}$ et la connexion affine ∇. Dans notre approche non-riemannienne, nous avons introduit les variables suivantes : la métrique $\mathbf{g}$, la torsion $\aleph$ et la courbure $\mathfrak{R}$ formulées à partir de ∇. Ces tenseurs sont nécessaires pour définir la forme d'énergie potentielle $W(\mathbf{g}, \aleph, \mathfrak{R})$. Il s'agit maintenant de définir les variables duales correspondantes. Nous pouvons indentifier le tenseur de contrainte d'ordre 2, couramment noté σ

$$\sigma := 2\,\frac{\partial W}{\partial \mathbf{g}} \tag{4.6.1}$$

Il sera nécessaire de notifier et nommer respectivement le tenseur d'ordre 3 et le tenseur d'ordre 4

$$\frac{\partial W}{\partial \aleph}, \qquad \frac{\partial W}{\partial \mathfrak{R}} \tag{4.6.2}$$

puis écrire les équations du mouvement. Nos investigation se porteront sur une loi de comportement élastique avec dislocations et/ou disclinations, du à la présence des tenseurs de torsion et de courbure. Par exemple nous avons les formes d'énergie suivantes :

$$W(\mathbf{g}, \aleph), \qquad W(\mathbf{g}, \mathfrak{R}), \qquad W(\mathbf{g}, \aleph, \mathfrak{R}) \tag{4.6.3}$$

dont les formes respectives projetées dans un système de coordonnées holonome se manipulent plus aisément :

$$W(g_{ij}, \aleph^k_{ij}), \qquad W(g_{ij}, \mathfrak{R}^k_{lij}), \qquad W(g_{ij}, \aleph^k_{ij}, \mathfrak{R}^k_{lij}) \tag{4.6.4}$$

Les première et dernière formes font intervenir la torsion, critère clé d'une approche par la géométrie de Cartan ou non-riemannienne. Le premier objectif sera ainsi de bien détailler cette contribution à la théorie du second gradient et son utilisation pour étudier les milieux faiblement continus. Nous pourrons dans cette démarche introduire les invariants associés aux tenseurs de torsion et de courbure. On rappelle que les démonstrations sont basées sur une projection des tenseurs dans une base holonome. Dans une base non holonome les définitions de la torsion et de la courbure sont plus générales : $\aleph^c_{ab} = \Gamma^c_{ab} - \Gamma^c_{ba} - \aleph^c_{0ab}$ et $\mathfrak{R}^c_{dab} = \Gamma^c_{ab,d} - \Gamma^c_{db,a} + \Gamma^m_{ab}\Gamma^c_{dm} - \Gamma^m_{db}\Gamma^c_{am} - \aleph^m_{0da}\Gamma^c_{mb}$. Dans ce cas il sera nécessaire de prendre en compte le vecteur covariant de Cartan $\aleph_0$ en étudiant les constantes de structure de Cartan $\aleph^c_{0ab} \neq 0$.

Propagation d'onde. (*chapitre 3*)

Nous pouvons envisager une fonction d'énergie potentielle de la forme : $W(\varepsilon, \tilde{\aleph}_0)$. Un premier exemple considère une énergie potentielle de la forme :

$$W(\varepsilon, \tilde{\aleph}_0) =$$

$$\frac{a_1}{2}\, Tr^2(\varepsilon) + \frac{a_2}{2}\, Tr(\varepsilon^2) + a_3\, Tr(\mathbf{M}\varepsilon) Tr(\varepsilon) + a_4\, Tr(\mathbf{M}\varepsilon^2) + \frac{a_5}{2}\, Tr^2(\mathbf{M}\varepsilon)$$

où $a_i, i = 1, ..., 5$ sont les constantes élastiques. Dans le chapitre 3, nous avons considéré $a_1 = \lambda_0$, $a_2 = 2\mu_0$ (constantes de Lamé) et $a_3 = a_4 = a_5 = 0$. Et $\mathbf{M} := \mathbf{m} \otimes \mathbf{m}$ est le tenseur de structure (ordre 2) avec $\mathbf{m} := \tilde{\aleph}_0 / \|\tilde{\aleph}_0\|$.

Nous pouvons dans un premier temps supposer que $\tilde{\aleph}_0$ est uniforme (comme c'est le cas dans le chapitre 3) puis dans un second temps considérer $\tilde{\aleph}_0 = \tilde{\aleph}_0(\mathbf{x})$. Dans ce cas, si nous partons avec la même densité de masse variable $\rho := \rho_0\ \exp[\tilde{\aleph}_0(\mathbf{x}) \cdot \mathbf{x}]$, nous obtenons une équation du mouvement :

$$\operatorname{div}\left(\frac{\partial \psi}{\partial \nabla \mathbf{u}}\right) + \frac{\partial \psi}{\partial \nabla \mathbf{u}} : (\tilde{\aleph}_0 + \nabla^T \tilde{\aleph}_0 : \mathbf{x}) = \mathbf{u}_{tt} \tag{4.6.5}$$

Il serait aussi intéressant de comparer notre description de milieu hétérogène (densité de masse variable suivant une loi exponentielle) avec d'autres approches décrivant les ondes élastiques propagées dans ce type de milieu.

Remarque 4.6.1 *Les travaux effectués (chapitre 2 et 3) tiennent compte de l'effet de densité de masse non uniforme et des champs de discontinuité de champs scalaires ou vectoriels sur l'analyse de contrainte et de déformation dans les milieux faiblement continus. Nous n'avons pas pris en compte l'évolution (dépendance par rapport au temps) de ces champs, en examinant* $\partial_t[\aleph(t)]$ *et* $\partial_t[\mathfrak{R}(t)]$.

Indentation du verre. (*chapitre 4*)

Une perspective immédiate consiste à faire un lien avec la théorie du second gradient. Le verre est un matériau fragile et fréquemment utilisé dans la vie courante. Des fissures sont observables suite au processus d'indentation, qui définissent la présence d'un champ de discontinuité dans la structure du verre. Ces fissures ou prémices de fissures ont pu être tracées à partir du modèle analytique de Yoffe dans le chapitre 4. L'idée est de confronter ce présent modèle avec celui du second gradient et ainsi considérer le verre indenté comme un milieu faiblement continu. Une ébauche sous forme de poster a été proposée par Manuel Buisson pour la conférence *Matériaux 2010, Nantes 18-22 oct.* Compte tenu de l'interprétation physique des tenseurs qui interviennent (torsion, vecteur covariant de Cartan) et des conditions limites (charge de l'indenteur), l'intérêt d'une telle approche est la possibilité d'estimer l'historique de la déformation irréversible du verre et peut-être prévoir le bris du verre.

Nous pouvons aussi poursuivre nos investigations sur le modèle de Yoffe. Même si cela ne paraît pas aisé, nous pouvons tenter une résolution directe des équations à l'interface pour avoir des résultats totalement analytiques ou aussi prendre en compte le processus de décharge de l'indenteur dans la modélisation.

Appendices

Annexe A

Calcul indiciel

A.1 Connection and tensors

Let (y^i) and (x^α) two coordinate systems respectively associated to the tangent base $\{\mathbf{e}_i\}$ and $\{\mathbf{e}_\alpha\}$. Let the affine connection ∇ and its coefficients

$$\nabla_{\mathbf{e}_i}\mathbf{e}_j = \Gamma^k_{ij}\mathbf{e}_k, \qquad \nabla_{\mathbf{e}_\alpha}\mathbf{e}_\beta = \Gamma^\gamma_{\alpha\beta}\mathbf{e}_\gamma \tag{A.1.1}$$

The coordinate transformation of ∇ is

$$\begin{aligned}
\Gamma^\gamma_{\alpha\beta}\mathbf{e}_\gamma &= \nabla_{\mathbf{e}_\alpha}\mathbf{e}_\beta \\
&= \nabla_{J^i_\alpha\mathbf{e}_i}\left(J^j_\beta\mathbf{e}_j\right) \\
&= J^i_\alpha\left[\nabla_{\mathbf{e}_i}\left(J^j_\beta\right)\mathbf{e}_j + J^j_\beta\nabla_{\mathbf{e}_i}\mathbf{e}_j\right] \\
&= J^i_\alpha\left[\nabla_{A^\alpha_i\mathbf{e}_\alpha}\left(J^j_\beta\right)\mathbf{e}_j + J^j_\beta\Gamma^k_{ij}\mathbf{e}_k\right] \\
&= J^i_\alpha\left[A^\alpha_i J^j_{\alpha\beta}\mathbf{e}_j + J^j_\beta\Gamma^k_{ij}\mathbf{e}_k\right]
\end{aligned}$$

say

$$\left[\Gamma^\gamma_{\alpha\beta}\right] = \left[\left(J^i_\alpha J^j_\beta A^\gamma_k\right)\Gamma^k_{ij}\right] + J^j_{\alpha\beta}A^\gamma_j \tag{A.1.2}$$

Let the biconnection $\nabla^2 = \nabla\circ\nabla$

$$\begin{aligned}
\nabla_{\mathbf{e}_\lambda}\left[\nabla_{\mathbf{e}_\alpha}\mathbf{e}_\beta\right] &= \nabla_{\mathbf{e}_\lambda}\left[\Gamma^\mu_{\alpha\beta}\mathbf{e}_\mu\right] \\
&= \nabla_{\mathbf{e}_\lambda}\left[\Gamma^\mu_{\alpha\beta}\right]\mathbf{e}_\mu + \Gamma^\mu_{\alpha\beta}\left[\nabla_{\mathbf{e}_\lambda}\mathbf{e}_\mu\right] \\
&= \Gamma^\mu_{\alpha\beta,\lambda}\mathbf{e}_\mu + \Gamma^\mu_{\alpha\beta}\Gamma^\gamma_{\lambda\mu}\mathbf{e}_\gamma \\
&= \left[\Gamma^\gamma_{\alpha\beta,\lambda} + \Gamma^\mu_{\alpha\beta}\Gamma^\gamma_{\lambda\mu}\right]\mathbf{e}_\gamma
\end{aligned}$$

Without going into details, the coordinate transformation of ∇^2 is

$$\begin{aligned}\left[\Gamma^{\gamma}_{\alpha\beta,\lambda}+\Gamma^{\mu}_{\alpha\beta}\Gamma^{\gamma}_{\lambda\mu}\right] &= \left[J^i_\alpha J^j_\beta J^l_\lambda A^\gamma_k\left(\Gamma^k_{ij,l}+\Gamma^d_{ij}\Gamma^k_{ld}\right)\right]\\ &+ \left(J^i_{\alpha\lambda}J^j_\beta A^\gamma_k + J^i_\lambda J^j_{\alpha\beta}A^\gamma_k + J^i_\alpha J^j_{\beta\lambda}A^\gamma_k\right)\Gamma^k_{ij}\\ &+ J^i_\mu J^l_\lambda J^j_{\alpha\beta}A^\gamma_j A^\mu_{il} + J^i_{\mu\lambda}J^j_{\alpha\beta}A^\mu_i A^\gamma_j\end{aligned} \tag{A.1.3}$$

The equalities (A.1.2) and (A.1.3) show that the connection ∇ and the biconnection ∇^2 are not tensors, according to (2.2.6). But in the both equalities, if the terms out of the brackets vanish then the components are components of tensor. These quantities are symmetric with respect to α, β for (A.1.2) and with respect to α, λ for (A.1.3). Then the torsion (2.2.7) and the curvature (2.2.8) are defined, with respect to the affine connection ∇, on the base $\{\mathbf{e}_a\}$ associated to coordinate system (y^a).

A.2 Indentification of coefficients

Let us apply the Lemma 2.3.2 to the equation

$$\Lambda^{ij,kl}h_{ij,kl} + \Lambda^{ij,k}h_{ij,k} + \Lambda^{ij}h_{ij} = \Lambda^{ij,kl}h_{ij|k|l} + \Pi^{ij,k}h_{ij|k} + \Pi^{ij}h_{ij},$$

for the identification of the coefficients of $h_{ij,k}$ and h_{ij}. Let us recall that

$$\begin{aligned}\Lambda^{ij,kl}h_{ij|k|l} &= \Lambda^{ij,kl}[h_{ij,kl} - \Gamma^a_{ik}h_{aj,l} - \Gamma^a_{jk}h_{ia,l} - \Gamma^a_{ik,l}h_{aj} - \Gamma a_{jk,l}h_{ia}\\ &- \Gamma^b_{il}h_{bj,k} + \Gamma^b_{il}(\Gamma^c_{bk}h_{cj} + \Gamma^{jk}_c h_{bc}) - \Gamma^b_{jl}h_{ib,k}\\ &+ \Gamma^b_{jl}(\Gamma^c_{ik}h_{cb} + \Gamma^c_{bk}h_{ic}) - \Gamma^b_{kl}h_{ij,b} + \Gamma^b_{kl}(\Gamma^c_{ib}h_{cj} + \Gamma^c_{jb}h_{ic})]\end{aligned}$$

and

$$\Pi^{ij,k}h_{ij|k} = \Pi^{ij,k}[h_{ij,k} - \Gamma^a_{ik}h_{aj} - \Gamma^a_{jk}h_{ia}].$$

The equation of the coefficients of $h_{ij,k}$ is

$$\Lambda^{ij,k}h_{ij,k} = -\Lambda^{ij,kl}[\Gamma^a_{ik}h_{aj,l} + \Gamma^a_{jk}h_{ia,l} + \Gamma^b_{il}h_{bj,k} + \Gamma^b_{jl}h_{ib,k} + \Gamma^b_{kl}h_{ij,b}] + \Pi^{ij,k}h_{ij,k}.$$

The following permutations are necessary to refind the common factor $h_{ij,k}$ in all the terms in right hand side (above) :

- $a \longleftrightarrow i$ and $l \longleftrightarrow k$ for $\Lambda^{ij,kl}\Gamma^a_{ik}h_{aj,l}$
- $a \longleftrightarrow j$ and $l \longleftrightarrow k$ for $\Lambda^{ij,kl}\Gamma^a_{jk}h_{ia,l}$
- $b \longleftrightarrow i$ then $b \to a$ for $\Lambda^{ij,kl}\Gamma^b_{il}h_{bj,k}$

– $b \longleftrightarrow j$ then $b \to a$ for $\Lambda^{ij,kl}\Gamma^b_{jl}h_{ib,k}$

– $k \longleftrightarrow b$ for $\Lambda^{ij,kl}\Gamma^b_{kl}h_{ij,b}$.

Then, according to symmetry of Λ and h, the equation of the coefficients of $h_{ij,k}$

$$(1/2)(\Pi^{ij,k} + \Pi^{ji,k}) = \Lambda^{ij,k} + 2\Gamma^i_{al}\Lambda^{aj,kl} + 2\Gamma^j_{al}\Lambda^{ia,kl} + \Gamma^k_{bl}\Lambda^{ij,bl}.$$

In the same way, the equation of the coefficients of h_{ij} is

$$\begin{aligned}\Lambda^{ij}h_{ij} &= \Lambda^{ij,kl}[-\Gamma^a_{ik,l}h_{aj} - \Gamma^a_{jk,l}h_{ia} + \Gamma^b_{il}(\Gamma^c_{bk}h_{cj} + \Gamma^c_{jk}h_{bc}) + \Gamma^b_{jl}(\Gamma^c_{ik}h_{cb} + \Gamma^c_{bk}h_{ic}) \\ &+ \Gamma^b_{kl}(\Gamma^c_{ib}h_{cj} + \Gamma^c_{jb}h_{ic})] - \Pi^{ij,k}\Gamma^a_{ik}h_{aj} - \Pi^{ij,k}\Gamma^a_{jk}h_{ia} + \Pi^{ij}h_{ij}.\end{aligned}$$

The following permutations are necessary to refind the common factor h_{ij} in all the terms in right hand side (above) :

– $a \longleftrightarrow i$ for $\Lambda^{ij,kl}\Gamma^a_{ik,l}h_{aj}$ and $\Pi^{ij,k}\Gamma^a_{ik}h_{aj}$

– $a \longleftrightarrow j$ for $\Lambda^{ij,kl}\Gamma^a_{jk,l}h_{ia}$ and $\Pi^{ij,k}\Gamma^a_{jk}h_{ia}$

– $c \longleftrightarrow i$ for $\Lambda^{ij,kl}\Gamma^b_{il}\Gamma^c_{bk}h_{cj}$ and $\Lambda^{ij,kl}\Gamma^b_{kl}\Gamma^c_{ib}h_{cj}$

– $c \longleftrightarrow j$ for $\Lambda^{ij,kl}\Gamma^b_{jl}\Gamma^c_{bk}h_{ic}$ and $\Lambda^{ij,kl}\Gamma^b_{kl}\Gamma^c_{jb}h_{ic}$

– $c \longleftrightarrow i$ and $b \longleftrightarrow j$ for $\Lambda^{ij,kl}\Gamma^b_{il}\Gamma^c_{jk}h_{bc}$ and $\Lambda^{ij,kl}\Gamma^b_{jl}\Gamma^c_{ik}h_{cb}$.

Then, according to symmetry of Λ and h, the equation of the coefficients of h_{ij} is

$$\begin{aligned}(1/2)(\Pi^{ij} + \Pi^{ji}) &= \Lambda^{ij} + \Gamma^i_{ak,l}\Lambda^{aj,kl} + \Gamma^j_{ak,l}\Lambda^{ia,kl} \\ &- \Gamma^b_{al}\Gamma^i_{bk}\Lambda^{aj,kl} - \Gamma^b_{cl}\Gamma^j_{bk}\Lambda^{ic,kl} \\ &- \Gamma^i_{bl}\Gamma^j_{ck}\Lambda^{bc,kl} - \Gamma^j_{bl}\Gamma^i_{ck}\Lambda^{bc,kl} \\ &- \Gamma^b_{kl}\Gamma^i_{cb}\Lambda^{cj,kl} - \Gamma^b_{kl}\Gamma^j_{cb}\Lambda^{ci,kl} \\ &+ (1/2)\Gamma^i_{ak}(\Pi^{aj,k} + \Pi^{ja,k}) + (1/2)\Gamma^j_{ak}(\Pi^{ia,k} + \Pi^{ai,k}).\end{aligned}$$

A.3 Components of biconnection

Let us consider

$$\Gamma^k_{ij,l} + \Gamma^m_{ij}\Gamma^k_{lm}$$

In the previous expression, the decompositions with respect to the permutation $i \longleftrightarrow j$ (for Γ^m_{ij} and $\Gamma^k_{ij,l}$) and $l \longleftrightarrow m$ (for Γ^k_{lm}) give :

$$\Gamma^k_{ij,l} + \Gamma^m_{ij}\Gamma^k_{lm} = \mathbb{S}^k_{ij,l} + \mathbb{T}^k_{ij,l} + \mathbb{S}^m_{ij}\mathbb{S}^k_{lm} + \mathbb{S}^m_{ij}\mathbb{T}^k_{lm} + \mathbb{T}^m_{ij}\mathbb{S}^k_{lm} + \mathbb{T}^m_{ij}\mathbb{T}^k_{lm}$$

We apply the permutation between i and l on the previous expression. We obtain the following decomposition :

$$\mathbb{S}^k_{ij,l} + \mathbb{T}^k_{ij,l} + \mathbb{S}^m_{ij}\mathbb{S}^k_{lm} + \mathbb{S}^m_{ij}\mathbb{T}^k_{lm} + \mathbb{T}^m_{ij}\mathbb{S}^k_{lm} + \mathbb{T}^m_{ij}\mathbb{T}^k_{lm}$$

$$= (1/2)\left[\mathbb{S}^k_{ij,l} + \mathbb{S}^m_{ij}\mathbb{S}^k_{lm} + \mathbb{S}^m_{ij}\mathbb{T}^k_{lm} + \mathbb{S}^k_{lj,i} + \mathbb{S}^m_{lj}\mathbb{S}^k_{im} + \mathbb{S}^m_{lj}\mathbb{T}^k_{im}\right]$$

$$+(1/2)\left[\mathbb{S}^k_{ij,l} + \mathbb{S}^m_{ij}\mathbb{S}^k_{lm} + \mathbb{S}^m_{ij}\mathbb{T}^k_{lm} - \mathbb{S}^k_{lj,i} - \mathbb{S}^m_{lj}\mathbb{S}^k_{im} - \mathbb{S}^m_{lj}\mathbb{T}^k_{im}\right]$$

$$+(1/2)\left[\mathbb{T}^k_{ij,l} + \mathbb{T}^m_{ij}\mathbb{T}^k_{lm} + \mathbb{T}^m_{ij}\mathbb{S}^k_{lm} + \mathbb{T}^k_{lj,i} + \mathbb{T}^m_{lj}\mathbb{T}^k_{im} + \mathbb{T}^m_{lj}\mathbb{S}^k_{im}\right]$$

$$+(1/2)\left[\mathbb{T}^k_{ij,l} + \mathbb{T}^m_{ij}\mathbb{T}^k_{lm} + \mathbb{T}^m_{ij}\mathbb{S}^k_{lm} - \mathbb{T}^k_{lj,i} - \mathbb{T}^m_{lj}\mathbb{T}^k_{im} - \mathbb{T}^m_{lj}\mathbb{S}^k_{im}\right]$$

Then we develop the expression in the right hand side. On the one hand we have :

$$\mathbb{S}^k_{ij,l} - \mathbb{S}^k_{lj,i} + \mathbb{T}^k_{ij,l} - \mathbb{T}^k_{lj,i} = \Gamma^k_{ij,l} - \Gamma^k_{lj,i}$$

and

$$\mathbb{S}^k_{ij,l} + \mathbb{S}^k_{lj,i} + \mathbb{T}^k_{ij,l} + \mathbb{T}^k_{lj,i} = \Gamma^k_{ij,l} + \Gamma^k_{lj,i}$$

And on the other hand we have in first part :

–

$$\begin{aligned}\mathbb{S}^m_{ij}\mathbb{S}^k_{lm} - \mathbb{S}^m_{lj}\mathbb{S}^k_{im} &= (1/4)\left(\Gamma^m_{ij}\Gamma^k_{lm} - \Gamma^m_{lj}\Gamma^k_{im}\right) + (1/4)\left(\Gamma^m_{ij}\Gamma^k_{ml} - \Gamma^m_{lj}\Gamma^k_{mi}\right)\\ &+ (1/4)\left(\Gamma^m_{ji}\Gamma^k_{lm} - \Gamma^m_{jl}\Gamma^k_{im}\right) + (1/4)\left(\Gamma^m_{ji}\Gamma^k_{ml} - \Gamma^m_{jl}\Gamma^k_{mi}\right)\end{aligned}$$

–

$$\begin{aligned}\mathbb{S}^m_{ij}\mathbb{T}^k_{lm} - \mathbb{S}^m_{lj}\mathbb{T}^k_{im} &= (1/4)\left(\Gamma^m_{ij}\Gamma^k_{lm} - \Gamma^m_{lj}\Gamma^k_{im}\right) - (1/4)\left(\Gamma^m_{ij}\Gamma^k_{ml} - \Gamma^m_{lj}\Gamma^k_{mi}\right)\\ &+ (1/4)\left(\Gamma^m_{ji}\Gamma^k_{lm} - \Gamma^m_{jl}\Gamma^k_{im}\right) - (1/4)\left(\Gamma^m_{ji}\Gamma^k_{ml} - \Gamma^m_{jl}\Gamma^k_{mi}\right)\end{aligned}$$

–

$$\begin{aligned}\mathbb{T}^m_{ij}\mathbb{T}^k_{lm} - \mathbb{T}^m_{lj}\mathbb{T}^k_{im} &= (1/4)\left(\Gamma^m_{ij}\Gamma^k_{lm} - \Gamma^m_{lj}\Gamma^k_{im}\right) - (1/4)\left(\Gamma^m_{ij}\Gamma^k_{ml} - \Gamma^m_{lj}\Gamma^k_{mi}\right)\\ &- (1/4)\left(\Gamma^m_{ji}\Gamma^k_{lm} - \Gamma^m_{jl}\Gamma^k_{im}\right) + (1/4)\left(\Gamma^m_{ji}\Gamma^k_{ml} - \Gamma^m_{jl}\Gamma^k_{mi}\right)\end{aligned}$$

–

$$\begin{aligned}\mathbb{T}^m_{ij}\mathbb{S}^k_{lm} - \mathbb{T}^m_{lj}\mathbb{S}^k_{im} &= (1/4)\left(\Gamma^m_{ij}\Gamma^k_{lm} - \Gamma^m_{lj}\Gamma^k_{im}\right) + (1/4)\left(\Gamma^m_{ij}\Gamma^k_{ml} - \Gamma^m_{lj}\Gamma^k_{mi}\right)\\ &- (1/4)\left(\Gamma^m_{ji}\Gamma^k_{lm} - \Gamma^m_{jl}\Gamma^k_{im}\right) - (1/4)\left(\Gamma^m_{ji}\Gamma^k_{ml} - \Gamma^m_{jl}\Gamma^k_{mi}\right)\end{aligned}$$

The sum of the four right hand sides of the four previous equations is equal to $\Gamma^m_{ij}\Gamma^k_{lm} - \Gamma^m_{lj}\Gamma^k_{im}$. And we have in second part :

–

$$\begin{aligned}\mathbb{S}^m_{ij}\mathbb{S}^k_{lm} + \mathbb{S}^m_{lj}\mathbb{S}^k_{im} &= (1/4)\left(\Gamma^m_{ij}\Gamma^k_{lm} + \Gamma^m_{lj}\Gamma^k_{im}\right) + (1/4)\left(\Gamma^m_{ij}\Gamma^k_{ml} + \Gamma^m_{lj}\Gamma^k_{mi}\right)\\ &+ (1/4)\left(\Gamma^m_{ji}\Gamma^k_{lm} + \Gamma^m_{jl}\Gamma^k_{im}\right) + (1/4)\left(\Gamma^m_{ji}\Gamma^k_{ml} + \Gamma^m_{jl}\Gamma^k_{mi}\right)\end{aligned}$$

–

$$\begin{aligned}\mathbb{S}^m_{ij}\mathbb{T}^k_{lm} + \mathbb{S}^m_{lj}\mathbb{T}^k_{im} &= (1/4)\left(\Gamma^m_{ij}\Gamma^k_{lm} + \Gamma^m_{lj}\Gamma^k_{im}\right) - (1/4)\left(\Gamma^m_{ij}\Gamma^k_{ml} + \Gamma^m_{lj}\Gamma^k_{mi}\right)\\ &+ (1/4)\left(\Gamma^m_{ji}\Gamma^k_{lm} + \Gamma^m_{jl}\Gamma^k_{im}\right) - (1/4)\left(\Gamma^m_{ji}\Gamma^k_{ml} + \Gamma^m_{jl}\Gamma^k_{mi}\right)\end{aligned}$$

–

$$\begin{aligned}\mathbb{T}^m_{ij}\mathbb{T}^k_{lm} + \mathbb{T}^m_{lj}\mathbb{T}^k_{im} &= (1/4)\left(\Gamma^m_{ij}\Gamma^k_{lm} + \Gamma^m_{lj}\Gamma^k_{im}\right) - (1/4)\left(\Gamma^m_{ij}\Gamma^k_{ml} + \Gamma^m_{lj}\Gamma^k_{mi}\right)\\ &- (1/4)\left(\Gamma^m_{ji}\Gamma^k_{lm} + \Gamma^m_{jl}\Gamma^k_{im}\right) + (1/4)\left(\Gamma^m_{ji}\Gamma^k_{ml} + \Gamma^m_{jl}\Gamma^k_{mi}\right)\end{aligned}$$

–

$$\begin{aligned}\mathbb{T}^m_{ij}\mathbb{S}^k_{lm} + \mathbb{T}^m_{lj}\mathbb{S}^k_{im} &= (1/4)\left(\Gamma^m_{ij}\Gamma^k_{lm} + \Gamma^m_{lj}\Gamma^k_{im}\right) + (1/4)\left(\Gamma^m_{ij}\Gamma^k_{ml} + \Gamma^m_{lj}\Gamma^k_{mi}\right)\\ &- (1/4)\left(\Gamma^m_{ji}\Gamma^k_{lm} + \Gamma^m_{jl}\Gamma^k_{im}\right) - (1/4)\left(\Gamma^m_{ji}\Gamma^k_{ml} + \Gamma^m_{jl}\Gamma^k_{mi}\right)\end{aligned}$$

The sum of the four right hand sides of the four previous equations is equal to $\Gamma^m_{ij}\Gamma^k_{lm} + \Gamma^m_{lj}\Gamma^k_{im}$.

Consequently,

$$\begin{aligned}&\mathbb{S}^k_{ij,l} + \mathbb{T}^k_{ij,l} + \mathbb{S}^m_{ij}\mathbb{S}^k_{lm} + \mathbb{S}^m_{ij}\mathbb{T}^k_{lm} + \mathbb{T}^m_{ij}\mathbb{S}^k_{lm} + \mathbb{T}^m_{ij}\mathbb{T}^k_{lm}\\ &= (1/2)\left(\Gamma^k_{ij,l} + \Gamma^m_{ij}\Gamma^k_{lm} - \Gamma^k_{lj,i} - \Gamma^m_{lj}\Gamma^k_{im}\right) + (1/2)\left(\Gamma^k_{ij,l} + \Gamma^m_{ij}\Gamma^k_{lm} + \Gamma^k_{lj,i} + \Gamma^m_{lj}\Gamma^k_{im}\right)\\ &= \mathbb{B}_{lij} + \mathbb{A}_{lij}\end{aligned}$$

Annexe B

Équation des ondes

B.1 Wave propagation equation

B.1.1 Units

- Lagrangean density $\mathcal{L}$: N/m^2
- mass density (per volume unit) ρ : kg/m^3
- constants of Lamé λ_0, μ_0 : N/m^2
- scalar strain energy ψ : $(m/s)^2$
- elasticity tensor of the material $\mathbb{E}$: $(m/s)^2$
- displacement vector $\mathbf{u}$: m
- vector $\tilde{\aleph}_0$: m^{-1}

We recall the time (unit s) derivation $\mathbf{u}_t := (\partial \mathbf{u}/\partial t)$. And the operators gradient ∇ and divergence div refer to the derivation with respect to $\mathbf{x} = (x_1, x_2, x_3)$ (unit m).

B.1.2 Equation

The Lagrangean density function takes the form of

$$\mathcal{L}(\mathbf{u}_t, \nabla \mathbf{u}) := (\rho/2)\|\mathbf{u}_t\|^2 - \rho\ \psi(\nabla \mathbf{u})$$

On the one hand, we consider a mass density

$$\rho := \rho_0\ \exp(\tilde{\aleph}_0 \cdot \mathbf{x}) \tag{B.1.1}$$

where ρ_0 is constant and non null. For linearized elasticity without initial stress, the (scalar) energy takes the form[1] of

$$\psi\left(\nabla \mathbf{u}\right) = (1/2)\varepsilon : \mathbb{E}\left[\varepsilon\right] \tag{B.1.2}$$

where $\mathbb{E}$ is the elasticity tensor of the material (4-order tensor), its components are labeled $\mathbb{E}_{ijkl}$. For the sake of the simplicity, we only consider an isotropic non homogeneous continuum with

$$\rho_0\ \mathbb{E}_{ijkl} = \lambda_0\ \delta_{ij}\delta_{kl} + \mu_0\left(\delta_{ik}\delta_{jl} + \delta_{il}\delta_{jk}\right)$$

[1] Recall : $\varepsilon = (1/2)\left(\nabla \mathbf{u} + \nabla^{\mathrm{T}}\mathbf{u}\right)$ is non-dimensionnal.

where λ_0 and μ_0 are constants of Lamé. Without going into details, we have

$$(1/2)\varepsilon : \mathbb{E}\,[\varepsilon] = (\lambda_0/2\rho_0)\ \mathrm{Tr}^2(\varepsilon) + (\mu_0/\rho_0)\ \mathrm{Tr}(\varepsilon^2) \tag{B.1.3}$$

According to (B.1.2) and (B.1.3) we deduce

$$\frac{\partial\psi}{\partial\nabla\mathbf{u}} = (\lambda_0/\rho_0)\ \mathrm{Tr}(\varepsilon)\ \mathbb{I} + 2(\mu_0/\rho_0)\ \varepsilon \tag{B.1.4}$$

and

$$\mathrm{div}\left(\frac{\partial\psi}{\partial\nabla\mathbf{u}}\right) = [(\lambda_0/\rho_0) + (\mu_0/\rho_0)]\,\nabla\,(\mathrm{div}\mathbf{u}) + (\mu_0/\rho_0)\ \Delta\mathbf{u} \tag{B.1.5}$$

On the other hand, the linear momentum equation is

$$\frac{\partial}{\partial t}\,(\mathbf{p}_t) + \mathrm{div}\mathbf{P}_{\nabla\mathbf{u}} = 0 \tag{B.1.6}$$

with

$$\mathbf{p}_t := \frac{\partial\mathcal{L}}{\partial\mathbf{u}_t} = \rho\ \mathbf{u}_t, \qquad \mathbf{P}_{\nabla\mathbf{u}} := \frac{\partial\mathcal{L}}{\partial\nabla\mathbf{u}} = -\rho\ \frac{\partial\psi}{\partial\nabla\mathbf{u}}$$

Applying Leibniz's rules for the divergence leads to

$$\mathrm{div}\mathbf{P}_{\nabla\mathbf{u}} = -\left[\rho\ \mathrm{div}\left(\frac{\partial\psi}{\partial\nabla\mathbf{u}}\right) + \frac{\partial\psi}{\partial\nabla\mathbf{u}}\ (\nabla\rho)\right]$$

which, according to (B.1.1), takes the form of

$$\mathrm{div}\mathbf{P}_{\nabla\mathbf{u}} = -\left[\rho\ \mathrm{div}\left(\frac{\partial\psi}{\partial\nabla\mathbf{u}}\right) + \rho\ \frac{\partial\psi}{\partial\nabla\mathbf{u}}(\tilde{\aleph}_0)\right]$$

Finally the linear momentum equation (B.1.6) takes the form of (the common factor $\rho \neq 0$ is dropped)

$$\mathrm{div}\left(\frac{\partial\psi}{\partial\nabla\mathbf{u}}\right) + \frac{\partial\psi}{\partial\nabla\mathbf{u}}(\tilde{\aleph}_0) = \mathbf{u}_{tt}$$

According to (B.1.4) and (B.1.5), we obtain the wave propagation equation :

$$(\lambda_0 + \mu_0)\,\nabla\,(\mathrm{div}\mathbf{u}) + \mu_0\ \Delta\mathbf{u} + \lambda_0\mathrm{Tr}\varepsilon\ \mathbb{I}(\tilde{\aleph}_0) + 2\mu_0\ \varepsilon(\tilde{\aleph}_0) = \rho_0\ \mathbf{u}_{tt}$$

B.2 Confluent hypergeometric equation

The Kummer's function of the first kind is noticed $\mathcal{M}\,(a,b;r)$ and second kind $\mathcal{U}\,(a,b;r)$, a, b, $r \in \mathbb{C}$. We assume the convergence conditions : $\Re(b) > \Re(a) > 0$ e.g. [2]. The integral representations of these functions are then

$$\begin{aligned}
\frac{\Gamma(b-a)\Gamma(a)}{\Gamma(b)}\ \mathcal{M}\,(a,b;r) &= \int_0^1\ e^{zt}t^{a-1}(1-t)^{b-a-1}\ dt \\
\Gamma(a)\ \mathcal{U}\,(a,b;r) &= \int_0^\infty\ e^{-zt}t^{a-1}(1+t)^{b-a-1}\ dt
\end{aligned}$$

Let us recall the general confluent hypergeometric differential equation

$$\begin{aligned} y'' &= -\left[\frac{2A}{r}+2f'+\frac{bh'}{h}-\frac{h''}{h'}\right]y'-\left[\left(\frac{bh'}{h}-h'-\frac{h''}{h'}\right)\left(\frac{A}{r}+f'\right)\right]y \\ &- \left[\frac{A(A-1)}{r^2}+\frac{2Af'}{r}+f''+(f')^2-\frac{a(h')^2}{h}\right]y \end{aligned}$$

where the unknown is $y=y(r)$, and $f=f(r)$ and $h=h(r)$ are C^2-functions with $h\neq 0$. The parameters are $a,b,A\in\mathbb{C}$. If we consider $f(r)=a_1r$ and $h(r)=a_2r$ with $a_1,a_2\in\mathbb{C}$ e.g. [16], then

$$\begin{aligned} y'' &= -\left[(2a_1-a_2)+\frac{2A+b}{r}\right]y' \\ &- \left[(a_1(a_1-a_2))+\frac{a_1(2A+b)-a_2(A+a)}{r}+\frac{A(A+b-1)}{r^2}\right]y \end{aligned}$$

Once constants a, b, A, a_1 and a_2 are known, functions

$$\left\{r^{-A}e^{-a_1r}\mathcal{M}(a,b;a_2r),\quad r^{-A}e^{-f(r)}\mathcal{U}(a,b;a_2r)\right\} \tag{B.2.1}$$

form a base of solutions of the confluent hypergeometric equation (above).

B.3 Cylinder

If we identify the equation of the motion (3.4.3) with the above confluent hypergeometric equation, the parameters a, b, a_1, a_2 and A are solutions of the following system

$$\left\{\begin{aligned} 2a_1-a_2 &= 2\aleph_0 \\ 2A+b &= 1 \\ a_1(a_1-a_2) &= \omega^2 \\ a_1(2A+b)-a_2(A+a) &= 2\left(1-2c^2\right)\aleph_0 \\ A(A+b-1) &= -1 \end{aligned}\right. \tag{B.3.1}$$

which may be separated to

$$\left\{\begin{aligned} 2A+b &= 1 \\ A(A+b-1) &= -1 \end{aligned}\right. \tag{B.3.2}$$

and

$$\left\{\begin{aligned} 2a_1-a_2 &= 2\aleph_0 \\ a_1(a_1-a_2) &= \omega^2 \end{aligned}\right. \tag{B.3.3}$$

and

$$a_1\left(2A+b\right)-a_2\left(A+a\right)=2\left(1-2c^2\right)\aleph_0 \tag{B.3.4}$$

The system (B.3.2) gives the solutions sets

$$\{A=-1,b=3\},\qquad \{A=1,b=-1\} \tag{B.3.5}$$

From the system (B.3.3), we have

$$a_1^2-2\aleph_0 a_1+\omega^2=0 \tag{B.3.6}$$

The solutions a_1 and a_2 depend on the sign of the discriminant $\left(\aleph_0^2-\omega^2\right)$.

- If $\left(\aleph_0^2-\omega^2\right)>0$ then we have either

$$\left\{a_1=\aleph_0+\sqrt{\aleph_0^2-\omega^2},a_2=2\sqrt{\aleph_0^2-\omega^2}\right\}$$

  or

$$\left\{a_1=\aleph_0-\sqrt{\aleph_0^2-\omega^2},a_2=-2\sqrt{\aleph_0^2-\omega^2}\right\}$$

- If $\left(\aleph_0^2-\omega^2\right)<0$ then we have either

$$\left\{a_1=\aleph_0+i\sqrt{\omega^2-\aleph_0^2},a_2=2i\sqrt{\omega^2-\aleph_0^2}\right\}$$

  or

$$\left\{a_1=\aleph_0-i\sqrt{\omega^2-\aleph_0^2},a_2=-2i\sqrt{\omega^2-\aleph_0^2}\right\}$$

- If $\left(\aleph_0^2-\omega^2\right)=0$ then we have $\{a_1=\aleph_0,a_2=0\}$

From the system (B.3.4) we have

$$a=-\frac{2\left(1-2c^2\right)\aleph_0-a_1+a_2A}{a_2} \tag{B.3.7}$$

and according to the values of a_1 and a_2, we have respectively

- If $\left(\aleph_0^2-\omega^2\right)>0$ then we have

$$a=\left[\left(4c^2-1\right)\aleph_0+3\sqrt{\omega^2-\aleph_0^2}\right]/\left[2\sqrt{\omega^2-\aleph_0^2}\right]$$

  or

$$a=\left[\left(1-4c^2\right)\aleph_0+3\sqrt{\omega^2-\aleph_0^2}\right]/\left[2\sqrt{\omega^2-\aleph_0^2}\right]$$

  .

- If $\left(\aleph_0^2-\omega^2\right)<0$ then we have

$$a=\left[\left(4c^2-1\right)\aleph_0+3i\sqrt{\omega^2-\aleph_0^2}\right]/\left[2i\sqrt{\omega^2-\aleph_0^2}\right]$$

  or

$$a=\left[\left(1-4c^2\right)\aleph_0+3i\sqrt{\omega^2-\aleph_0^2}\right]/\left[2i\sqrt{\omega^2-\aleph_0^2}\right]$$

  .

- If $\left(\aleph_0^2-\omega^2\right)=0$ then a is not defined.

Variable change (case $\aleph_0^2 - \omega^2 = 0$). Let $x = 2\sqrt{\xi r}$ and $\alpha = \alpha(r)$

$$\frac{\partial \alpha}{\partial r} = \frac{\partial \alpha}{\partial x}\frac{\partial x}{\partial r} = \frac{\partial \alpha}{\partial x}\left(\frac{\partial x}{\partial \xi r}\frac{\partial \xi r}{\partial r}\right) = \frac{\partial \alpha}{\partial x}\left(\frac{2\xi}{x}\right)$$

and

$$\begin{aligned}
\frac{\partial^2 \alpha}{\partial r^2} &= \frac{\partial}{\partial r}\left(\frac{\partial \alpha}{\partial r}\right) \\
&= \frac{\partial}{\partial x}\left(\frac{\partial \alpha}{\partial x}\frac{\partial x}{\partial r}\right)\frac{\partial x}{\partial r} \\
&= \frac{\partial}{\partial x}\left(\frac{\partial \alpha}{\partial x}\frac{\partial x}{\partial \xi r}\frac{\partial \xi r}{\partial r}\right)\frac{\partial x}{\partial \xi r}\frac{\partial \xi r}{\partial r} \\
&= \frac{\partial^2 \alpha}{\partial x^2}\left(\frac{\partial x}{\partial \xi r}\frac{\partial \xi r}{\partial r}\right)^2 + \frac{\partial \alpha}{\partial x}\frac{\partial}{\partial x}\left(\frac{\partial x}{\partial \xi r}\frac{\partial \xi r}{\partial r}\right)\frac{\partial x}{\partial \xi r}\frac{\partial \xi r}{\partial r} \\
&= \frac{\partial^2 \alpha}{\partial x^2}\left(\frac{4\xi^2}{x^2}\right) - \frac{\partial \alpha}{\partial x}\left(\frac{4\xi^2}{x^3}\right)
\end{aligned}$$

Thus we have

$$\begin{aligned}
(\xi r - 1)\,\alpha &= \left[\frac{x^2}{4} - 1\right]\alpha \\
r\frac{\partial \alpha}{\partial r} &= \frac{x}{2}\frac{\partial \alpha}{\partial x} \\
r^2\frac{\partial^2 \alpha}{\partial r^2} &= \frac{x^2}{4}\frac{\partial^2 \alpha}{\partial x^2} - \frac{x}{4}\frac{\partial \alpha}{\partial x}
\end{aligned}$$

B.4 Beam

For $\Delta_\Theta := \aleph_1^2 - \omega^2 > 0$ the general angle solution of (3.5.13) is

$$\Theta(x,t) = \left[C_1\, e^{\sqrt{\aleph_1^2-\omega^2}x} + C_2\, e^{-\sqrt{\aleph_1^2-\omega^2}x}\right] e^{-\aleph_1 x},$$

for $\Delta_\Theta := \aleph_1^2 - \omega^2 < 0$ that is

$$\Theta(x,t) = \left[C_1\, e^{i\sqrt{\omega^2-\aleph_1^2}x} + C_2\, e^{-i\sqrt{\omega^2-\aleph_1^2}x}\right] e^{-\aleph_1 x}$$

and for $\Delta_\Theta := \aleph_1^2 - \omega^2 = 0$ that is

$$\Theta(x,t) = [C_1 + C_2\, x]\, e^{-\aleph_1 x}.$$

For $\Delta_U := \aleph_1^2 - \dfrac{\omega^2}{c^2} > 0$, the general displacement solution, associated with homogeneous second equation of (3.5.13), is

$$U(x) = \left[K_1\ e^{\sqrt{\aleph_1^2 - \frac{\omega^2}{c^2}}x} + K_2\ e^{-\sqrt{\aleph_1^2 - \frac{\omega^2}{c^2}}x}\right] e^{-\aleph_1 x},$$

for $\Delta_U := \aleph_1^2 - \dfrac{\omega^2}{c^2} < 0$, that is

$$U(x) = \left[K_1\ e^{i\sqrt{\frac{\omega^2}{c^2} - \aleph_1^2}x} + K_2\ e^{-i\sqrt{\frac{\omega^2}{c^2} - \aleph_1^2}x}\right] e^{-\aleph_1 x}$$

for $\Delta_U := \aleph_1^2 - \dfrac{\omega^2}{c^2} = 0$, that is

$$U(x) = [K_1 + K_2\ x]\, e^{-\aleph_1 x}.$$

Now, we aim to search for a particular solution of the second equation of (3.5.13). Let us note $\phi(x) := (1 - c^2)\ \Theta' + 2c^2\aleph_1\ \Theta$. The second equation of (3.5.13) is reformulated by

$$U'' + 2\aleph_1\ U' + (\omega^2/c^2)\ U = \phi(x)\ c^{-2}. \tag{B.4.1}$$

Lemma B.4.1 *For $\Delta_\Theta \neq 0$, a particular solution of equation (B.4.1) is*

$$U^{part}(x) = \left[(1 - c^2)\ \Theta'(x) + 2c^2\aleph_1\ \Theta(x)\right] / \left[(1 - c^2)\ \omega^2\right]. \tag{B.4.2}$$

Proof. Let us remark that ϕ depends on the angle Θ, and consequently on the sign of the discriminant Δ_Θ. Then let us consider the following numbers, with respect to Δ_Θ and $\aleph_1$

$$\begin{cases} \beta_1 &= -\aleph_1 + \sqrt{\Delta_\Theta} \\ \beta_2 &= -\aleph_1 - \sqrt{\Delta_\Theta} \\ \gamma_1 &= -\aleph_1 + i\sqrt{-\Delta_\Theta} \\ \gamma_2 &= -\aleph_1 - i\sqrt{-\Delta_\Theta} \\ \beta_0 &= -\aleph_1 \end{cases}$$

and the two functions

$$\begin{cases} f_1(k) &= \left[\left(1 - c^2\right) C_1\right] k + 2\aleph_1 c^2 C_1 \\ f_2(k) &= \left[\left(1 - c^2\right) C_2\right] k + 2\aleph_1 c^2 C_2 \end{cases}$$

If $\Delta_\Theta > 0$ then

$$\phi(x) = f_1(\beta_1)\, e^{\beta_1 x} + f_2(\beta_2)\, e^{\beta_2 x}, \tag{B.4.3}$$

a particular solution of (B.4.1) takes the form of

$$U(x) = \left[\frac{f_1(\beta_1)\, e^{\beta_1 x}}{\beta_1^2 + 2\aleph_1\beta_1 + (\omega/c)^2} + \frac{f_2(\beta_2)\, e^{\beta_2 x}}{\beta_2^2 + 2\aleph_1\beta_2 + (\omega/c)^2}\right] c^{-2} \tag{B.4.4}$$

If $\Delta_\Theta < 0$ then

$$\phi(x) = f_1(\gamma_1)\, e^{\gamma_1 x} + f_2(\gamma_2)\, e^{\gamma_2 x}, \tag{B.4.5}$$

a particular solution of (B.4.1) takes the form of

$$U(x) = \left[\frac{f_1(\gamma_1)\, e^{\gamma_1 x}}{\gamma_1^2 + 2\aleph_1\gamma_1 + (\omega/c)^2} + \frac{f_2(\gamma_2)\, e^{\gamma_2 x}}{\gamma_2^2 + 2\aleph_1\gamma_2 + (\omega/c)^2}\right] c^{-2} \tag{B.4.6}$$

In both previous cases the particular solution depends on the sign of Δ_Θ but does not depend on the value of Δ_U. After simplification the particular solution takes the common form of

$$U = U^{part}(x) = \frac{\left(1-c^2\right)\Theta'(x) + 2c^2\aleph_1\Theta(x)}{\left(1-c^2\right)\omega^2} \tag{B.4.7}$$

with the corresponding $\Theta(x)$ according to the sign of Δ_Θ.

□

If $\Delta_\Theta = 0$ then

$$\phi(x) = (\phi_1 + \phi_2 x)\, e^{\beta_0 x} \tag{B.4.8}$$

with

$$\begin{aligned} \phi_1 &= -(1-c^{-2})\left(\Theta_2 - \aleph_1\Theta_1\right) + 2\aleph_1\Theta_1 \\ \phi_2 &= (1-c^{-2})\aleph_1\Theta_2 + 2\aleph_1\Theta_2 \end{aligned}$$

In such a case, the solution of (B.4.1) takes the form of

$$\left\{\begin{aligned} U(x) &= (U_1 + U_2 x)\, e^{\beta_0 x} \\ U_1 &= -\left(C_2 + c^2 C_2 + C_1\aleph_1 - 3c^2 C_1\aleph_1\right) / \left(c^2\aleph_1^2 - \omega^2\right) \\ U_2 &= \left(C_2 - 3c^2 C_2\aleph_1\right)\left(c^2\aleph_1^2 - \omega^2\right) \end{aligned}\right. \tag{B.4.9}$$

Different cases. Since $0 < c^2 < 1$ then $\Delta_U < \Delta_\Theta$, the possible cases are

$$\Delta_\Theta > 0 \Longrightarrow \Delta_U > 0 \tag{B.4.10}$$

$$\Delta_\Theta > 0 \Longrightarrow \Delta_U = 0 \tag{B.4.11}$$

$$\Delta_\Theta > 0 \Longrightarrow \Delta_U < 0 \tag{B.4.12}$$

$$\Delta_\Theta = 0 \Longrightarrow \Delta_U < 0 \tag{B.4.13}$$

$$\Delta_\Theta < 0 \Longrightarrow \Delta_U < 0 \tag{B.4.14}$$

In the general case, the solutions of

$$\Theta''(x) + 2\aleph_1\, \Theta'(x) + \omega^2\, \Theta = 0 \tag{B.4.15}$$

are determined according to the sign of Δ_Θ. The solutions of

$$U''(x) + 2\aleph_1\, U'(x) + (\omega/c)^2\, U = \phi(x)\, c^{-2} \tag{B.4.16}$$

are determined according to the sign of Δ_U (homogeneous solution) and Δ_Θ (particular solution). The general solution of (3.5.13) is given in respect with the non dimensionnal parameters ω, c and $\aleph_1$.

Application. For illustration, we consider the bending and transversal wave within a clamped-clamped beam are studied : the boundary conditions are $\Theta(0) = \Theta(1) = 0$ and $U(0) = U(1) = 0$. In the case $\{\aleph_2 = 0, \aleph_1 \neq 0\}$, according to the boundary condition, for (B.4.10) and (B.4.11) the solutions of (3.5.13) are trivial $\Theta(x) = 0$ and $U(x) = 0$. For (B.4.12) and (B.4.13), the angle is null $\Theta(x) = 0$ and consequently the transversal displacement is the solution of homogeneous equation $U'' + 2\aleph_1 U' + (\omega^2/c^2) U = 0$:

$$U(x) = \left[U_1 \, e^{i\sqrt{\frac{\omega^2}{c^2} - \aleph_1^2}x} + U_2 \, e^{-i\sqrt{\frac{\omega^2}{c^2} - \aleph_1^2}x}\right] e^{-\aleph_1 x} \tag{B.4.17}$$

And U_1 and U_2 are solutions of

$$\begin{cases} U_1 + U_2 &= 0 \\ U_1 \, e^{i\sqrt{\frac{\omega^2}{c^2} - \aleph_1^2}} + U_2 \, e^{-i\sqrt{\frac{\omega^2}{c^2} - \aleph_1^2}} &= 0 \end{cases}$$

Non trivial solutions exist if and only if $\sin\left[\sqrt{(\omega/c)^2 - \aleph_1^2}\right] = 0$. The eigenfrequencies are then, e.g. [74]

$$\omega_n = \sqrt{c^2\left(n^2\pi^2 + \aleph_1^2\right)}, \qquad n = 1, ..., \infty \tag{B.4.18}$$

The most interesting case (B.4.14) has been studied in details in a previous section.

Remark B.4.1 *If $\{\aleph_2 \neq 0, \aleph_1 = 0\}$ and $\{\aleph_2 \neq 0, \aleph_1 \neq 0\}$ are introduced into equation (3.5.10), then according to the previous boundary conditions we show directly that the solutions are trivial ($C_1 = C_2 = 0$ and $K_1 = K_2 = 0$). This is the reason why we have detailed the case $\{\aleph_2 = 0, \aleph_1 \neq 0\}$ in this paper.*

Annexe C

Modèle d'indentation

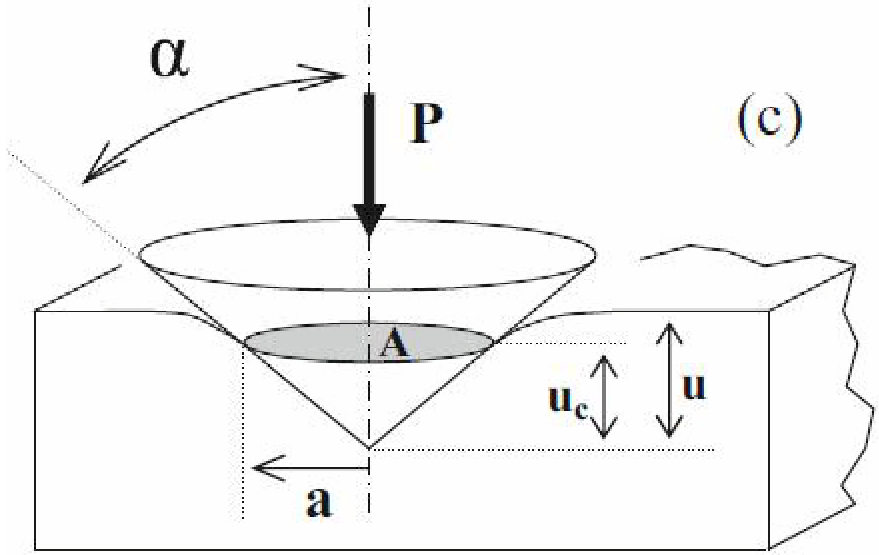

Fig. C.0.1 – Indentation de Vickers avec un indenteur conique. Cette figure est extraite de [6].

C.1 Identification of parameters

C.1.1 Fourier series : recalls

Let be a T-periodic function $f : D \subset \mathbb{R} \longrightarrow \mathbb{C}$ and the following coefficients for $n = 1, ..., \infty$

$$\begin{cases} a_0 &= (1/T)\int_{-T/2}^{T/2} f(t)dt \\ a_n &= (2/T)\int_{-T/2}^{T/2} f(t)\cos(\frac{2\pi nt}{T})dt \\ b_n &= (2/T)\int_{-T/2}^{T/2} f(t)\sin(\frac{2\pi nt}{T})dt \end{cases} \tag{C.1.1}$$

The Fourier series $\mathcal{FS}(f)$ associated with the function f is the trigonometric series for which the general term is defined according to the coefficients (C.1.1) :

$$[\mathcal{FS}(f)](t) = a_0 + \sum_{n\in\mathbb{N}^*}[a_n\cos(nt) + b_n\sin(nt)] \tag{C.1.2}$$

where the series is defined $\forall\ t \in D$:

$$\sum_{n\in\mathbb{N}^*}[a_n\cos(nt) + b_n\sin(nt)] = \lim_{N\longrightarrow\infty}\sum_{n=1}^{N}[a_n\cos(nt) + b_n\sin(nt)] \tag{C.1.3}$$

According to (C.1.1), if f is even then $b_n = 0$ pour $n = 1, ..., \infty$ and if f is odd then $a_0 = 0$ and $a_n = 0$ pour $n = 1, ..., \infty$. We have the following definitions and theorems e.g. [78] :

Definition C.1.1 *A function $f : [a, b] \subset \mathbb{R} \longrightarrow \mathbb{R}$ is a function of bounded variation if for any subdivision τ of $[a, b]$: $\tau = [t_0 = a, ..., t_{i-1}, t_i, t_{i+1}, ..., t_l = b]$, we have*

$$\sup_{\tau}\sum_{i=0}^{n-1}|f(t_{i+1}) - f(t_i)| < \infty \tag{C.1.4}$$

Theorem C.1.1 *If f is a function of bounded variation in the period interval, then the Fourier series of f is semi-convergent at each point $t \in \mathbb{R}$ to the arithmetic mean of the left-hand limit[1] $f(t-0)$ and the right-hand limit[2] $f(t+0)$:*

$$\lim_{N\longrightarrow\infty}\{a_0 + \sum_{n=1}^{N}[a_n\cos(nt) + b_n\sin(nt)]\} = \frac{1}{2}[f(t-0) + f(t+0)] \tag{C.1.5}$$

or

$$[\mathcal{FS}(f)](t) = \frac{1}{2}[f(t-0) + f(t+0)] \tag{C.1.6}$$

[1] $f(t-0) = \lim_{t\longrightarrow 0^-} f(t)$
[2] $f(t+0) = \lim_{t\longrightarrow 0^+} f(t)$

Theorem C.1.2 *(Theorem of unicity of Cantor) If the Fourier series converges to the null function, i.e.*

$$\forall\ t \in \mathbb{R},\ \lim_{N \longrightarrow \infty} \{a_0 + \sum_{n=1}^{N} [a_n \cos(nt) + b_n \sin(nt)]\} = 0 \tag{C.1.7}$$

then all the coefficients are null : $a_0 = 0$, $a_n = 0$ and $b_n = 0$ for $n = 1, ..., \infty$.

Let us also recall the following theorem :

Theorem C.1.3 *(Inequality of finite increases) Let $f : [a, b] \subset \mathbb{R} \longrightarrow \mathbb{R}$ a function continuous for $a \leq x \leq b$, differentiable for $a < x < b$ and it exists a constant $k > 0$ such that $|f'(x)| \leq k$ for $a < x < b$. Then*

$$|f(a) - f(b)| \leq k|a - b| \tag{C.1.8}$$

Let us recall the definition of a Lipschitzian function :

Definition C.1.2 *A function $f : I \subset \mathbb{R} \longrightarrow \mathbb{R}$ is k-Lipschitzian if it exists a constant $k > 0$ such that $\forall\ x, y \in I : |f(x) - f(y)| \leq k|x - y|$.*

Properties C.1.1 *Any Lipschitzian function is a function of bounded variation, e.g [78].*

C.1.2 Approximation in Fourier series

Let the following functions f_1 et f_2 defined for $\theta \in [-\pi/2; \pi/2]$ et $r \in \mathbb{R}_+$:

$$\begin{aligned} f_1(r, \theta) &= \frac{P(1 - 2\nu + 2(-2 + \nu)\cos\theta)}{2\pi r^2} + \frac{4B(-2 + \nu - (-5 + \nu)\cos^2\theta)}{r^3} \\ &+ p\cos^2\theta + q\sin^2\theta \\ f_2(r, \theta) &= \frac{1}{2}\cos\theta \left[-2p + 2q + \frac{8B(1 + \nu)}{r^3} + \frac{P - 2P\nu}{\pi r^2(1 + \cos\theta)}\right] \sin\theta \end{aligned}$$

where P, B, q and p are scalar parameters. Next we will fix the variable r and only θ is variable. Both functions f_1 and f_2 are defined for $\theta \in [-\pi/2; \pi/2]$ and we prolong these by periodicity of period $T = \pi$. The Fourier series of f_1 is labeled $\mathcal{FS}(f_1)$ and the Fourier series of f_2 is labeled $\mathcal{FS}(f_2)$. The function f_1 is even with respect to θ and the function f_2 is odd with respect to θ. Consequently we have

$$\mathcal{FS}(f_1) = a_0 + \sum_{n \in \mathbb{N}^*} a_n \cos(n\theta), \qquad \mathcal{FS}(f_2) = \sum_{n \in \mathbb{N}^*} b_n \sin(n\theta) \tag{C.1.9}$$

with the coefficients

$$a_0 = \frac{2}{\pi}\int_0^{\pi/2} f_1(\theta)d\theta$$

$$a_n = \frac{4}{\pi}\int_0^{\pi/2} f_1(\theta)\cos(2n\theta)d\theta$$

$$b_n = \frac{4}{\pi}\int_0^{\pi/2} f_2(\theta)\sin(2n\theta)d\theta$$

According to the theorem C.1.3 and definition C.1.2, the functions $\cos\theta$, $\cos^2\theta$, $\sin^2\theta$, $\cos\theta\sin\theta$ and $(\cos\theta\sin\theta)/(1+\cos\theta)$ are Lipschitzian for $\theta \in [-\pi/2;\pi/2]$. Indeed, all the derivatives of these functions are bounded for $\theta \in [-\pi/2;\pi/2]$. $\forall\ \theta_1, \theta_2 \in [-\pi/2;\pi/2]$ and $\theta_1 < \theta < \theta_2$:

$$\begin{aligned}
|\cos\theta_1 - \cos\theta_2| &\leq |\sin\theta||\theta_1-\theta_2| \leq |\theta_1-\theta_2| \\
|\cos^2\theta_1 - \cos^2\theta_2| &\leq |-2\sin\theta\cos\theta||\theta_1-\theta_2| \leq 2|\theta_1-\theta_2| \\
|\sin^2\theta_1 - \sin^2\theta_2| &\leq |2\sin\theta\cos\theta||\theta_1-\theta_2| \leq 2|\theta_1-\theta_2| \\
|\cos\theta_1\sin\theta_1 - \cos\theta_2\sin\theta_2| &\leq |-\sin^2\theta+\cos^2\theta||\theta_1-\theta_2| \leq 2|\theta_1-\theta_2| \\
|\frac{\cos\theta_1\sin\theta_1}{1+\cos\theta_1} - \frac{\cos\theta_2\sin\theta_2}{1+\cos\theta_2}| &\leq |\frac{-\sin^2\theta+\cos^2\theta}{(1+\cos\theta)} + \frac{\cos\theta\sin^2\theta}{(1+\cos\theta)^2}| \leq 3|\theta_1-\theta_2|
\end{aligned}$$

Consequently, the functions f_1 and f_2 are Lipschitzian and, according to the property C.1.1, these are functions of bounded variation in the period interval $[-\pi/2;\pi/2]$. According to the theorem C.1.1, the Fourier series $\mathcal{FS}(f_1)$ and $\mathcal{FS}(f_2)$ are respectively convergent to f_1 and f_2 for $\theta \in [-\pi/2;\pi/2]$

$$[\mathcal{FS}(f_1)](\theta) = f_1(\theta), \qquad [\mathcal{FS}(f_2)](\theta) = f_2(\theta)$$

since f_1 and f_2 are also continuous for $\theta \in [-\pi/2;\pi/2]$. If the functions f_1 and f_2 are null then, according to the theorem C.1.2, all the coefficients of $\mathcal{FS}(f_1)$ and $\mathcal{FS}(f_2)$ are null. In particular, from (C.1.9), $a_0 = 0$, $a_1 = 0$ and $b_1 = 0$. However the equation $f_1(\theta) = 0$ corresponds to the equation $\sigma_U^{rr} = \sigma_{Bo}^{rr} + \sigma_{bl}^{rr}$ and the equation $f_2(\theta) = 0$ corresponds to the equation $\sigma_U^{r\theta} = \sigma_{Bo}^{r\theta} + \sigma_{bl}^{r\theta}$, for $\theta \in [-\pi/2;\pi/2]$. We find

$$a_0 = \frac{4B\pi^2(1+\nu) + r(\pi^2(p+q)r^2 + P(-8+\pi+4\nu-2\pi\nu))}{2\pi^2 r^3}$$

$$a_1 = \frac{r(3\pi^2(p-q)r^2 + 8P(-2+\nu)) - 12B\pi^2(-5+\nu)}{6\pi^2 r^3}$$

$$b_1 = \frac{12B\pi^2(1+\nu) + r(3\pi^2(-p+q)r^2 - 2P(-8+3\pi)(-1+2\nu))}{6\pi^2 r^3}$$

The calculus have been done by using Mathematica. Let us begin with the equation $b_1 = 0$ to estimate the parameter B :

$$B = \frac{r(16P - 6P\pi + 3p\pi^2 r^2 - 3\pi^2 q r^2 - 32P\nu + 12P\pi\nu)}{12\pi^2(1+\nu)} \tag{C.1.10}$$

Then, let us introduce B into the equation $a_0 = 0$ to estimate the parameter p :

$$p = -\frac{P(-8 - 3\pi - 20\nu + 6\pi\nu)}{6\pi^2 r^2} \tag{C.1.11}$$

Then, let us introduce p into the equation $a_1 = 0$ to estimate the parameter q :

$$q = -\frac{P(-88 + 21\pi + 124\nu - 48\pi\nu - 40\nu^2 + 12\pi\nu^2)}{18\pi^2 r^2} \tag{C.1.12}$$

Finally, according to the equation $P = p\,\pi a^2$, we have the radius r related to the interface inclusion/matrix, labeled R :

$$R = a\,\frac{\sqrt{8 + \pi(3 - 6\nu) + 20\nu}}{\sqrt{6\pi}} \tag{C.1.13}$$

which only depends on parameters which characterize the material (Poisson ratio ν) and the indenter (radius a of the pressure disc). The value $r = R$ is respectively introduced into (C.1.12) and (C.1.10). We obtain :

$$\begin{aligned} B &= \frac{aP(16 - 20\nu + \pi(-3 + 6\nu))\sqrt{8 + \pi(3 - 6\nu) + 20\nu}}{36\sqrt{6\pi^5}} \\ q &= \frac{P(-88 + 124\nu - 40\nu^2 + 3\pi(7 - 16\nu + 4\nu^2))}{3a^2\pi(-8 - 3\pi - 20\nu + 6\pi\nu)} \end{aligned}$$

Remark C.1.1 *The parameters B, q and p are the unknown factors of a linear system of three equations : $a_0 = 0$, $a_1 = 0$, $b_1 = 0$. Thus we have chosen an arbitrary order to have the expressions of B, p, q : B according to $b_1 = 0$, then p according to $a_0 = 0$, then q according to $a_1 = 0$. These also depend on the radius r (fixed), and also on the Poisson ratio ν and on the force P or on the radius a. We gauge r according to the equation $P = p\pi a^2$ with the previous expression of p (P is simplified). Finally we introduce that into the expression of q and B, which consequently depend on ν, a and P.*

Remark C.1.2 *The values of R, q and B are approximations because we have used only three null coefficients from the Fourier series ($a_0 = 0$, $a_1 = 0$, $b_1 = 0$). Let us recall that all the coefficients are null in such a case.*

C.2 Polar equations

The equations at the interface inclusion/matrix are rewritten : a system of two equations with one unknown $R = r\ a$ (adimensionnal)

$$\begin{cases} \alpha + \dfrac{\beta}{R^2} + \dfrac{\gamma}{R^3} &= 0 \\ \lambda + \dfrac{\mu}{R^2} + \dfrac{\tau}{R^3} &= 0 \end{cases} \tag{C.2.1}$$

with

$$\begin{cases} \alpha &= p\cos^2\theta + q\sin^2\theta \\ \beta &= \dfrac{P(1-2\nu+2(-2+\nu)\cos\theta)}{2a^2\pi} \\ \gamma &= \dfrac{4B(-2+\nu-(-5+\nu)\cos^2\theta)}{a^3} \\ \lambda &= -2p+2q \\ \mu &= \dfrac{8B(1+\nu)}{a^3} \\ \tau &= \dfrac{P-2P\nu}{\pi a^2(1+\cos\theta)} \end{cases} \tag{C.2.2}$$

According to [83], the stress fields on the inclusion (Boussinesq and blister) are distinguished according to their dependence on the radius : the Boussinesq field depends on the adimensionnal radius R^{-2} and the blister field depends on R^{-3}. We consider then both formal unknown factors : $X = R^{-2}$ and $Y = R^{-3}$. Thus the system (C.2.1) takes the form of

$$\begin{cases} \alpha + \beta\ X + \gamma\ Y &= 0 \\ \lambda + \mu\ X + \tau\ Y &= 0 \end{cases} \tag{C.2.3}$$

which is a linear system of two equations with two unknown X and Y. The method of substitution allows to propose the following solutions :

$$X = \frac{\lambda\gamma - \tau\alpha}{\tau\beta - \mu\gamma}, \qquad Y = \frac{\beta\lambda - \alpha\mu}{\gamma\mu - \beta\tau} \tag{C.2.4}$$

Since the scalars $\{\alpha, \beta, \gamma, \lambda, \mu, \tau\}$ depend on the parameters B, q and p, the variables X and Y depend on these. We introduce into X and Y the parameters previously evaluated

$$\begin{aligned} B &= \frac{aP(16-20\nu+\pi(-3+6\nu))\sqrt{8+\pi(3-6\nu)+20\nu}}{36\sqrt{6\pi^5}} \\ q &= \frac{P(-88+124\nu-40\nu^2+3\pi(7-16\nu+4\nu^2))}{3a^2\pi(-8-3\pi-20\nu+6\pi\nu)} \\ p &= \frac{P}{\pi\ a^2} \end{aligned}$$

The factor (P^2/a^4) appears into numerator and denominator of ratios (C.2.4). Consequently, X and Y depend only on the variable θ, and also on the Poisson ratio ν. According to X, the form R^2 takes the form of

$$R^2[\theta] = \frac{3(-1+\nu)[1+\nu+2(1+\nu)\cos\theta-3(-1+\nu)\cos 2\theta]\sec^2[\theta/2]}{8(-1+\nu^2+(-3+6\nu)\cos 2\theta)} \tag{C.2.5}$$

where $\sec\theta = 1/\cos\theta$. And according to Y, the second form R^3 takes the form of

$$R^3[\theta] = -\frac{N}{D} \tag{C.2.6}$$

with the numerator

$$\begin{aligned} N &= \sqrt{8+\pi(3-6\nu)+20\nu}(-8-3\pi-20\nu+6\pi\nu) \\ &\times (16-20\nu+\pi(-3+6\nu))(1+\nu+2(1+\nu)\cos\theta-3(-1+\nu)\cos 2\theta) \end{aligned}$$

and the denominator

$$\begin{aligned} D &= 6\sqrt{6\pi^3}(-40+12\pi+88\nu-21\pi\nu+20\nu^2-6\pi\nu^2 \\ &+ (6\pi(5-11\nu+2\nu^2)-8(8-23\nu+5\nu^2))\cos\theta \\ &+ (-32+15\pi+92\nu-33\pi\nu-20\nu^2+6\pi\nu^2)) \end{aligned}$$

Then we note $R^2 = r_1$ and $R^3 = r_2$.

Remark C.2.1 *The resolution of the system (C.2.1) is not a mathematical resolution, which would consist to solve the first equation then the second equation and finally to intersect both sets of solutions. We have introduced two variables which describe the action of both stress field in the inclusion, namely the Boussinesq field and the blister field. We have conserved the assumptions of loading since we have used the values of B, q, p previously evaluated. Our objective is to propose forms of polar functions $R = R(\theta)$, to draw the form of the inclusion (deformed).*

C.3 Auto-similarity

The uniform pressure p is solution of the equation $P = p\pi a^2$ and it is calculated according to the parameters R, B and q, which are previously identified. We have used the adapted equation for a Vickers test [43], [26] :

$$\begin{aligned}
\pi a^2 &= (49/2)h^2 \\
\pi a^2 &= (49/2)(u_r^{bl}(R,0) + u_r^{Bo}(R,0))^2 \\
\pi a^2 &= (49/2)P^2(...)^2 \\
\pi a^2 &= (49/2)p^2\pi^2 a^4(...)^2
\end{aligned}$$

where the term in brackets (...) depends on $G = E/(2+2\nu)$ and ν. The expression of p thus depends on E (Young modulus) and ν (Poisson ratio) :

$$p = E\sqrt{-\frac{27\pi^2(-8-3\pi-20\nu+6\pi\nu)}{49[(8+3\pi(-2+\nu)-10\nu)(3+\nu-2\nu^2)]^2}} \tag{C.3.1}$$

We etablish the relation between the densification volume ΔV and the load P. We have $P = p\ a^2\ \pi$ which involves that the radius $a = \sqrt{P/p\pi}$.

$$\begin{aligned}
\frac{E\ \Delta V}{Pa} &= \frac{(1-2\nu)(1+\nu)(16-20\nu+\pi(-3+6\nu))\sqrt{8+\pi(3-6\nu)+20\nu}}{27\sqrt{6\pi^3}} \\
\Delta V &= \phi(\nu)\ \frac{Pa}{E} \\
\Delta V &= \phi(\nu)\ \frac{P^{3/2}}{E\sqrt{p\pi}}
\end{aligned}$$

and, according to (C.3.1) $p = p(E,\nu)$, we have

$$\Delta V = f(E,\nu)\ P^{3/2} \tag{C.3.2}$$

The exposant (3/2) of the load P is a consequence of the auto-similar characteristic of the indenter, and this information has been suggested by reviewer for publication in journal "Matériaux et Techniques" (2008).

C.4 Equations in cylindrical system

Onto the orthonormal basis $(\mathbf{e}_r, \mathbf{e}_\theta, \mathbf{e}_z)$, the equilibrium equation (without external force) is in cylindrical coordinates (with $\partial_\theta = 0$) :

$$\left\{\begin{aligned}
\frac{\partial\sigma^{rr}}{\partial r} + \frac{\partial\sigma^{rz}}{\partial z} + \frac{\sigma^{rr}-\sigma^{\theta\theta}}{r} + \sigma^{rr}\aleph_0 &= 0 \\
\frac{\partial\sigma^{zr}}{\partial r} + \frac{\partial\sigma^{zz}}{\partial z} + \frac{\sigma^{zr}}{r} + \sigma^{rz}\aleph_0 &= 0
\end{aligned}\right. \tag{C.4.1}$$

Let us define the longitudinal velocity c_L^2 and the transversal velocity c_T^2,

$$\begin{cases} c_L^2 & := & \dfrac{\lambda+2\mu}{\rho} \\ c_T^2 & := & \dfrac{\lambda+2\mu}{\rho} \\ c_L^2 - 2c_T^2 & := & \dfrac{\lambda}{\rho} \end{cases} \tag{C.4.2}$$

and with the relations between the stress and the displacement, the equations (C.4.1) become

$$\begin{cases} c_L^2 \dfrac{\partial^2 u}{\partial r^2} + (\dfrac{c_L^2}{r} + c_L^2 \aleph_0)\dfrac{\partial u}{\partial r} + 2c_T^2 \dfrac{\partial^2 u}{\partial z^2} + (-\dfrac{c_L^2}{r^2} + \dfrac{c_L^2 - 2c_T^2}{r}\aleph_0)u \\ \qquad + c_L^2 \dfrac{\partial^2 w}{\partial r \partial z} + (c_L^2 - 2c_T^2)\aleph_0 \dfrac{\partial w}{\partial z} = 0 \\ 2c_T^2 \dfrac{\partial^2 w}{\partial r^2} + (\dfrac{2c_T^2}{r} + 2c_T^2 \aleph_0)\dfrac{\partial w}{\partial r} + c_L^2 \dfrac{\partial^2 w}{\partial z^2} \\ \qquad + c_L^2 \dfrac{\partial^2 u}{\partial z \partial r} + (\dfrac{c_L^2}{r} + 2c_T^2 \aleph_0)\dfrac{\partial u}{\partial z} = 0 \end{cases} \tag{C.4.3}$$

Let us introduce the following scales

$$\begin{cases} t & = & T\tilde{t}, & time \\ r & = & L\tilde{r}, & radius \\ z & = & L\tilde{z}, & depth \\ \aleph_0 & = & \dfrac{\tilde{\aleph}_0}{L}, & defect \\ u & = & R\tilde{u}, & radial\ \ displacement \\ w & = & R\tilde{w}, & vertical\ \ displacement \end{cases} \tag{C.4.4}$$

where the letters with the "tilde" have no dimension. Next the non-dimensional variables will be noticed without the "tilde". The following choice of the time variable

$$T = \frac{R}{c_L} \tag{C.4.5}$$

induces that (C.4.3) becomes non-dimensional

$$\left\{\begin{array}{rcl} \frac{\partial^2 u}{\partial r^2} + (\frac{1}{r} + \aleph_0)\frac{\partial u}{\partial r} + 2c^2\frac{\partial^2 u}{\partial z^2} + (-\frac{1}{r^2} + \frac{1-2c^2}{r}\aleph_0)u & & \\ + \frac{\partial^2 w}{\partial r \partial z} + (1-c^2)\aleph_0\frac{\partial w}{\partial z} & = & 0 \\ 2c^2\frac{\partial^2 w}{\partial r^2} + (\frac{2c^2}{r} + 2c^2\aleph_0)\frac{\partial w}{\partial r} + \frac{\partial^2 w}{\partial z^2} & & \\ + \frac{\partial^2 u}{\partial z \partial r} + (\frac{1}{r} + 2c^2\aleph_0)\frac{\partial u}{\partial z} & = & 0 \end{array}\right. \tag{C.4.6}$$

Table des figures

1.1.1 Interprétation géométrique de la torsion : Deux champs de vecteurs $\mathbf{u}$ et $\mathbf{v}$. De tout point P, le transport parallèle de $\mathbf{u}$ et $\mathbf{v}$ le long de $\mathbf{v}$ ou $\mathbf{u}$ donne respectivement $\mathbf{u}_R^{||}$ et $\mathbf{v}_Q^{||}$. (a) = $\nabla_{\mathbf{v}}\mathbf{u}$, (b) = $\nabla_{\mathbf{u}}\mathbf{v}$, (c) = $[\mathbf{u},\mathbf{v}]$ et (d) = $\aleph(\mathbf{u},\mathbf{v})$. Cf [40]. 3
1.1.2 Transformation d'un point $\mathbf{M}$ par φ et d'une fibre $\mathbf{OM}$ par $\nabla\varphi$. Cf [75] . 5
1.1.3 Déformations d'un solide : transformation holonome φ_1, transformation non-holonome φ_2. Cf [74] 6
1.1.4 Circuit de Burgers dans un cristal. Cf [74] 7
1.1.5 Dislocations de Volterra : (a) Translations relatives de deux surfaces (lèvres du cylindre). (b) Rotations relatives de deux surfaces (disclinations). Cf [74] 7
1.1.6 Circuit de Cartan. Cf [73] 8

3.4.1 Thick-walled cylinder with inner radius p and outer radius q. 55
3.4.2 Norm of the determinant $|det(\omega, c, r_1)|$ vs. real frequency ω of the inhomogeneous aluminium cylinder. 59
3.5.1 Deformation of an element of Timoshenko beam : the figure is extracted of [75]. 63
3.5.2 Three first modal angle $\Theta_n/\exp(-\aleph_1 x)$ for heterogeneous beam with $d_\aleph$ = 0.1, 1, or 10 (plain thick Θ_1, plain thin Θ_2, dotted Θ_3). 68
3.5.3 Three first modal angle Θ_n (attenuated) for heterogeneous beam with $d_\aleph$ = 0.1 (plain thick Θ_1, plain thin Θ_2, dotted Θ_3). 68
3.5.4 Three first modal angle Θ_n (attenuated) for heterogeneous beam with $d_\aleph$ = 1 (plain thick Θ_1, plain thin Θ_2, dotted Θ_3). 69
3.5.5 Three first modal angle Θ_n (attenuated) for heterogeneous beam with $d_\aleph$ = 10 (plain thick Θ_1, plain thin Θ_2, dotted Θ_3). 69
3.5.6 Three first modal displacement $U_n/\exp(-\aleph_1 x)$ for heterogeneous beam with $d_\aleph = 0.1$ (plain thick U_1, plan thin U_2, dotted U_3). 70
3.5.7 Three first modal attenuated displacement U_n (attenuated) for heterogeneous beam with $d_\aleph = 0.1$ (plain thick U_1, plan thin U_2, dotted U_3). . . . 70
3.5.8 Three first modal displacement $U_n/\exp(-\aleph_1 x)$ for heterogeneous beam with $d_\aleph = 1$ (plain thick U_1, plan thin U_2, dotted U_3). 71
3.5.9 Three first modal displacement U_n (attenuated) for heterogeneous beam with $d_\aleph = 1$ (plain thick U_1, plan thin U_2, dotted U_3). 71

3.5.10 Three first modal displacement $U_n/\exp(-\aleph_1 x)$ for heterogeneous beam with $d_\aleph = 10$ (plain thick U_1, plan thin U_2, dotted U_3). 72
3.5.11 Three first modal displacement $U_n/$ (attenuated) for heterogeneous beam with $d_\aleph = 10$ (plain thick U_1, plan thin U_2, dotted U_3). 72

4.3.1 Semi-inclusion embedded to the semi-infinite matrix, pressure p in vertical arrow, pressure q the other. Cf [12]. 80
4.5.1 Densification volume $[\mu m]$ with respect to the load $[mN]$ for 4 types of glass. According to [12]. 85
4.5.2 Data for 4 types of glass. According to [43] and [12]. 85
4.5.3 Global densification -(4.5.6) with respect to the Poisson's ratio ν. 86
4.5.4 Blister shape for the silica glass with a beginning of defect. Cf [11], [12]. . 87
4.5.5 The angular localization with respect to the Poisson's ratio. 87

C.0.1 Indentation de Vickers avec un indenteur conique. Cette figure est extraite de [6]. 109

Bibliographie

[1] Agiasofitou EK, Lazar M. Conservation and balance laws in linear elasticity, *Journal of Elasticity* 94, (2009), 69-85.

[2] Abramowitz M, Stegun IA. *Handbook of Mathematical Functions*, National Bureau of Standards Applied Mathematics Series 55 (1964), p 555, p 358.

[3] Antonio Tamarasselvame N, Buisson M, Sangleboeuf JC. Densification of glass beneath an indenter : dependence of the shape of the deformed zone on the Poisson's ratio, *Proceeding for International Conference on Fracture (ICF12) Ottawa 2009.*

[4] Antonio Tamarasselvame N, Rakotomanana RL. On the Form-Invariance of Lagrangian Function for Higher Gradient Continuum, accepté dans *Mechanics of Generalized Continua*, edited by H. Altenbach, G.A. Maugin, V.I. Erofeev, (Springer 2010, to appear), chap 15, 291-322.

[5] Antonio Tamarasselvame N, Buisson M, Rakotomanana RL. Wave Propagation within a Non Homogeneous Body, en soumission.

[6] Bernard C, Keryvin V, Sangleboeuf JC, Rouxel T. Indentation creep of window glass around glass transition, *Mechanics of Materials* 42, (2010), 196-206.

[7] Bertram A, Svendsen B. On Material Objectivity and Reduced Constitutive Equations, *Archive of Mechanics* 53(6), (2001), 653-675.

[8] Bilby BA, Smith E. Continuous distributions of dislocations : a new application of the method of non Riemanian geometry, *Proc. Roy. Soc. London* A 231, (1955), 263-273.

[9] Bilby BA, Gardner LRT, Stroh AN. Continuous distributions of dislocations and the theory of plasticity, *Actes du IX^{éme} du Congrès de Mécanique Appliquée*, (1957), 35-44.

[10] Buisson M, Sangleboeuf JC, Keryvin V, Rouxel T. Champ de pression non isotrope approchant le champ des contraintes d'indentation d'un verre, *18ème Congrès Français de Mécanique*, (2007), Session 5/0492.

[11] Buisson M, Sangleboeuf JC, Antonio Tamarasselvame N. Low Indentation of Glass, Analytical Calculus, *eProceedings of 9th International Mathematica Symposium*, (2008), Maastricht, The Netherlands, http ://internationalmathematicasymposium.org.

[12] Buisson M, Sangleboeuf JC, Antonio Tamarasselvame N. Indentation faible charge : influence du coefficient de Poisson sur la densification et sur la forme des zones affectées. Une étude analytique, *Matériaux et Techniques hors-série 2008*.

[13] Cartan E. Sur les variétés à connexion affine et la théorie de la relativité généralisée I partie, *Ann. Ec. Norm.* 40, (1923), 325.

[14] Cartan E. *On manifolds with an affine connection and the theory of general relativity*, English translation of the French original by A. Magnon and A. Ashtekar, Bibliopolis, Napoli, (1986).

[15] Cermelli P, Gurtin ME. Geometrically necessary dislocations in viscoplastic single crystals and bicrystals undergoing small deformations, *International Journal of Solids and Structures* 39, (2002), 6281-6309.

[16] Challamel N, Andrade A, Camotim D. An Analytical Study on the Lateral-Torsional Buckling, *International Journal of Structural Stability and Dynamics* 7(3), (2007), 445-447.

[17] Challamel N, Rakotomanana RL, Le Marrec L. A dispersive wave equation using nonlocal elasticity, *CR Mécanique* 337, (2009), 591-595.

[18] Choquet-Bruhat Y, De Witt-Morette C, Dillard-Bleick M. *Analysis manifolds and physics*, North-Holland, New-York, (1977), part 3 and part 5.

[19] Cosserat E, Cosserat F. *Théorie des corps déformables*, Hermann, Paris, (1909), translated into English by D. Delphenich (2007).

[20] Edelen DGB, Lagoudas DC. *Gauge Theory and Defects in Solids*, North-Holland, New-York, (1988).

[21] Ehlers J. The nature and concept of spacetime, *The Physicist's concept of nature*, Edited by J. Mehra, Reidel Publishing Compagny, Dordrecht-Holland, (1973), 71-91.

[22] Eringen CA. *Nonlocal continuum field theories*, Springer, New-York, (2002).

[23] Epstein M. The Eshelby tensor and the theory of continuous distributions of inhomogeneities, *Mechanics Research Communications* 29, (2002), 501-506.

[24] Eshelby JD. The determination of the elastic field of an ellipsoidal inclusion, and related problems, communicated by R. E. Peierls, F.R.S. (1957), Collected Works of J.D. Eshelby, *The Mechanics of Defects and Inhomogeneities, Solid Mechanics and its Applications*, Xanthippi Markenscoff and Anurag Gupta (Eds.), Springer, (2006).

[25] Feng G, Qu S, Huang Y, Nix WD. An analytical expression for the stress field around an elastoplastic indentation-contact, *Acta Materiala* 55, (2007), 2929-2938.

[26] Fischer-Cripps AC. *Nanoindentation*, Springer, (2004).

[27] Forest S, Sab K. Cosserat overall modelling of heterogenous materials, *Mechanics Research Communications* 25(4), (1998), 449-454.

[28] Fleck NA, Hutchinson JW. Strain gradient plasticity, Hutchinson JW, Wu TY (Eds.), *Adv. in Appl. Mech.* 33, Academic Press, (1997), 295-361.

[29] Fleck NA, Hutchinson JW. A reformulation of strain gradient plasticity, *Journal of the Mechanics and Physics of Solids* 49, (2001), 2245-2271.

[30] Gao H, Huang Y, Nix WD, Hutchinson JW. Mechanism-based strain gradient plasticity I : Theory, *Journal of the Mechanics and Physics of Solids* 47, (1999), 1239-1263.

[31] Gao XL, Park SK. Variational formulation of a simplified strain gradient elasticity theory and its application to a pressurized thick-walled cylinder problem, *International Journal of Solids and Structures* 44, (2007), 7486-7499.

[32] Germain P. La méthode des puissances virtuelles en mécanique des milieux continus, première partie : théorie du second gradient, *J Mécanique*, 12, (1973), 235-274.

[33] Goldstein H. Classical Mechanics, *Addison-Wesley Series in Physics*, 2nd edition, Addison-Wesley, Massachusets, (1980).

[34] Gonseth F. *Les fondements des mathématiques : De la géométrie d'Euclide à la relativité générale et à l'intuitionisme*, Librairie scientifique et technique Albert Blanchard, Paris, (1926).

[35] Grady D. Scattering as mechanism for structured shock waves in metals, *Journal of the Physics and Mechanics of Solids* 46(10), (1998), 2017-2032.

[36] Gutkin MY, Aifantis EC. Dislocations and disclinations in gradient elasticity, *Phy Stat Sol b* 214, (1999), 245-284

[37] Gurtin ME. *Configurationnal forces as basis concepts of continuum physics*, Springer, New-York, (2000).

[38] Huang Y, Gao H, Nix WD, Hutchinson JW. Mechanism-based strain gradient plasticity II. Analysis, *Journal of the Mechanics and Physics of Solids* 48, (2000), 99-128.

[39] Huang Y, Chen J. The role of intrinsic material length scales in micro-indentation simulations, *Computational Materials Science* 25, (2002), 253-263.

[40] Hehl FW, Obukhov YN. Elie Cartan's torsion geometry and in field theory, an essay, *Annales de la Fondation Louis de Broglie* 32(2-3), (2007), 157-194.

[41] Hirao M, Ogi H, Suzuki N, Ohtani T. Ultrasonic attenuation peak during fatigue of polycrystalline copper, *Acta Materiallia* 48, (2000), 517-524.

[42] Ji H, Keryvin V, Rouxel T, Hammouda T. Densification of window glass under very high pressure and its relevance to Vickers indentation, *Scripta Mater* 55, (2006), 1159-1162.

[43] Ji H. *Mécanique et physique de l'indentation du verre*, Thèse, Université de Rennes 1, LARMAUR, (2007).

[44] Katanaev MO. Wedge dislocation in the Geometric Theory of Defects, *Theoretical and mathematical physics* 35(2), (2003), 733-744

[45] Keryvin V. Indentation of bulk metallic glasses : Relationships between shear bands observed around the prints and hardness, *Acta Materiala* 55, (2007), 2565-2578.

[46] Kleinert H. Nonholonomic mapping principle for classical and quantum mechanics in spaces with curvature and torsion, *General Relativity and Gravitation* 32 (5), (2000), 769-839.

[47] Kienzler R, Herrmann G. *Mechanics in Material Space*, Spinger, Berlin, (2000), chap 1.

[48] Kondo K. Non-Riemanian geometry of imperfect crystals from macroscopic viewpoint, *Memoirs of the unifying study of basic prblems in engineering sciances by means of geometry* vol I, Division D, Tokyo : Gakujutsu Benken Fukyu-Kai, (1955).

[49] Kröner E. Dislocation : a new concept in the continuum theory of plasticity, *J Math Phys* 42, (1963), 27-37.

[50] Kröner E. Continuum theory of defects, *Physique des défauts*, les Houches July 28 - August 29, North-Holland Publishing, Ed. by Balian et al., (1981), 219-315.

[51] Lazar M. An elastoplastic theory of dislocations as a physical field with torsion, *Journal Physics A : Math Gen 35*, (2002), 1983-2004.

[52] Lazar M, Maugin GA. Defect in gradient micropolar elasticity II : edge dislocation and wedge dislocation, *Journal of Mechanics and Physics of Solids* 52, (2004), 2285-2307.

[53] Lazar M, Maugin GA. Nonsingular stress and strain field of dislocations and disclinations in first strain gradient elasticity, *International Journal of Engineering Science* 43, (2005), 1157-1184.

[54] Lazar M, Maugin GA, Aifantis E. Dislocations in second strain gradient elasticity, *International Journal of Solids and Structure* 43, (2006), 1787-1817.

[55] Le KC, Stumpf H. Nonlinear continuum theory of dislocations, *Int J Eng Science* 34(3), (1996), 339-358.

[56] Le KC, Stumpf H. On the determination of the crystal reference in nonlinear continuum theory of dislocations, *Proc R Soc Lond A* 452, (1996), 359-371.

[57] Lovelock D, Rund H. *Tensors, differential forms and variational principles*, Wiley, (1975).

[58] Lubarda VA. The effects of couple stresses on dislocation strain energy, *International Journal of Solids and Structures* 40, (2003), 3807-3826.

[59] Markenscoff X, Gupta A. (éditeurs), Collected Works of J.D. Eshelby, *The Mechanics of Defects and Inhomogeneities*, Springer,(2006).

[60] Marsden JE, Hughes TJR. *Mathematical Foundations of Elasticity*, Prentice Hall, New-Jersey, (1983).

[61] Maugin GA. *Material Inhomogeneities in Elasticity*, Chapman and Hall, (1993).

[62] Maugin GA. Material forces : concepts and applications, *Appl. Mech. Rev.* 48, (1995), 247-285.

[63] Mindlin RD, Tiersten HF. Effects of couple-stresses in linear elasticity, *Arch. Ration. Mech. Anal.* 11, (1962), 415-448.

[64] Mindlin RD. Micro-structure in linear elasticity, *Arch. Ration. Mech. Anal.* 16, (1964), 51-78.

[65] Mindlin RD. Second gradient of strain and surface-tension in linear elasticity, *International Journal of Solids and Structures* 1, (1965), 417-438.

[66] Mindlin RD, Eshel NN. On first strain-gradient theories in linear elasticity, *International Journal of Solids and Structures* 4, (1968), 109-124.

[67] Nakagawa S, Nihei KT, Myer LR. Stop-pass behavior of acoustic waves in a 1D fractured system, *Journal of Acoustical Society of America* 107(1), (2000), 40-50.

[68] Nakahara M. *Geometry, Topology and Physics*, Graduate student series in Physics IOP Publishing, (1996).

[69] Noll W. Materially uniform simple bodies with inhomogeneities, *Archive for Rational Mechanics and Analysis* 27, (1967), 1-32.

[70] Onda I. Propagation and apparent attenuation of elastic waves in a heterogeneous medium with certain periodic structures, *Bulletin of the Earthquake Research Institute* 42, (1964), 427-447.

[71] Papargyri-Beskou S, Polyzos D, Beskos DE. Wave dispersion in gradient elastic solids and structures, *International Journal of Solids and Structures* 46, (2009), 3751-3759.

[72] Popov V, Kröner E. On the dynamic theory of elastoplastic medium with microstructure, *Computational Material Sciences* 16, (1999), 218-236.

[73] Rakotomanana RL. Contribution à la modélisation géométrique et thermodynamique d'une classe de milieux faiblement continus, *Archive of Rational Mechanics and Analysis* 141, (1997), 199-236.

[74] Rakotomanana RL. *A geometric approach to thermomechanics of dissipating continua*, Birkauser, Boston (2003).

[75] Rakotomanana RL. *Eléments de dynamique des structures et solides déformables*, Presses Polytechniques et Universitaires Romandes, Lausanne, (2009).

[76] Rakotomanana RL. Some class of SG continuum models to connect various length scales in plastic deformation, *Mechanics of material forces*, edited by P. Steimann and G. A. Maugin, Springer, (2005), chap 32.

[77] Rouxel T, Sangleboeuf JC, Guin JP, Keryvin V, Sorarù GD. Surface damage resistance of gel-derived oxycarbide glasses : hardness, toughness and scratchability, *J. Am. Ceram. Soc.* 84(10), (2001), 2220-2224.

[78] Schwartz L. *Mathematics for the physical sciences*, Hermann, Publishers in Arts and Science, Paris, (1966), chap 4 - chap 5.

[79] Svendsen B, Bertram A. On frame-indifference and form-invariance in constitutive theory, *Acta Mechanica* 132, (1999), 195-207.

[80] Svendsen B, Neff P, Menzel A. On Constitutive and configurational aspects of models for gradient continua with microstructure, *Z Angew Math Mech* 89(8), (2009), pp 687-697.

[81] Toupin RA. Elastic materials with couple stresses, *Arch. Ration. Mech. Anal.* 11, (1962), 385-414.

[82] Tsuchida E, Kouris D, Jasiuk I. *Hemispherical Inhomogeneity Subjected to a Concentrated Force*, Micromechanics and Inhomogeneity : The Toshio Mura Anniversary Volume, by G. J. Weng, M. Taya, H. Abe, Springer, (February 1990).

[83] Yoffe EH. Elastic Stress Fields caused by indenting brittle materials, *Phil. Mag. A* 46(4), (1982), 617-628.

[84] Yoshida S, Sangleboeuf JC, Rouxel T. Quantitative evaluation of indentation-induced densification in glass, *J. Mater. Res.* 20(12), (2005), 3404-3412.

[85] Wang CC. Geometric structure of simple bodies, or mathematical foundation for the theory of continuous distributions of dislocations, *Archive of Rational Mechanics and Analysis* 27, (1967), 33-94.

[86] Zhang X, Sharma P. Inclusions and inhomogeneities in strain gradient elasticity with couple stresses and related problem, *International Journal of Solids and Structure* 42, (2005), 3833-3851.

[87] Zhao J, Pedroso D. Strain gradient theory in orthogonal curvilinear coordinates, *International Journal of Solids and Structure* 45, (2008), 3507-3520.

Modèle de second gradient adapté aux milieux faiblement continus et mécanique d'Eshelby appliquée à l'indentation du verre

Dans une première partie, notre étude porte sur les milieux faiblement continus avec une approche basée sur la géométrie non riemannienne. Nous considérons un corps solide déformable modélisé par une variété riemannienne munie d'une connexion affine. Un tel modèle est une extension d'un autre qui considère une connexion euclidienne, laquelle dérive du tenseur métrique imposé par l'espace ambiant. La masse par unité de volume peut être supposée non constante et le corps peut contenir des défauts décrits par des champs de discontinuité de champs scalaires ou de champs vectoriels définis sur la variété. Dans ce cas, en plus du tenseur métrique, nous utilisons nécessairement la torsion introduite par Cartan ou la courbure, deux tenseurs associés à la connexion affine. Nous disposons ainsi d'un modèle de milieu continu du second gradient. Les investigations prennent en compte les effets de ces champs tensoriels dans l'analyse de la déformation du corps. Comme application, nous décrivons l'atténuation spatiale d'une onde propagée dans un milieu non homogène. Dans une seconde partie, notre étude porte sur une modélisation de l'indentation Vickers du verre. Nous considérons un modèle qui utilise le schéma d'inclusion d'Eshelby dans une matrice semi-infinie, pour analyser les champs de contrainte et de déplacement durant le processus de charge. L'objectif est de déterminer la densification du verre sous l'indenteur. Les résultats semi-analytiques obtenus sont confrontés de manière positive avec des données expérimentales fournies par le LARMAUR.

Second gradient model for weakly continuous media and mechanics of Eshelby applied to indentation of glass

In a first part, we deal with the weakly continuous media according to non Riemannian geometry. We consider a solid body modelled by a Riemannian manifold endowed with an affine connection. This model is an extension of the one which considers an Euclidean connection, which derives from the metric tensor induced by the ambiant space. The mass per volume unit may be assumed non constant and some defects, described by discontinuity fields of scalar fields or vectorial fields defined on the manifold, may appear in the body. In a such case, in addition of the metric, we necessary use the torsion introduced by Cartan or the curvature, both tensors associated with the affine connection. This corresponds to a second gradient continuum model. The investigations take into account the effects of these tensor fields on the analysis of the deformation of the body. As application, we describe the attenuation of wave propagation within a non homogeneous body. In a second part, we deal with the modelling of the Vickers indentation of glass. We consider a model which uses the schema of inclusion of Eshelby into a semi-infinite matrix, to analyse the stress and displacement fields during the loading process. The objective is to determine the densification of the glass beneath the indenter. The semi-analytical results are positively compared with experimental data which are issue from LARMAUR.